Preparation and properties of molecular sieving membranes(Dissertation_全文)

AUTHOR(S):

Kuraoka, Koji

Preparation and properties of molecular sieving membranes

Koji Kuraoka

2000

Preface

The studies presented in this thesis have been carried out at Osaka National Research Institute, AIST during 1993-2000.

The author wishes to express his sincerest gratitude to Professor Yoshiki Chujo of Kyoto University for his continuing interest, guidance and encouragement in this work.

The author's grateful thanks are also due to Dr. Tetsuo Yazawa of Osaka National Research Institute, AIST for his guide to this research, insightful discussion and hearty encouragement.

The author wishes to express his deep gratitude to Professor Hajime Tamon and Professor Kazuyuki Hirao for their helpful advice and suggestions.

It is also a pleasure to acknowledge the hospitality, collaboration and helpful advice of the member of Advanced Glass Section, Osaka National Research Institute, AIST. Sincere thanks are due to Ms. Yoshiko Ishida for her assistance.

Finally, the author sincerely thanks his wife, Mrs. Yoko Kuraoka for her supports and encouragement. The author also wishes to express his deep appreciation to his parents, Mr. Naotsugu Kuraoka and Mrs. Hiroko Kuraoka for their supports.

Koji Kuraoka

Advanced Glass Section,
Department of Optical Materials,
Osaka National Research Institute, AIST,
2000

Contents

General Introduction

General Introduction

Membrane science has developed since the first synthesis of membranes almost 40 years ago, which has been driven by strong technological needs and commercial expectations. Membranes are understood to be thin barriers between two phases through which transport takes place under the action of a driving force such as a pressure difference and a chemical or electrical potential difference. There are two big categories in material classification of membranes such as organic membranes and inorganic membranes. Because of distinct advantages that organic membranes (polymer membranes) offer compared with inorganic membranes, including production cost-efficiency and performance, commercial separations are dominated by organic membranes. However, intensive research efforts are being development and improvement of inorganic membranes for use in separations that are poorly, if at all, attainable by conventional organic membranes. In general, inorganic membranes have advantages for high temperature separations, due to their relatively high thermal stability. They can also be used in environments that require high chemical stability and biocompatibility. These exceptional properties of inorganic membranes have challenged many research laboratories around the world to formulate novel synthesis routes that will lead to end products tailored to specific applications and without the typical weakness of ceramic and other inorganic materials, such as poor reproductivity and intrinsic brittleness.

Membrane can be divided into two categories according to their structures: dense membranes (non porous membranes) and porous membranes [1, 2]. The dense membranes include typical polymer membranes and metal films such as Pt [3], Au, Pd [4, 5], Ag alloys [6]. The porous membranes are porous polymer membranes and typical inorganic membranes such as the membranes prepared by sol-gel method. In this thesis, molecular sieving membranes are investigated. The molecular sieving membranes are typical porous membranes. Thus the porous membranes are described in detail here.

The properties of gas flow in porous media depend on the ratio of the number of molecule-molecule collisions to that of molecule-pore wall collisions [1, 7]. The Knudsen number, Kn is a characteristic parameter defining different regions of this ration. That number is defined by $Kn=\lambda/d_p$ with λ being the mean free path of the gas molecules and d_p being the characteristic pore diameter. The value of Kn separates three main flow regimes of gaseous diffusion:

(i) Viscous flow: $Kn<<1$, $\lambda<<d_p$

(ii) Knudsen flow: $Kn>>1$, $\lambda>>d_p$

(iii) Transition flow (Viscous flow+Knudsen flow): $Kn=1$, $\lambda=d_p$

When the pore walls strongly adsorb gas molecules, surface flow occurs. Molecular sieving (activated diffusion) is a separate class and occurs when the pore diameter is a factor of 1-5 larger than the molecular diameter. Figure 1 schematically shows the different mechanisms that may occur in a porous membrane for a pore of cylindrical shape [2]. They are (a) viscous flow; (b) Knudsen flow; (c) surface flow; and (d) molecular sieving (activated diffusion).

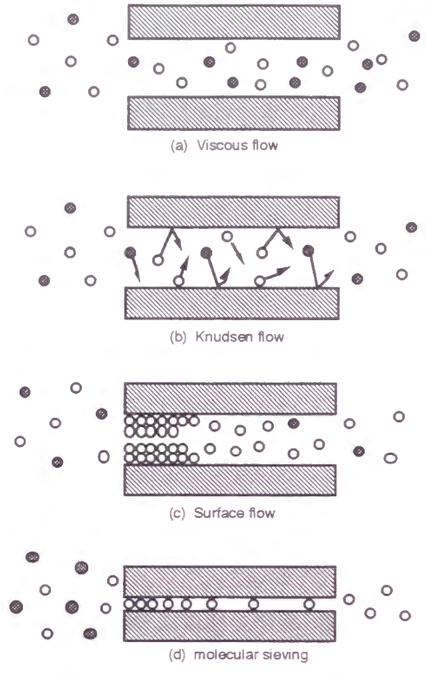

Fig. 1 Transport mechanisms for gaseous mixtures through porous media

(a) viscous flow

In this flow mechanism, the mean distance between molecule-molecule collisions in the gas phase (the mean free path) is much smaller than the pore size (Kn<<1), and the driving force for transport through the membrane is the total pressure gradient. This flow can be described by Darcy's law [1, 7]. In capillaries with small diameter, the flow is laminar and if the gas velocity near the pore walls equals zero (no slip flow), molar flux can be described by Hargen-Poiseuille law [1]:

$$J = \frac{r^2}{8\eta}\frac{P}{RT}\frac{dP}{dz} \qquad (1)$$

In actual porous media, Eq. (1) should be modified to account for the porosity (the number of capillaries per unit volume) and the tortuosity, τ (the complexity of the structure) as follows:

$$J = \frac{\varepsilon}{\tau}\frac{r^2}{8\eta}\frac{P}{RT}\frac{dP}{dz} \qquad (2)$$

In the steady state, the fluxes in and out of any cross section of a pore are equal. Therefore P(dP/dz) is constant and Eq. (2) integrates over the thickness L of the porous medium gives the permeation:

$$F = -\frac{J}{\Delta P} = \frac{\varepsilon}{8\eta\tau}\frac{r^2}{RTL}P_m \qquad (3)$$

where the mean pressure, $P_m=0.5(P_1+P_2)$ and P_1 and P_2 the pressure at the inlet and outlet respectively. Equation (3) shows that the permeation is proportional to the radius squared (r^2) and the mean pressure.

(b) Knudsen flow

This mechanism occurs when the mean free path is much larger than the mean pore diameter (Kn>>1). Thus collisions between molecules in the gas phase are rare, and transport takes place through the diffusion molecules with pore walls. The flow of a single gas in a long capillary under the driving force of a concentration pressure gradient can be described by the Knudsen equation [7, 8]:

$$J = -\frac{2}{3}\bar{v}\, r\frac{dc}{dz} \quad \text{or} \quad J = -\frac{2}{3}\bar{v}\, r\frac{1}{RT}\frac{dP}{dz} \qquad (4)$$

with the mean velocity of the gas molecules $\bar{v}$ given by:

$$\bar{v} = \left(\frac{8RT}{\pi M}\right)^{0.5} \qquad (5)$$

In actual porous media, geometrical effects play an important role, similar to that discussed for viscous flow, and Eq. (4) should be modified by a term ε/τ. Furthermore in derivation of Eq.

(4), it is assumed that the molecules are secularly reflected after collisions with the wall. This assumption is usually not true. The walls have a certain roughness and this causes diffuse reflection. This effect is given by a term $1/\theta$ (θ is unity for smooth wall, otherwise it is larger).

Using these terms and inserting Eq. (5) into Eq. (4), the expression for the Knudsen flow in a porous membrane is as follows:

$$J = -\frac{2}{3}\frac{\varepsilon r}{\tau\theta}\left(\frac{8}{\pi RTM}\right)^{0.5}\frac{dP}{dz} \tag{6}$$

After integration of Eq. (6) over the membrane thickness, L, the permeation is expressed:

$$F = -\frac{J}{\Delta P} = \frac{2\varepsilon r}{3\tau\theta L}\left(\frac{8}{\pi RTM}\right)^{0.5} \tag{7}$$

Eq. (7) shows that the permeation of a single gas in the Knudsen regime is proportional to the mean pore radius, r, independent of the pressure and proportional to $M^{-0.5}$.

(c) surface flow [1, 9]

The surface flow mechanism appears when the diffusing molecules exhibit strong affinity with the materials making the pore walls and a dense layer covered on the pore surface. The adsorbed molecules on the pore walls diffuse along the pore surface by moving from one adsorptive site to another. The actual mechanism of the surface flow is rather complicated and three main mechanisms have been considered:

The hydrodynamic model [10, 11]: The adsorbed molecules is considered as a liquid film in this model. This film can glide along the surface under the pressure gradient.

The hopping model [12]: This model assumes that the adsorbed molecules can move on the surface by hopping over a certain distance with a certain velocity.

The random walk model [13-15]: This model is based on the two-dimensional form of Fick's law and many papers used this model.

The surface flux, J_s for a single gas is generally described by the two-dimensional Fick's law for relatively low surface concentration as follows:

$$J_s = -\frac{\varepsilon}{\tau}D_s\frac{dC_s}{dz} \tag{8}$$

where C_s is the surface concentration of the adsorbed molecules (mol/m^2). Expressed in terms of directly measurable parameters this gives:

$$J_s = -\rho(1-\varepsilon)\left(\frac{\varepsilon}{\tau}\right)D_s\frac{dq}{dz} \tag{9}$$

where $C_s = q\rho(1-\varepsilon)$, and $\rho(1-\varepsilon)$ is the density of the porous media. To consider that the influence of the pore size on the magnitude of the surface flow:

$$q = \theta_s \bullet S_w \bullet c_{sat} \tag{10}$$

and

$$S_w = 2\frac{\varepsilon}{\rho\, r} \tag{11}$$

where θ_s is the occupancy, defined as the mole fraction occupied by adsorption relative to a monolayer with sorption capacity c_{sat} in mol/m2 and S_w is the surface area of the porous medium.

Substituting Eq. (10), (11) into Eq. (9) one obtains:

$$J_s = -\frac{2\varepsilon^2}{\tau}\frac{D_s}{r}c_{sat}\frac{d\theta_s}{dL} \tag{12}$$

Equation (12) implies that Js increases strongly with decreasing the average pore size.

(d) molecular sieving (activated diffusion) [7, 16]

The molecular sieving mechanism occurs when the pore size becomes molecular dimension which can exhibit selectivity according to the size of the gas molecules. This mechanism is called activated diffusion, configurational diffusion or micropore diffusion [16]. The activated diffusion may be viewed as surface diffusion at the limit at which the pore size becomes comparable to the molecular size. With the gradient of the gas concentration in the pores as the driving force, the expression that relates the activated diffusion coefficient to the adsorption isotherm is analogous to that for surface flow. Many of the methods adapted to study the surface flow and the relationships developed for that flow also apply to the activated diffusion due to many similarities between them [17]. The value for the activated diffusion coefficient covers a very broad range, from 10^{-7} to 10^{-20} m^2/s. The activated diffusion and Knudsen flow are the main two transport mechanisms of interest for the porous permselective membranes. For Knudsen flow, the permselectivity is determined by the ratio of the molecular weights as mentioned above, but in the case of the activated diffusion, the diffusion coefficients of two gases are strong functions of the molecular shape and size, the pore size and the strength of the interactions between pore wall and gas molecules.

There are two big categories for making membranes; (1) Liquid phase method and (2) Vapor phase method. Here these important techniques for making membranes will be described.

(i) Sol-gel method

(ii) Elution method

(iii) CVD (Chemical Vapor Deposition) method

(iv) Sputtering method

(i) Sol-gel method [9, 18]

The sol-gel method using metal alkoxide is one of the most effective methods for the preparation of membranes. The membranes such as Al_2O_3 [19, 20], TiO_2 [21, 22], SiO_2 [23-26] are prepared by this method. The method is composed of sol preparation with solvents, subsequent gelation and removal of the solvents. Using alkoxysilanes as precursors, Si-OH groups will be formed by hydrolysis of alkoxy groups and with condensation of hydroxyl groups, Si-O-Si bonds will be obtained. These reactions are catalyzed by acids or bases. With further hydrolysis and condensation, siloxane networks are developed via crosslinking of oligomers. And by removing the solvents with heating or drying, xerogels are obtained. Generally, xerogels are porous materials and are used for the membranes. The structure of the obtained xerogels are affected by many parameters such as reaction temperature, solvents, pressure, amounts of water, kinds of catalyst and amounts of catalyst.

The sol-gel process can be divided into two main routes which are schematically shown in Fig. 2. These two main routes are the particulate sol route and the polymeric sol route [18]. In the particulate sol route, a faster hydrolysis rate is obtained by using a precursor with a fast hydrolysis rate and by reacting the precursor with excess water. A particulate sol is obtained by this route (Fig. 2). The elementary particle size ranges, depending on the system and processing conditions, from 3 to 15 nm and these particles form loosely bound agglomerates with sizes ranging from 5 to 100 nm [9]. During removing the solvents, the particulate sol transforms to a gel structure consisting of inter linked chains of particles or agglomerates and a xerogel with meso to macro pores (pore diameter of more than 2 nm) finally. In the polymeric sol route, the hydrolysis rate is kept low by adding small amounts of water, using acid catalysts and choosing a precursor which hydrolyzes relatively slowly. The final stage of this process is a strongly interlinked gel network (Fig. 2) with a structure different from that obtained from the particulate sol route. The xerogels with micro pore

(pore diameter of less than 2 nm) are obtained by removing solvent completely.

Organic-inorganic hybrid membranes are also made by this method [27-30]. One of the advantages of the sol-gel method to prepare organic-inorganic hybrid membranes is that the reaction can be carried out at comparatively low temperature, while the conventional melting process of silica glasses requires much high temperature. Another advantage of this method is that this reaction can be treated in low viscosity solution. This allows to obtain homogeneous solution of organic polymer and inorganic materials. Thus, it enables us to introduce organic groups into inorganic materials without derioration of their functionalities.

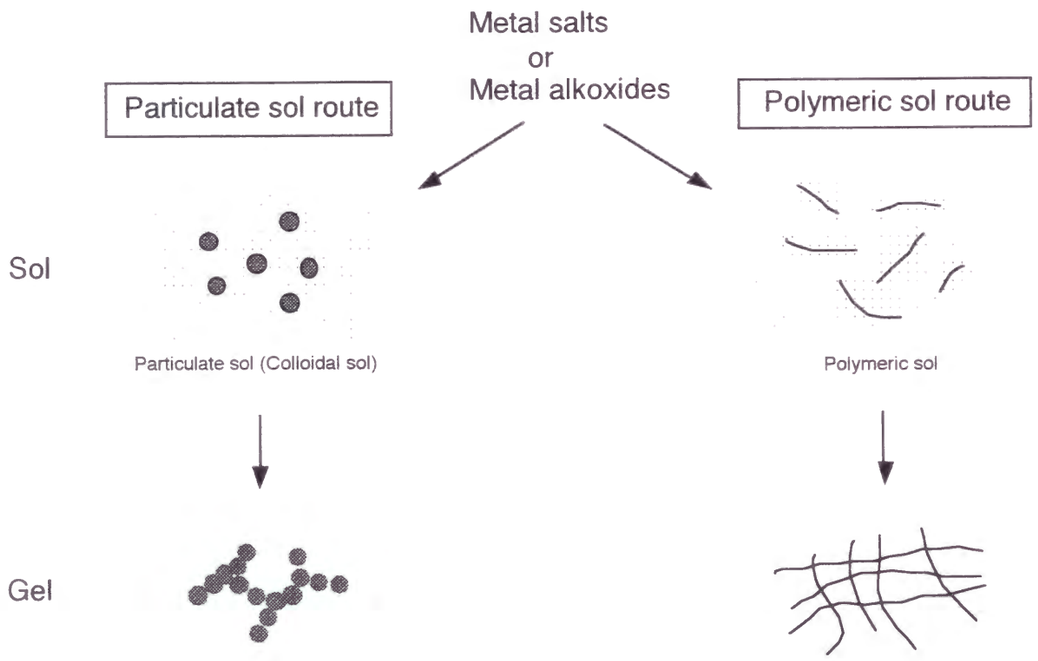

Fig. 2 Scheme of sol-gel routes. Particulate sol route and polymeric sol route.

(ii) Elution method (leaching method)

One of the most famous membranes prepared by elution method is a porous glass membrane. Porous glass membranes are produced by leaching a phase separated glass in the system of SiO_2-B_2O_3-Na_2O [31]. Figure 3 indicates a flow chart of making porous glasses. A typical composition is 70 wt% SiO_2-23 wt% B_2O_3-7 wt% Na_2O reported in the investigations of Hood and Nordberg [32, 33]. The two phase region (miscibility gap) is a large composition range. This miscibility gap is well-known as Vycor glass.

Under certain time and temperature conditions, the homogeneous glass is separated into two phases (Silica-rich phase and Borate-rich phase). Silica-rich phase is insoluble in mineral acids. However borate-rich phase is easily soluble in the acids. After the borate-rich phase is dissolved out of this heterogeneous glass structure with the acids, a porous skeleton of substantially insoluble silica-rich phase is left. The phase separation occurs at 773 K to 1073 K. A visible sign for the phase separation is that glass exhibits increasing opalescence with increasing heat treatment temperature. Because the pore sizes are controlled with the heat treatment temperature. The heat treatment time also influences the phase separation. Therefore, there are many possibilities of producing porous glass by changing glass composition, heat treatment temperature and time.

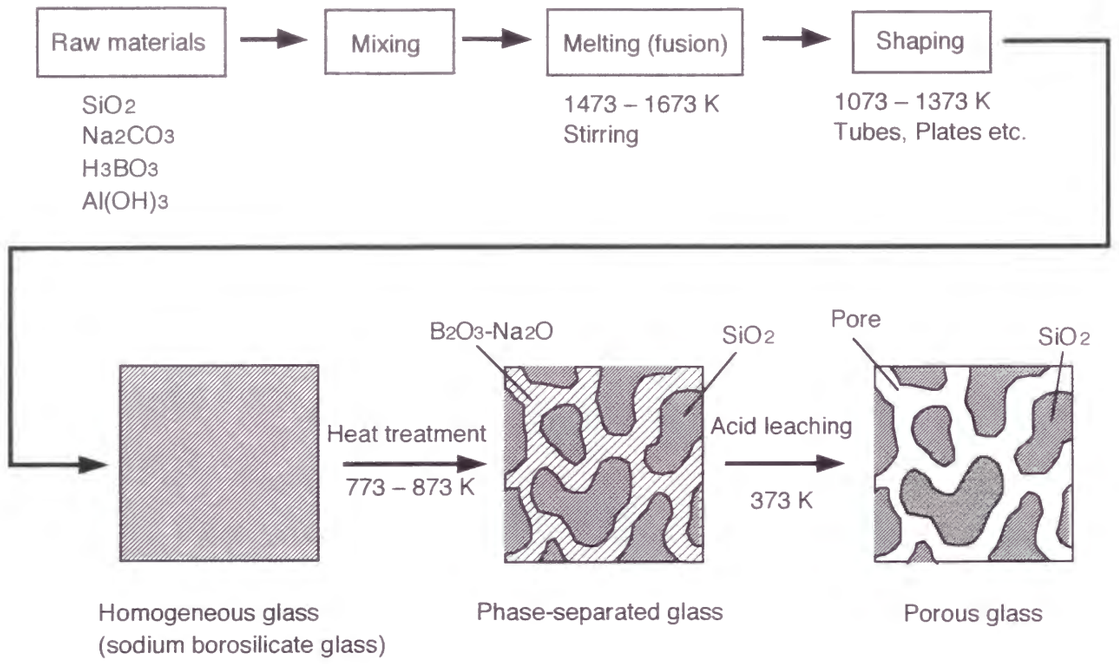

Fig. 3 Flow chart of making porous glass.

(iii) CVD method

Chemical vapor deposition (CVD) method has been used for preparing inorganic molecular sieving membranes with an ultramicroporous layers of silica [34-36], zirconia or titania [37-39]. In this process, heat is supplied through resistive heating, infrared heating, laser beam or plasma to effect a gas phase chemical reaction involving metal complex. The metals and metal oxides are produced from the reaction deposits by nucleation and growth on the substrates which are placed in CVD reactor. Effective reactants should be quite volatile and for this reason metal carbonyls, hydride and organic compounds such as alkoxides are commonly used.

(iv) Sputtering method

Sputtering method is an effective method to make thin films that cannot be prepared by other methods, such as sol-gel method, electroless plating and evaporation method. And the rates of evaporation for various metals using this method are similar. It doesn't involve another physical vapor deposition, such as thermal evaporation. Instead the method entails the use of rapid ion bombardment with an inert gas (Ar etc.) to dislodge atoms of selected solid materials and then deposit them onto a nearby target substrate. Its deposition rate is in general lower than those of thermal evaporation processes. For comparison, the deposition rates for the resistive heating (thermal evaporation) and the sputtering methods are approximately > 1 μm/min and < 0.1 μm/min, respectively [2]. Recently, this method has been used to make a thin effective separation layer on various substrate for inorganic membranes. Thin films of Pd and Pd-Ag alloys have been prepared by several researchers according to this method [40, 41]. Thin dense metal membranes on porous supports have been widely studied to achieve a high permselectivity and a relatively high flux at the same time [42].

In this thesis, the author is engaged in the study of the preparation and characterization of inorganic molecular sieving membranes. The basic concept of this study is shown in Fig. 4. The chapters in Fig. 4 are corresponding to the chapters of this thesis. To control pore size (pore diameter of subnano-nanometer scale), the author applies sol-gel method, elution method, CVD method and sputtering method. Control of potential of the prepared pore surface is also studied to give affinity for certain gas with surface modification. In addition, molecular dispersion of organic polymer in inorganic matrix is studied to introduce functionality of organic polymers and to make new materials (inorganic-organic hybrids).

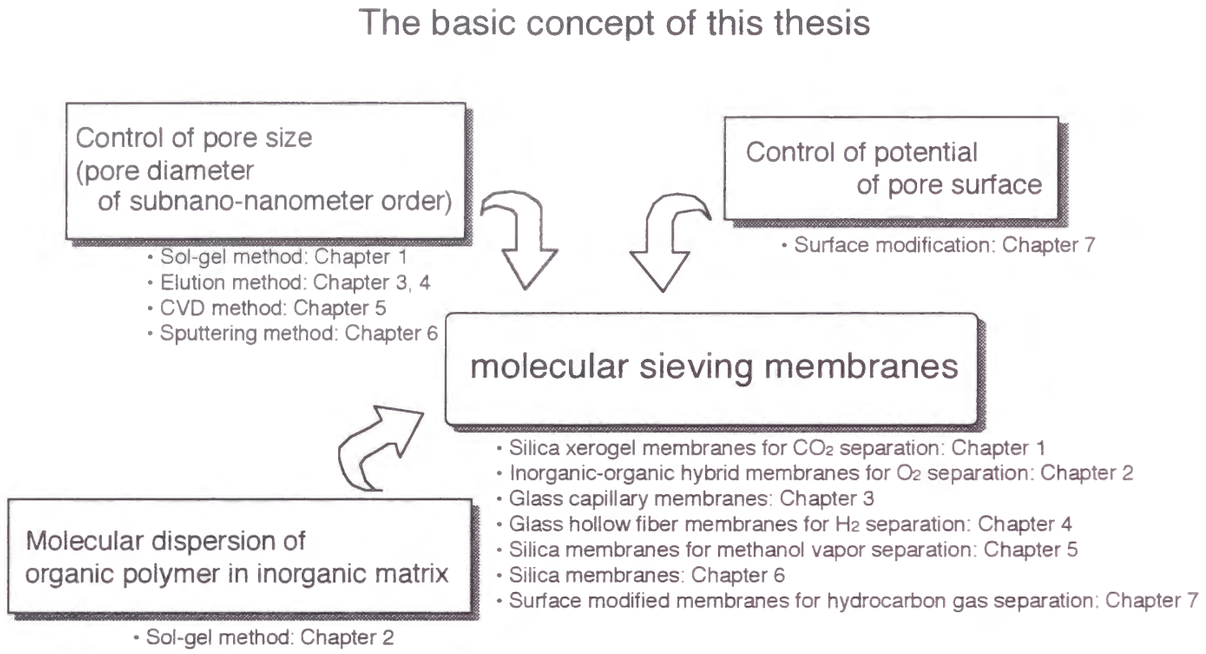

Fig. 4 The basic concept of this thesis

This thesis has been classified with preparation method mainly. In Part I, the membranes prepared by liquid phase method have been studied. In Part I-1, the membranes prepared by sol-gel method are described. In Chapter 1, the microporous silica xerogel membrane with pore diameter less than 1 nm coated on porous glass support has been successfully prepared by a novel sol-gel method. This method is characterized by low water content and low heat treatment temperature. This membrane indicated highly selective separation of CO_2. Selectivities of CO_2 (the ratios of permeances, CO_2/N_2) were increased as relative humidities were increased. The details of the preparation condition, structure, gas permeation property for the membrane are investigated. In Chapter 2, preparation and property of the inorganic-organic hybrid membranes are described. This membrane is SiO_2-poly(N-vinylpyrrolidone)- N,N'-disalicylidenethylenediaminatocobalt(II) hybrid

and inorganic matrix and organic matrix are dispersed at a molecular level. The detail preparation method, thermal stability, structure and O_2 permeance are shown. In Part I-2, the membranes prepared by acid leaching are described. In Chapter 3, glass capillary membranes prepared by elution of alkali metal ions from alkali silicate glasses are investigated. Permeation properties of He, N_2, CO_2 and pore structure of the membranes are investigated. In Chapter 4, glass hollow fiber membranes have been prepared by acid leaching. The composition of the glass hollow fibers are well-known composition of phase-separated glasses. H_2 permeation property and mechanism of micropore formation are described.

In Part II, the membranes prepared by vapor phase method have been studied. In Chapter 5, the membranes prepared by CVD (Chemical Vapor Deposition) method are described. Silica membranes have been prepared by depositing silica on porous glass tubes with the aid of evacuation using tetraethoxysilane as a reactant in the temperature range of 673-773 K. The basic permeation properties of methanol vapor in gas phase are investigated. In Chapter 6, the membranes prepared by sputtering method are described. The silica tubular glass membranes with thin, dense silica layers on porous glass supports have been prepared by sputtering using the novel sputtering apparatus for tubular supports. This apparatus has holder for tubular supports and a rotation mechanism. The sputtering conditions of the membranes and the basic gas permeation properties are reported.

In Part III, the surface modification of the pores by organosilicon compounds is described. In Chapter 7, the porous glass membranes have been prepared by surface modification with organosilicon compounds having various length of carbon chain. These compounds are generally indicated as R-$(CH_3)_2$-Si-Cl, R=C_nH_{2n+1} (R=1, 3, 8, 18). The detail surface modification method, hydrocarbon gas permeation properties and thermal stability are described.

References

1. S.-T. Hwang and K. Kammermeyer, *Membranes in separations* (JOHN WILEY & SONS, New York, 1975).
2. H.P. Hsieh, *Inorganic membranes for separation and reaction* (ELSEVIER, Amsterdam, 1996).
3. H. Zhao, A. Li, J. Gu and G. Xiong, *J. Mater. Sci.*, **34**, 1 (1999).
4. S. Uemiya, N. Sato, H. Ando, Y. Kude, T. Matsuda and E. Kikuchi, *J. Membrane Sci.*, **56**, 303 (1991).
5. S. Uemiya, T. Matsuda and E. Kikuchi, *J. Membrane Sci.*, **56**, 315 (1991).
6. M.J. Hampden-Smith and T.T. Kodas, *Chem. Vap. Deposition*, **1 (1)**, 8 (1995).
7. A.J. Burggraaf and L. Cot, *Fundamentals of inorganic membrane science and technology* (ELSEVIER SCIENCE B.V., Amsterdam, 1996).
8. M. Knudsen, *Ann. Physik (Leipzig)*, **28**, 75 (1909).
9. R.R. Bhave, *Inorganic membranes synthesis, characteristics and applications* (CHAPMAN & HALL, London, 1991).
10. E.R. Gilliland, R.F. Baddour and J.L. Russell, *AIChE J.*, **4**, 90 (1958).
11. R.F. Batholemew and E.A. Flood, *Can. J. Chem.*, **43**, 1968 (1965).
12. R.K. Smith and A.B. Metzner, *J. Phys. Chem.*, **68**, 2741 (1964).
13. S.-T. Hwang and K. Kammermeyer, *Can. J. Chem. Eng.*, **44**, 82 (1966).
14. T. Okubo and H. Inoue, *J. Chem. Eng. Japan*, **20**, 590 (1987).
15. K. Keizer, R.J.R. Uhlhorn, R.J. Vanvuren and A.J. Burggraaf, *J. Membrane Sci.*, **39**, 285 (1988).
16. S.V. Sotirchos and V.N. Burganos, *MRS Bull.*, **24 (3)**, 41 (1999).
17. A.B. Shelekhin, A.G. Dixon and Y.H. Ma, *AIChE J.*, **41**, 58 (1995).
18. C.J. Brinker and G.W. Scherer, *Sol-gel science: the physics and chemistry of sol-gel processing* (ACADEMIC PRESS, INC., San Diego, 1990).
19. B.E. Yoldas, *Amer. Ceram. Soc. Bull.*, **54**, 289 (1975).
20. B.E. Yoldas, *Amer. Ceram. Soc. Bull.*, **54**, 286 (1975).
21. R.J.R. Uhlhorn, K. Keizer and A.J. Burggraaf, *J. Membrane Sci.*, **66**, 271 (1992).
22. Z. Zeng, X. Xiao, Z. Gui and L. Li, *J. Membrane Sci.*, **136**, 153 (1997).
23. C.J. Brinker, T.L. Ward, R. Sehgal, N.K. Raman, S.L. Hietala, D.M. Smith, D. Hua and T.J. Headley, *J. Membrane Sci.*, **77**, 165 (1993).
24. B.N. Nair, T. Yamaguchi, T. Okubo, H. Suematsu, K. Keizer and S. Nakao, *J. Membrane Sci.*, **135**, 237 (1997).
25. R.M.d. Vos and H. Verweij, *J. Membrane Sci.*, **143**, 37 (1998).
26. R.M.d. Vos and H. Verweij, *Science*, **279**, 1710 (1998).
27. H. Schmidt, H. Scholze and A. Kaiser, *J. Non-Cryst. Solids*, **63**, 1 (1984).
28. T. Saegusa and Y. Chujo, *J. Macromol. Sci.*, **A27 (13&14)**, 1603 (1990).
29. M. Toki, T.Y. Chow, T. Ohnaka, H. Samura and T. Saegusa, *Polymer Bull.*, **29**, 653 (1992).
30. Y. Chujo and T. Saegusa, *Adv. Polym. Sci.*, **100**, 11 (1992).
31. O.V. Mazurin and E.A. Porai-Koshits, *Phase separation in glass* (Elsevier Science Publishers B. V., Amsterdam, 1984).
32. H.P. Hood and M.E. Nordberg, USA Patent, 2,106,744 (1938).
33. H.P. Hood and M.E. Nordberg, USA Patent, 2,221,709 (1940).
34. G.R. Gavalas, C.E. Megiris and S.W. Nam, *Chem. Eng. Sci.*, **44**, 1829 (1989).
35. J.C.S. Wu, H. Sabol, G.W. Smith, D.L. Flowers and P.K.T. Liu, *J. Membrane Sci.*, **96**, 275 (1994).
36. S. Morooka, S. Yan, K. Kusakabe and Y. Akiyama, *J. Membrane Sci.*, **101**, 89 (1995).
37. M. Tsapatsis, S. Kim, S.W. Nam and G. Gavalas, *Ind. Eng. Chem. Res.*, **30**, 2152 (1991).
38. L.G.J.d. Haart, Y.S. Lin, K.J.d. Vries and A.J. Burggraaf, *J. Europ. Ceram. Soc.*, **8**, 59

(1991).

39. H.Y. Ha, S.W. Nam, T.H. Lim, I.-H. Oh and S.-A. Hong, *J. Membrane Sci.*, **111**, 81 (1996).

40. J. Shu, B.P.A. Grandjean, A.V. Neste and S. Kaliaguine, *Can. J. Chem. Eng.*, **69**, 1036 (1991).

41. V. Jayaraman and Y.S. Lin, *J. Membrane Sci.*, **104**, 251 (1995).

42. Y.H. Ma, *MRS Bull.*, **24 (3)**, 46 (1999).

Part I Liquid phase method

Part I-1 Sol-gel method

Chapter 1: Preparation of silica xerogel membrane and its carbon dioxide separation

1. 1 Abstract

Silicate xerogel membrane was coated on tubular porous glass support by sol-gel method. This membrane has micropores with diameter less than 1 nm and high gas selectivity. From IR study, it was found that this membrane had fused-silica like structure. Permeations of N_2, He and CO_2 were investigated at 298 K and 373 K. At 298 K, the He/N_2 selectivity factor (ratio of the permeance) and the CO_2/N_2 selectivity factor attained about 20 and about 50, respectively. The influence of alternated temperature of 298 K and 373 K on the selectivity factors was also investigated. The selectivity factors changed reversibly between high value at 298 K and low value at 373 K. The influence of humidity on permeations was investigated at 303 K. Permeances of N_2 and He decreased rapidly as increased humidity. Permeance of CO_2 decreased slower than those of N_2 and He. It was found that the permeation characteristics of this membrane were strongly related to humidity.

1. 2 Introduction

For the last decade, active researches on inorganic membranes have been carried out. Inorganic membranes have many advantages compared with organic membranes due to their chemical and thermal stability and high mechanical strength.

Almost all asymmetric membranes are made by the sol-gel method [1]. This method is based on the hydrolysis, condensation and polymerization of metal alkoxides and following sintering [2]. Sol is coated on the outer surface or inner surface of a porous support tube, which has a large pore size, and becomes a gel after drying. By conventional sol-gel method which is composed of deposition of particulate sol and calcination at relatively high temperature (more than 573 K), it is difficult to obtain porous membrane with pore size less than 2 nm [3].

However, the author found that microporous xerogel membrane with pore diameter less than 1 nm coated on porous glass support could be obtained by a novel sol-gel method. This xerogel prepared by evaporation of solvent from wet gel is distinguished from ordinary porous ceramic green bodies by its small pore size and correspondingly enormous surface area. This method is peculiar in application of low water content and low heat treatment temperature. The gas selectivity factor (the ratio of the permeance) of the membrane attained about 20 for He/N_2 system and about 50 for CO_2/N_2 system at 298 K.

In this chapter, the author indicates the preparation of this novel microporous xerogel membrane, and its gas separation characteristics.

1. 3 Experimental

1.3.1 Membrane preparation

Xerogel layer was prepared using the sol-gel method. The silicate sol composition was tetraethoxysilane(TEOS):C_2H_5OH:H_2O:HCl=1:20:2:0.01 in molar ratio. Commercially available reagent grade chemicals were used. The mixture was stirred for several hours at room temperature to obtain homogeneous sol. Porous glass tubes with pore diameter of 4 nm, outer diameter of 5 mm, inner diameter of 4 mm, and length of approximately 10 cm were used as the support. Support tubes with one end closed were dipped in the sol, withdrawn at a rate of 3 mm/s, and then they were dried at room temperature. After the dip-coating procedure repeated for 3 times, the tubes were heated to 423 K at the rate of 0.5 K/min and maintained at the temperature for 2 hours, and cooled to room temperature. These coating and heating procedures were repeated 2 times and final specimens were obtained. The membranes were stored in the atmosphere until the gas permeation measurements.

1.3.2 Infrared Spectroscopy

A part of the sol was dried at room temperature in a TEFLON beaker until it gelated, and then it was heat treated under the same conditions described above. Fourier transform infrared (FT-IR) spectrum was measured for investigating xerogel structure. FT-IR spectrometer PERKIN-ELMER 1760 connected with a personal computer PERKIN-ELMER 7700 was used.

1.3.3 Pore size measurement

Samples were prepared by the same procedure described in section 2.2. The nitrogen adsorption was measured by BELSORP 28, BEL JAPAN Inc. The specific surface area was determined by Langmuir plot and the pore size distribution was analyzed by MP-method [4].

1.3.4 Measurement of gas permeation

Single gas permeation of the membrane was measured using He, N_2, and CO_2. One end of the tubular membrane was sealed and the other end was connected to a Pyrex glass tube with epoxy resin. This membrane was supported in a gas flow cell. Pressure difference of the gases through the membranes was kept constant at 1 atm and the permeance at 298 K and 373 K was measured by a mass flow meter.

The effect of cyclic change of the temperature was also estimated. After the measurement of permeance at 298 K and 373 K, the sample was exposed to the atmosphere for a few days. Then the permeance was measured at 298 K and 373 K. The cycle of measurement and exposure was repeated several times.

The dependance of the ratio of permeation, He/N_2 and CO_2/N_2 on relative humidity was also measured. After drying the membrane at 353 K overnight, the membrane was exposed to various relative humidities (30 to 80%) at 303 K for 3 hours. Then the permeation rates were measured at 303 K.

1. 4 Results and discussion

1.4.1 Infrared spectroscopy

FT-IR spectra of xerogel, TEOS and fused-silica are presented in Fig. 1. As seen, xerogel shows no band between 3000 and 2800 cm^{-1} which correspond to the C-H stretching modes. This fact shows that xerogel doesn't contain TEOS nor its hydrolytic decomposition products.

Xerogel shows the band at ~960 cm^{-1} associated with the stretching mode of Si-OH and the wide band between ~3800 and ~3000 cm^{-1} associated with O-H group stretching vibrations [5]. These bands are typical of the porous gel structure and indicate that the xerogel contains physically adsorbed water and Si-OH groups.

On the other hand, both xerogel and fused-silica show also similar characteristic bands. The ~1220 cm^{-1} band is associated with the LO mode of the Si-O-Si asymmetric bond stretching vibration, while ~1080 cm^{-1} band is associated with the TO mode of the Si-O-Si asymmetric bond stretching vibration. The band at ~800 cm^{-1} is assigned to a network Si-O-Si symmetric bond stretching vibration. The band at ~460 cm^{-1} is associated with a network Si-O-Si bond bending vibration [5, 6]. The coincidence confirms the presence in the structural units of xerogel similar to those of fused-silica.

Thus the author can conclude that the xerogel is composed of almost pure silica whose molecular structure is similar to the fused-silica.

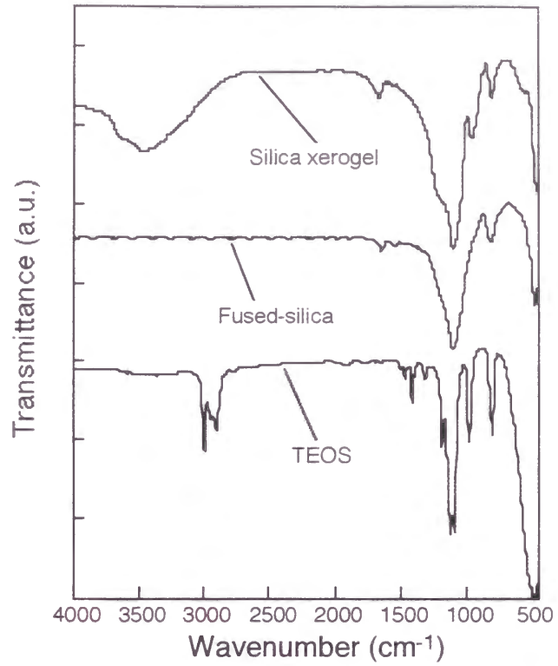

Fig. 1 IR spectra of xerogel, TEOS and fused-silica.

1.4.2 Pore size distribution

N_2 adsorption-desorption isotherm at 77 K of xerogel is shown in Fig. 2. So-called type I [7] or Langmuir type isotherm is obtained and the hysteresis loop was not observed. This type of isotherm is characteristic of microporous materials. The absence of the hysteresis indicates that mesopores and macropores are not present.

Figure 3 shows pore size distribution of xerogel determined with N_2 adsorption isotherm based on the MP-method [4]. The mean pore radius is only about 0.4 nm. The specific surface area based on a Langmuir plot is about 470 m^2/g. This mean pore radius is smaller than conventional ceramic materials, which are made with sol-gel method and were calcinated at a temperature higher than 573 K. Such a small pore was caused by lower water concentration in sol and lower heat treatment temperature. Under a low heat treatment temperature at 423 K, condensation rate of

intermediate hydroxides is kept low and thus particle growth is prevented. The low water content of H_2O/TEOS (molar ratio)=2, prefers the gel with weakly branched structure because of low hydrolysis rate. According to Brinker and Scherer [8], the molecules in the most weakly branched systems, prepared under the conditions where the condensation rate is low, tend to be overlapped each other at the gel point. Because the excluded volume effect is weak and the condensation rate remains low, the compliant structure can rather freely shrink with solvent removal. These conditions are therefore favorable for the preparation of membranes with fine pore texture. At the final stage of drying, the pores undergo a further compaction under the enormous capillary pressure. Consequently, a compact membrane that has micropores with diameter less than 1 nm can be obtained by this method.

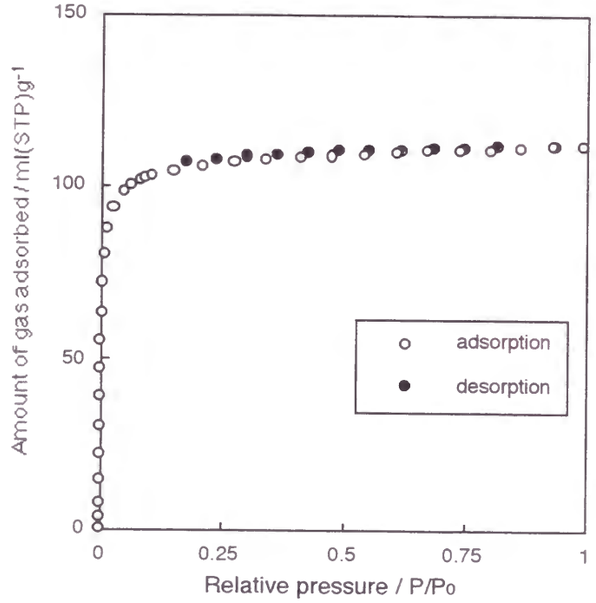

Fig. 2 N_2 adsorption-desorption isotherm at 77 K of xerogel.

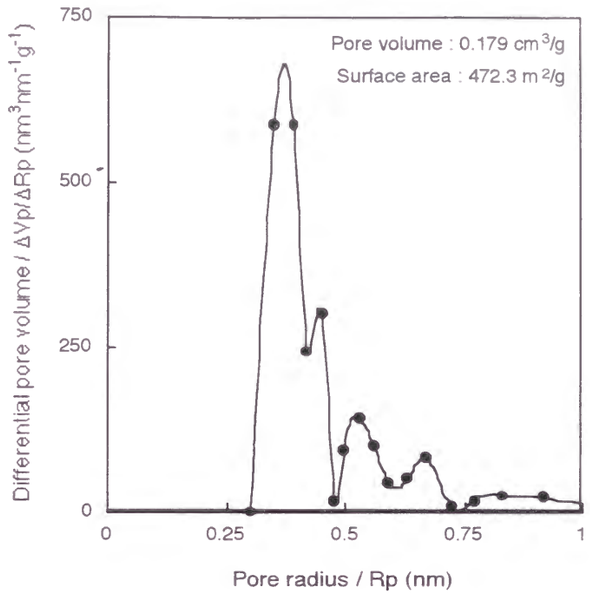

Fig. 3 Pore size distribution of xerogel.

Table 1 Permeation rates and the selectivity factors of CO_2 and He vs. N_2 through xerogel coated porous glass membrane.

	Permeation rate X10^{-6} (cm^3(STP)·cm^{-2}·s^{-1}·$cmHg^{-1}$)			Selectivity factor	
Temperature (K)	CO_2	He	N_2	P_{CO_2}/P_{N_2}[c]	P_{He}/P_{N_2}[d]
298 K[a]	14.2	5.97	0.294	48.3	20.3
373 K[a]	44.5	44.0	16.4	2.7	2.7
298 K[b]	59.3	54.3	30.5	1.9	1.8

[a]As prepared sample.
[b]Dry sample.
[c]Theoretical selectivity factor based on Knudsen flow is 0.8.
[d]Theoretical selectivity factor based on Knudsen flow is 2.6.

1.4.3 Permeation measurement

Table 1 shows single gas permeances of He, N_2 and CO_2 through the membrane at different temperatures for as prepared membrane and dry membrane which was cooled after the measurement at 373 K in draft of dry nitrogen. The table indicates the selectivity factor $\alpha=R_A/R_B$, where R_A and R_B are the permeances of gases A and B, respectively. Theoretical selectivity factors based on Knudsen flow are also indicated in the footnote of Table 1. At 298 K, the He/N_2 selectivity factor was 20.3, and He permeance of $5.97X10^{-6}$ ($cm^3(STP)\cdot cm^{-2}\cdot s^{-1}\cdot cmHg^{-1}$) was attained. At the same temperature, the CO_2/N_2 selectivity factor was 48.3, and permeance of CO_2 was $1.42X10^{-5}$($cm^3(STP)\cdot cm^{-2}\cdot s^{-1}\cdot cmHg^{-1}$). This selectivity factor is more than 60 times as large as the theoretical Knudsen value ($R_{CO_2}/R_{N_2}=0.8$). This value is comparable with the commercial organic membranes. At 373 K, the selectivity factor decreased to about 2. The dry membrane showed a low selectivity factor even at 298 K and high permeance of gases.

Figure 4 shows the effect on the CO_2/N_2 selectivity factors of the cyclic temperature change and exposure to the atmosphere. After a few days exposure to the atmosphere, the selectivity factor regains initial high value.

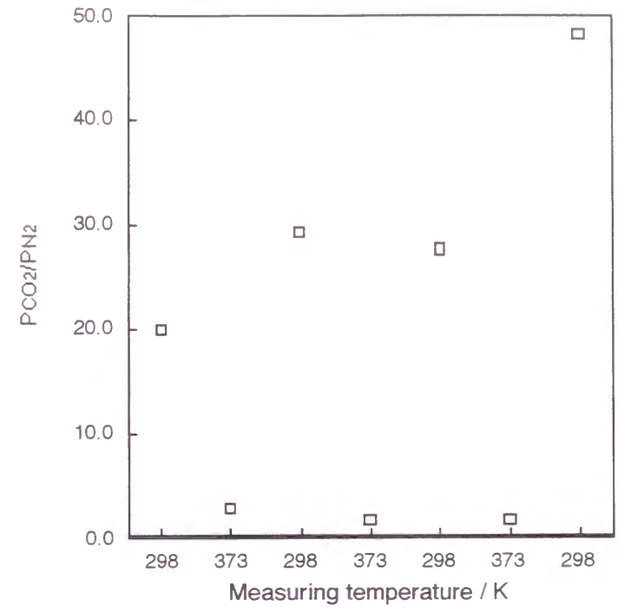

Fig. 4 Effect of temperature on the CO_2/N_2 selectivity factor. After the measurement at 298 K and at 373 K, the sample was exposed to the atmosphere each time.

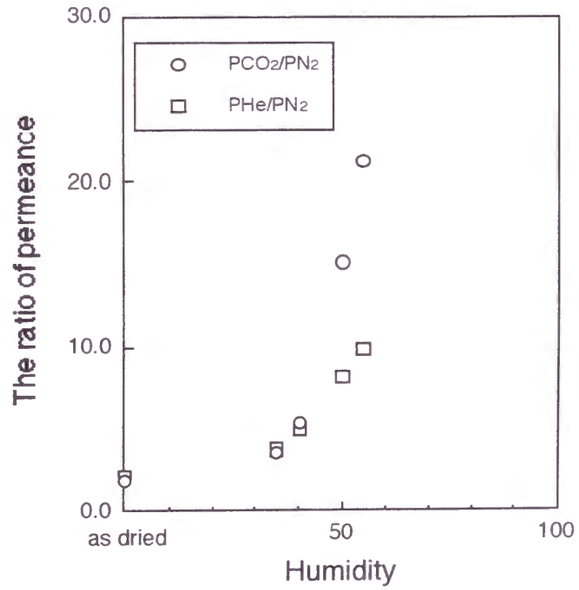

Fig. 5 The dependance of the ratio of permeation rates, He/N_2 and CO_2/N_2, on relative humidity.

The dependance of the ratio of permeation rates, He/N_2 and CO_2/N_2, on relative humidity is shown in Fig. 5. The ratio of permeances, CO_2/N_2, indicated high value as increasing relative humidity, but the ratio of permeances, He/N_2, was not so high and smaller than that of CO_2/N_2. Figure 6 shows H_2O adsorption-desorption isotherm at 303 K of xerogel. Amount of H_2O adsorbed was extremely much at low relative pressure. H_2O was easy to adsorbed on the xerogel. Comparing these facts with the result shown in Table 1, it is inferred that the separation of CO_2/N_2 is strongly related to the presence of adsorbed water. At 298 K and high relative humidities, pore surface is covered with water adsorbed from the atmosphere. CO_2 has a strong affinity to water and accordingly it can permeate through the micropores easily, though the adsorbed water prevents the permeation of N_2 by narrowing the pores (Fig. 7). Therefore, the CO_2/N_2 selectivity factor attains such a high value. At 373 K, however, adsorbed water is almost eliminated from xerogel layer, so the affinity of CO_2 to the pore becomes smaller and the effective pore size increases. So permeance of all gases becomes high and the high selectivity for CO_2 is lost.

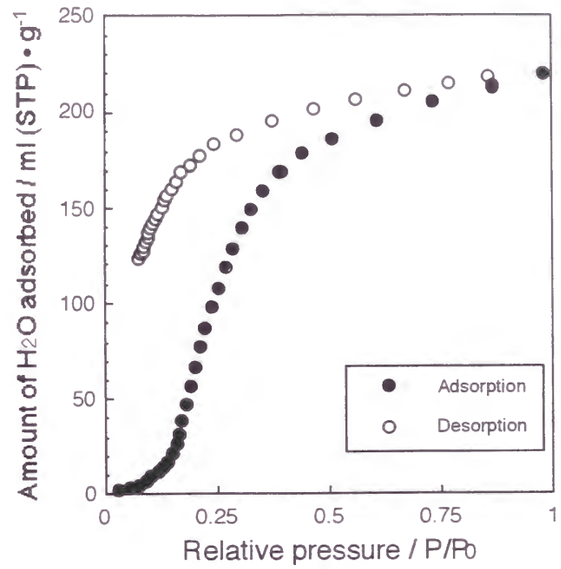

Fig. 6 H_2O adsorption-desorption isotherm at 303 K of xerogel.

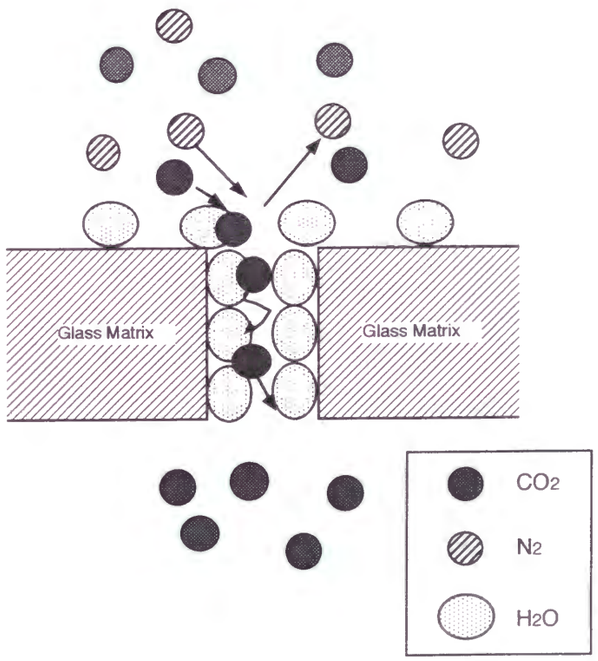

Fig. 7 Mechanism of gas permeation through the silica xerogel membrane.

1. 5 Conclusions

A microporous membrane of which pore diameter less than 1 nm was prepared by using sol-gel method with low water content and low heat treatment temperature, and gas separation property of this membrane was evaluated.

It was concluded that the membrane had fused-silica like structure by FT-IR study.

The He/N_2 selectivity factor and the CO_2/N_2 selectivity factor at 298 K indicated about 20 and about 50, respectively. These values are considerably higher than the theoretical Knudsen values. The author also investigated the effect of exposure to the atmosphere on the gas separation characteristics. The membrane indicated reversible behavior after the measurement at high temperature and exposure to the atmosphere. The ratio of the permeances, CO_2/N_2 strongly related to the relative humidities. That value increased as increasing the relative humidities. From these results, it is considered that these gas permeation characteristics were dependent on the adsorbed water on xerogel layer.

1. 6 References

1. A. Larbot, J.P. Fabre, C. Guizard and L. Cot, *J. Membrane Sci.*, **39**, 203 (1988).
2. M.W. Shafer, D.D. Awschalom and J. Warnock, *J. Appl. Phys.*, **61**, 5438 (1987).
3. T. Yazawa, H. Tanaka, H. Nakamichi and T. Yokoyama, *J. Membrane Sci.*, **60**, 307 (1991).
4. R.S. Mikhail, S. Brunauer and E.E. Bodor, *J. Colloid Interf. Sci.*, **26**, 45 (1968).
5. A. Bertoluzza, C. Fagnano, M.A. Morelli, V. Gottardi and M. Guglielmi, *J. Non-Cryst. Solids*, **48**, 117 (1982).
6. J. Wong and C.A. Angell, *Glass structure by spectroscopy* (MARCEL DEKKER, INC., New York, 1976).
7. S. Brunauer, L.S. Deming, W.E. Deming and E. Teller, *J. Am. Ceram. Soc.*, **62**, 1723 (1940).
8. C.J. Brinker and G.W. Scherer, *Sol-gel science: the physics and chemistry of sol-gel processing* (ACADEMIC PRESS, INC., San Diego, 1990).

Chapter 2: Preparation of inorganic-organic hybrid membrane and its oxygen separation property

2. 1 Abstract

Novel SiO_2-N,N'-disalicylideneethylenediaminatocobalt(II) (salcomine) hybrid membranes for oxygen separation were prepared by sol-gel method using poly(N-vinylpyrrolidone)(PVP) as mediation agents. From IR measurement and the papers reported previously, the structure of the membrane was assumed that inorganic segments (SiO_2) and organic ones (PVP, salcomine) were dispersed at a molecular level. This membranes indicated facilitated permeation of oxygen at high oxygen partial pressure and relatively high temperature. At 423 K, the O_2/N_2 selectivity factor was 6.1, and permeance of O_2 was 5.0 X 10^{-10} ($mol/m^{-2} \cdot s^{-1} \cdot Pa^{-1}$). This selectivity factor was more than 6 times as large as the theoretical Knudsen value (P_{O_2}/P_{N_2}=0.94).

2. 2 Introduction

Oxygen selective membranes were important for various fields such as medical field, oxygen-enriching combustion system, fuel cell system and have been attracted the attentions of many researchers. In organic polymer membrane, many researches have been made in the study of oxygen-enriching membranes. Most of the attention for such membranes has been focused on the synthesis of polymers in which the solubility of oxygen is greater than that of nitrogen. However, no permselective membrane has been successfully prepared by using this approach. On the other hand, in recent years, the method of oxygen carrier addition to improve the oxygen selectivity of an organic polymer gas separation membrane using at around room temperature has attracted tremendous attentions. These efforts have been developed in the forms of a facilitated transport using transition-metal complexes, such as cobalt porphyrin complexes [1] and cobalt Schiff base complexes[2]. The O_2/N_2 selectivity for the organic polymer membrane contained [α, α', α'', α'''-meso-tetrakis(o-pivalamidophenyl)porphinato]cobalt(II) was larger than 10 at room temperature [1]. However, the high O_2/N_2 selectivity only got at low pressure (below atmosphere pressure). All the above investigations (about organic polymer membranes) showed that the high O_2 selectivity could only be obtained at either low pressure or low operating temperature.

Recently, the synthesis of a large variety of inorganic-organic hybrids by sol-gel method has been reported. The advantage of sol-gel technique for the preparation of inorganic-organic hybrids is the fact that the reactions can be carried out at relatively low temperature, while the conventional melting fusion process for glasses requires high temperature. Thus, it enables the introduction of organic elements into inorganic matrices without deteriorating their functionalities. The most common method for the preparation of inorganic-organic hybrids is the utilization of hydrogen bonding interactions between polar functional groups of organic polymers and silanol groups of

silica gels. Organic polymers such as poly (2-methyl-2-oxazoline), poly (N-vinylpyrrolidone) have been incorporated homogeneously into silica gels by using such interactions at a molecular level [3, 4]. Without utilization of hydrogen bonding interaction, inorganic elements and organic ones are easily phase-separated and do not dispersed in a molecular level. Novel properties have been obtained by the incorporation of organic and inorganic elements at molecular level. Mechanical strength and thermal stability of organic polymers can be improved by the incorporation of inorganic elements. And brittleness of inorganic materials can also be improved by incorporation of organic elements.

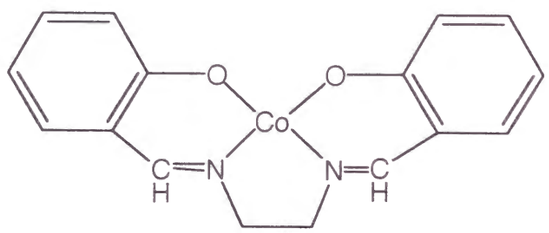

N,N'-disalicylideneethylenediaminatocobalt(II): salcomine, Co(salen)

Fig. 1 The structure of N,N'-disalicylideneethylenediaminatocobalt(II)

In this paper, preparation of SiO_2 and N,N'-disalicylideneethylenediaminatocobalt(II) (salcomine) hybrid membrane using poly (N-vinylpyrrolidone) (PVP) as mediation agents and its oxygen permeation property as oxygen selective membranes were reported. N,N'-Disalicylideneethylenediaminatocobalt(II) (salcomine) is one of the well-known oxygen carrier complexes (Fig. 1). It is interest to obtain membrane that can indicate high oxygen selectivity at high O_2 partial pressure and relatively high temperature that usual organic polymer

membranes didn't operate. As mentioned above, the integration of inorganic elements and organic elements at a molecular level may induce special properties that are different from original materials and can introduce organic functionalities into inorganic materials. However there are no interactions between salcomine and silica and it is difficult to integrate at a molecular level. To solve this problem, PVP was used as mediation agents. PVP has amide carbonyl groups in its structure. Utilization of hydrogen bonding interactions between amide carbonyl and silanol groups of silica and coordinate bonding interactions between nitrogen atoms of amide carbonyl groups and Co(II) of salcomines can disperse organic (PVP, salcomine) and inorganic elements (SiO_2) at a molecular level. Based on these concepts and to solve the problems of the reported organic polymer membranes for oxygen separation, the author prepared novel inorganic-organic hybrid membranes containing oxygen carrier complexes, SiO_2-PVP-salcomine hybrid membrane, by a sol-gel method.

2. 3 Experimental

2.3.1 Membrane preparation

Selective SiO_2-PVP-salcomine hybrid layer was prepared by sol-gel method. Sol composition was tetraethoxysilane(TEOS):C_2H_5OH:H_2O:HNO_3=1:20:2:0.01 in molar ratio, Poly-(N-vinylpyrrolidone) (PVP) was added in 11 wt% to TEOS and N,N'-disalicylideneethylenediaminatocobalt(II) (Salcomine) was added in 1 mol% to TEOS. Molecular weight of PVP was 630,000. Commercially available reagent grade chemicals were used. First, the mixture of H_2O, HNO_3, C_2H_5OH and TEOS was stirred for several hours at room temperature to obtain homogeneous sol. Continuously, PVP was added to the sol. After stirring for several hours, salcomine was added to the sol and it was stirred for several hours to obtain homogeneous sol. Porous alumina tubes (NGK Insulator, Ltd.) with mean pore diameter of 0.1 μm, outer diameter of 10 mm, inner diameter of 7 mm, and length of approximately 10 cm were used as the support. Support tubes with one end closed were dipped in the sol, withdrawn at a rate of 1 mm/s, and then they were dried at room temperature. The dip coating procedure was performed in a class 1000 clean room at 295 K and 50% relative humidity to avoid dusts which makes pinholes on membranes. After the dip-coating procedure had been repeated two times, the tubes were heated to 423 K at the rate of 0.5 K/min and maintained at that temperature for 2 hours, then cooled to room temperature at the same rate of heating. These coating and heating procedures were repeated twice and final specimens were obtained. The SiO_2-PVP hybrid membranes (without salcomine) were also prepared by the same procedure described above using the sol without addition of salcomine.

2.3.2 Infrared Spectroscopy

A part of each sol was dried at room temperature in a Teflon beaker until it gelated, then it was heat treated under the same conditions described above. Their fourier transform infrared

(FT-IR) spectra were measured for investigating the structures, using a FT-IR spectrometer (FTIR-8700, shimadzu).

2.3.3 Pore size measurement

Samples were prepared by the same procedure described above. The nitrogen adsorption was measured by BELSORP 28 (BEL JAPAN Inc.).

2.3.4 Measurement of gas permeation

Single gas permeation of the membrane was measured using He, N_2 and O_2 by the same procedure described previously [5] after drying at 373 K in a vacuum oven. One end of the tubular membrane was sealed and the other end was connected to a Pyrex glass tube with epoxy resin. This membrane was supported in a gas flow cell. The pressure difference of the gases through the membranes was kept constant at 1.01 X 10^5 Pa and the permeances at 298 K, 373 K and 423 K were measured by a mass flow meter.

2. 4 Results and discussion

2.4.1 Infrared spectroscopy

FT-IR spectra of SiO_2-PVP-salcomine, SiO_2-PVP and PVP are presented in Fig. 2. As seen, both hybrids show the band at ~960 cm^{-1} associated with the stretching mode of Si-OH [6]. This band is typical of the gel structure and indicates that the hybrids contain Si-OH groups. And these hybrids show similar characteristic bands. The ~1220 cm^{-1} band is associated with the LO mode of the Si-O-Si asymmetric bond stretching vibration, while ~1080 cm^{-1} band is associated with the TO mode of the Si-O-Si asymmetric bond stretching vibration. The band at ~800 cm^{-1} is assigned to a network Si-O-Si symmetric bond stretching vibration. The band at ~460 cm^{-1} is associated with a network Si-O-Si bond bending vibration [6, 7]. The coincidence confirms the presence of Si-O-Si networks in the hybrids.

On the other hand, both SiO_2-PVP and SiO_2-PVP-salcomine hybrids had other characteristic bands originated from PVP. Figure 3 shows high resolution FT-IR spectra of the hybrids and PVP (resolution of 0.5 cm^{-1}). The ~1650 cm^{-1} band is associated with the stretching band of amide carbonyl groups. These bands of the hybrids were shifted to the low wave-number region comparing with that of PVP. This fact supports the existence of the hydrogen bondings between amide carbonyl and silanol groups in the hybrids [3]. Thus, these hybrids were supposed that the inorganic segments (silica) and organic ones (PVP) were dispersed at a molecular level as same as the reported study previously [3, 4]. The spectra deference between SiO_2-PVP hybrid and SiO_2-PVP-salcomine hybrid was not observed because addition of salcomine was very small (only 1 mol% to TEOS). However, salcomine didn't homogeneously dissolve in the sol without PVP. Existence of PVP in the sol was important to dissolve salcomine into the sol homogeneously.

From this fact and the facts reported on organic membranes containing salcomines [2, 8], it was considered that salcomines were coordinated with nitrogen atoms in the PVP. Thus salcomines seemed to be dispersed with PVP at a molecular level. Therefore, it was assumed that SiO_2-PVP-salcomine hybrid also had inorganic-organic dispersed structure at a molecular level.

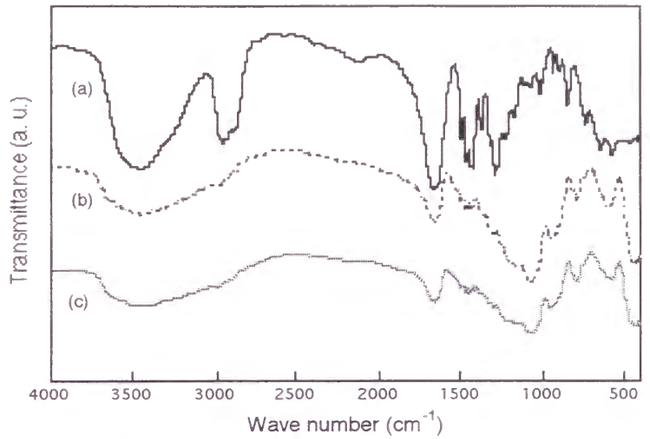

Fig. 2 IR spectra of (a) PVP, (b) SiO_2-PVP and (c) SiO_2-PVP-salcomine hybrids.

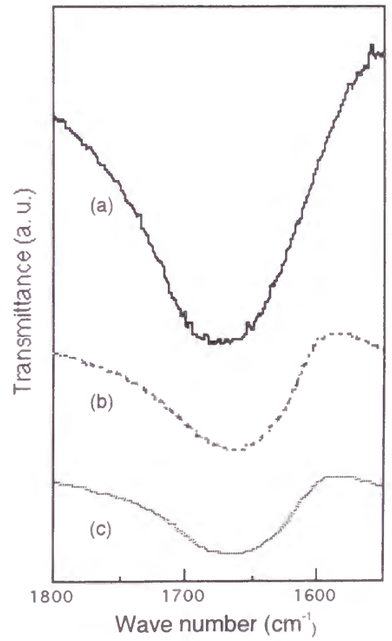

Fig. 3 High resolution IR spectra of (a) PVP, (b) SiO_2-PVP and (c) SiO_2-PVP-salcomine hybrids.

2.4.2 N_2 adsorption isotherm

N_2 adsorption-desorption isotherms at 77 K of SiO_2-PVP-salcomine, SiO_2-PVP hybrids and silica xerogel reported previously [9] are shown in Fig. 4. The deference between the silica xerogel and the hybrids was an existence of organic polymers. The isotherm of the silica xerogel was a so-called type I or Langmuir type isotherm. On the other hand, the isotherms of the hybrids were the so-called type II isotherm but the adsorption amounts were very small. Type I and type II isotherms follow the BDDT classification, which was originally proposed by Brunaer, Deming, Deming and Teller [10]. Type I isotherms are characteristic of microporous materials and type II isotherms are characteristic of non-porous materials [11]. As shown in Fig.4, the adsorption amounts of these hybrids were very small comparing to that of the silica xerogel. It has been reported by some researchers that the adsorption amounts of N_2 on ultramicroporous materials were also very small [12, 13]. Based on this result, it is considered that the pores of these hybrids are so small that N_2 cannot adsorb on the pores, and the adsorption amounts of the hybrids are small. This implies the structures of the hybrids were extremely dense.

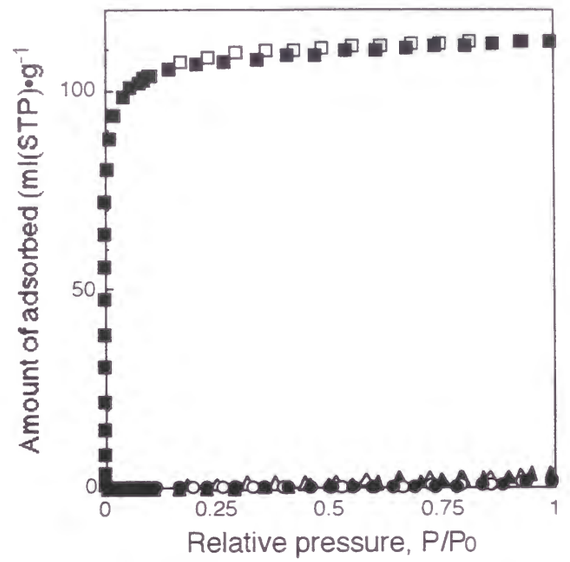

Fig. 4 N_2 adsorption-desorption isotherms of SiO_2-PVP-salcomine hybrid (○), SiO_2-PVP hybrid (△) and silica xerogel (□); solid symbols: adsorption, open symbols: desorption.

Table 1 Permeances and selectivity factors of He, N_2 and O_2 through SiO_2-PVP-salcomine hybrid membranes and SiO_2-PVP hybrid membrane at 298 K, 373 K and 423 K.

Sample	Temperature (K)	Permeance X 10^{10} (mol•m^{-2}•s^{-1}•Pa^{-1})			Selectivity factor	
		He	N_2	O_2	P_{O_2}/P_{N_2}[a]	P_{He}/P_{N_2}[b]
SiO_2-PVP-Salcomine membrane	298	21	0.84	1.2	1.4	25
	373	47	0.87	4.0	4.6	55
	423	74	0.84	5.0	6.1	86
SiO_2-PVP membrane	298	6.7	1.5	1.5	1.0	4.5
	373	15	1.1	1.2	1.0	13
	423	25	0.77	0.77	0.99	32

[a]Theoretical selectivity factor based on Knudsen flow is 0.94.

[b]Theoretical selectivity factor based on Knudsen flow is 2.6.

2.4.3 Permeation measurement

Table 1 shows single gas permeance of He, N_2 and O_2 through SiO_2-PVP-salcomine hybrid membrane and SiO_2-PVP hybrid membrane at 298 K, 373 K and 423 K. The table indicates the selectivity factor $\alpha=P_A/P_B$, where P_A and P_B are the permeances of gases A and B, respectively. Theoretical selectivity factors based on Knudsen flow are also indicated in the footnote of Table 1. SiO_2-PVP-Salcomine hybrid membrane indicated oxygen selectivity and helium selectivity even at high temperature. At 423 K, the He/N_2 selectivity factor was 86, and He permeance of 7.4 X 10^{-9} (mol•m^{-2}•s^{-1}•Pa^{-1}) was attained. At the same temperature, the O_2/N_2 selectivity factor was 6.1, and permeance of O_2 was 5.0 X 10^{-10} (mol•m^{-2}•s^{-1}•Pa^{-1}). This selectivity factor is more than 6 times as large as the theoretical Knudsen value (P_{O_2}/P_{N_2}=0.94). This value and measured temperature are quite impressive. Because usual organic membranes cannot withstand this high temperature. However, thermal stability of inorganic-organic hybrids was increased than that of only organic polymers, and it was reported that silica-PVP hybrids were stable at about 423 K [4]. Our hybrids are the almost same hybrid and it is supported that the permeances through the membranes didn't change after measuring at 423 K.

On the other hand, SiO_2-PVP hybrid membrane didn't have oxygen selectivity. At 423 K, the He/N_2 selectivity factor was 32, and He permeance of 2.5 X10^{-9} (mol•m^{-2}•s^{-1}•Pa^{-1}) was attained. At the same temperature, the O_2/N_2 selectivity factor was 0.99, and permeance of O_2 was 7.7 X 10^{-11} (mol•m^{-2}•s^{-1}•Pa^{-1}). Comparing these values with the results of SiO_2-PVP-salcomine hybrid membrane, it is supposed that the separation of O_2/N_2 is strongly related to the presence of salcomine. From IR and gas permeation measurements, it was suggested that the structure of the membrane is schematically shown in Fig. 5 (a). Silica and PVP were dispersed at a molecular level

due to the strong hydrogen bonding as described above between amide carbonyl and silanol groups. PVP and salcomines were also dispersed at a molecular level because nitrogen atoms of amide carbonyl groups were coordinated with Co(II) of salcomines as reported previously [2, 8]. Thus, salcomines were also dispersed in SiO_2-PVP hybrid at the molecular level. Co(II) in salcomine has six-coordination sites [14]. Planar four coordination sites were already coordinated by Shiff base as shown in Fig. 1 and, in general, oxygens can coordinate in residual two sites. However, in this case, one of the residual coordination site was coordinated with nitrogen atom in amide carbonyl groups and oxygen can coordinate at only one site (Fig. 5(b)). Oxygen was attracted to one of Co(II) of the coordinated salcomines, and it moved next Co(II) of the coordinated salcomines. By this way, oxygen permeation occurs. Although the O_2/N_2 selectivity through SiO_2-PVP-salcomine hybrid membrane at 298 K was not so high (P_{O_2}/P_{N_2}=1.4), the selectivity became higher with increasing temperature . It is considered that this is due to strength of Co(II)-oxygen complex bonds. In high partial pressure of oxygen, Co(II)-oxygen complex bonds are strong and salcomine releases oxygen at higher than 373 K. Thus oxygen is strongly trapped by salcomine at low temperature and mobility of oxygen is small. However, at higher than 373 K, oxygen mobility becomes higher and oxygen still has a strong affinity to salcomine, accordingly it can permeate through the membrane preferentially.

(a)

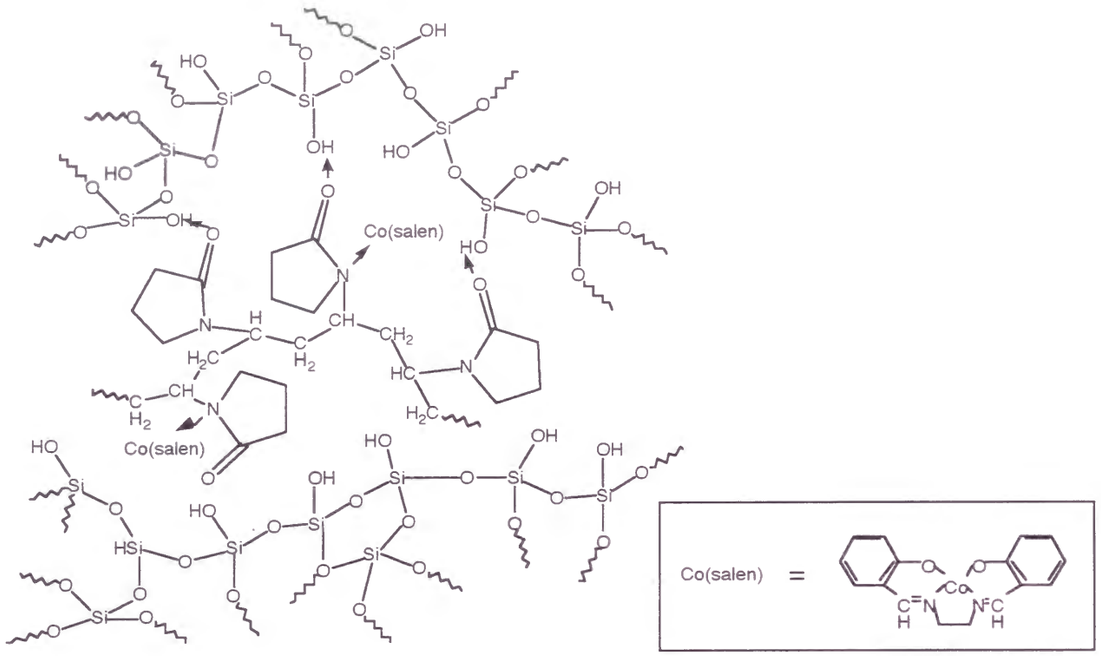

(b)

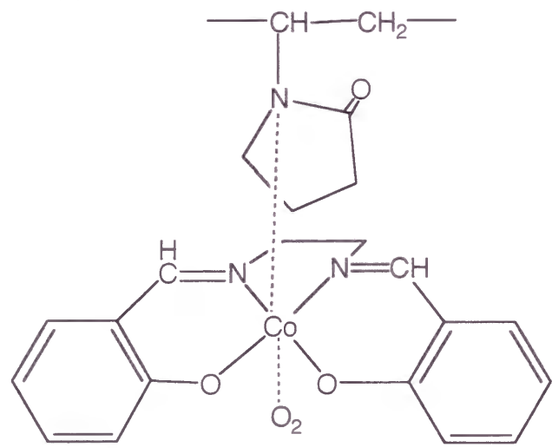

Fig. 5 Schematic representation of (a) the structure of SiO_2-PVP-salcomine hybrid and (b) coordination of oxygen.

2.5 Conclusions

SiO_2-N,N'-disalicylideneethylenediaminatocobalt(II) (salcomine) hybrid membranes for oxygen separation were prepared by sol-gel method using poly(N-vinylpyrrolidone)(PVP) as a mediation agent. From IR measurement and the papers reported previously, the structure of the membrane was assumed that inorganic segments (SiO_2) and organic ones (PVP, salcomine) were dispersed at a molecular level. This membranes indicated facilitated permeation of oxygen at high oxygen partial pressure and relatively high temperature. At 423 K, the O_2/N_2 selectivity factor was 6.1, and permeance of O_2 was 5.0 X 10^{-10} (mol/m$^{-2}\cdot$s$^{-1}\cdot$Pa^{-1}). This selectivity factor was more than 6 times as large as the theoretical Knudsen value (P_{O_2}/P_{N_2}=0.94).

2. 6 References

1. H. Nishide, M. Ohyanagi, O. Okada and E. Tsuchida, *Macromolecules*, **20**, 417 (1987).
2. E. Tsuchida, H. Nishide, M. Ohyanagi and H. Kawakami, *Macromolecules*, **20**, 1907 (1987).
3. Y. Chujo and T. Saegusa, *Adv. Polym. Sci.*, **100**, 11 (1992).
4. R. Tamaki, Y. Chujo, K. Kuraoka and T. Yazawa, *J. Mater. Chem.*, **9**, 1741 (1999).
5. T. Yazawa and H. Tanaka, *Ceram. Trans.*, **31**, 213 (1993).
6. A. Bertoluzza, C. Fagnano, M.A. Morelli, V. Gottardi and M. Guglielmi, *J. Non-Cryst. Solids*, **48**, 117 (1982).
7. J. Wong and C.A. Angell, *Glass structure by spectroscopy* (MARCEL DEKKER, INC., New York, 1976).
8. H. Nishide, M. Kuwahara, M. Ohyanagi, Y. Funada, H. Kawakami and E. Tsuchida, *Chem. Lett.*, 43 (1986).
9. K. Kuraoka, H. Tanaka and T. Yazawa, *J. Mater. Sci. Lett.*, **15**, 1 (1996).
10. S. Brunauer, L.S. Deming, W.E. Deming and E. Teller, *J. Am. Ceram. Soc.*, **62**, 1723(1940).
11. S.J. Gregg and K.S.W. Sing, *Adsorption, surface area and porosity* (ACADEMIC PRESS INC. (LONDON) LTD, London, 1982).
12. C.J. Brinker, T.L. Ward, R. Sehgal, N.K. Raman, S.L. Hietala, D.M. Smith, D. Hua and T.J. Headley, *J. Membrane Sci.*, **77**, 165 (1993).
13. M.H. Hassan, J.D. Way, P.M. Thoen and A.C. Dillon, *J. Membrane Sci.*, **104**, 27 (1995).
14. E. Tsuchida, *J. Macromol. Sci.-Chem.*, **A13**, 545 (1979).

Part I-2 Elution method

Chapter 3: Preparation of glass capillary membrane and its gas permeation property

3. 1 Abstract

The gas separation characteristics of ultra-microporous glass capillary membranes were investigated. Glass capillary membranes which had ultra-micropore (pore diameter less than 1 nm) were prepared by elution of alkali metal ions from glass capillaries. From elution treatment, it was found that alkali metal ions of 3.5 Na (Composition: 77.8 SiO_2, 22.2 Na_2O mol%) and 3.5 K (Composition: 77.8 SiO_2, 22.2 K_2O mol%) glass capillaries were completely eluted after 90 and 10 min with 3 mol/l HNO_3, 240 and 10 min with 3 mol/l CH_3COOH and 3 mol/l H_3PO_4, respectively. Permeations of N_2, He and CO_2 were measured at 298 K, 373 K and 473 K. Permeation rates of the 3.5 Na and 3.5 K glass capillary membranes were 1 - 10^{-1} ($cm^3(STP)\cdot cm^{-2}\cdot s^{-1}\cdot cmHg^{-1}$). The ratios of permeation rates, CO_2/N_2 and He/N_2, were similar to the theoretical Knudsen value.

3. 2 Introduction

Recently, due to their stability in organic solvent and at high temperature, inorganic membranes attracted many investigators and many researches have been done. In particular, glass membranes are expected as a promising membrane due to its facility of shaping and it can be shaped into glass capillaries. To shape into glass capillary has following advantages. The first advantage is to obtain large membrane area and small module size. The second one is to be able to be endowed with flexibility. The third one is to provide high shaping rate. That is directed toward the mass production of glass capillary membranes without difficulty.

Y. H. Ma et al. [1] and J. D. Way et al. [2] have reported microporous glass hollow fiber membranes which had high selectivities of gases. It was proposed that transport mechanism of these membranes was mainly surface flow and molecular sieving. However, it was not necessarily clear the composition of glass and formation process of ultra-micro pore.

It is well-known that alkali metal ions in glass are easy to diffuse compared with other metal ions (for example, Al^{3+} and B^{3+}) [3] and they are easily eluted by water and acid solution. It can be considered that pores which are made by elution of alkali metal ions are ultra-micro pore.

In this chapter, glass capillary membranes which had ultra-micro pore (pore diameter less than 1 nm) were prepared by elution of alkali metal ions. The author tries to explain formation of micropore in terms of elution of alkali metal ions from glass capillaries. Its gas separation characteristics are also reported.

3. 3 Experimental

3. 3. 1 Preparation of glass capillary membrane

Glass capillary membranes which had an outer diameter 0.30 mm and an inner diameter 0.24 mm were made from glass capillaries. The glass capillaries were prepared from following procedure. First, glass tubes which had an outer diameter 5 mm and inner diameter 4 mm were made of glass melts. Second, the glass tubes were shaped into the glass capillaries by redrawing. Glass capillaries compositions of the 3.5 Na and 3.5 K are $3.5SiO_2 \bullet Na_2O$ and $3.5SiO_2 \bullet K_2O$, respectively. Glass capillaries were cut in approximately 100 mm length. Then they were immersed in the solution of 3 mol/l HNO_3, 3 mol/l CH_3COOH and 3 mol/l H_3PO_4 at 371 K for a certain time until alkali metal ions were completely eluted. After that, they were washed with diluted water and dried at room temperature.

In order to determine time when alkali metal ions were completely eluted, a portion of acid solutions in which glass capillaries were immersed was taken out at a certain minutes intervals and measured Na^+ or K^+ concentrations with atomic absorption /flame emission spectrophotometer (Shimadzu AA-180, Shimadzu). Inductively coupled plasma spectrometry (ICP spectrometry: SPS-1200, Seiko) was used to detect elution of Si ion at the point that alkali ions were completely eluted.

3. 3. 2 Pore size measurement

Samples were prepared by the described above. The specific surface areas and the pore size distribution of samples were measured by the nitrogen adsorption (BELSORP 28, BEL JAPAN Inc.). The specific surface areas were determined by BET plots [4] and the pore size distributions was analyzed by MP methods [5].

3. 3. 3 Measurement of gas permeation

Single gas permeations of the membranes were measured using He, N_2, and CO_2 by the same procedure described previously [6]. One side of the capillary membranes was sealed and another side of that was connected to a Pyrex glass tube with epoxy resin. This membrane was supported in a gas flow cell. Pressure difference of the gases through the membranes was kept at 1 atm (1 atm = $1.013X10^5$ Pa) and the permeation rates at 298 K, 373 K and 473 K were measured by mass flow meter.

3. 4 Results and discussion

3. 4. 1 Elution rates of alkali metal ions

In an alkali-silicate glass, alkali metal ions occupied SiO_2 networks as shown in Fig. 1 [7]. Ionic crystal radii of Na^+ and K^+ are 0.102 and 0.155 nm, respectively [8]. In an acidic solution, H^+ ions diffused into glass and replaced the alkali metal ions, the alkali ions also easily moved in glass, therefore they were eluted in a solution and made pores in which diameter was about diameter of alkali metal ions.

Elution rates of alkali metal ions from the 3.5 Na glass capillaries are shown in Fig. 2 and those of the 3.5 K glass capillaries are shown in Fig. 3. Alkali metal ions of the 3.5 Na and 3.5 K glass capillaries were completely eluted after 90 and 10 min with 3 mol/l HNO_3, 240 and 10 min with 3 mol/l CH_3COOH and 3 mol/l H_3PO_4, respectively. Elution rates of the 3.5 K glass capillaries were much faster than those of the 3.5 Na capillaries. Many studies on elution of alkali metal ions from alkali silicate glasses in water were reported [9-11]. These papers also observed that the elution of K^+ from potassium silicate glasses was much faster than those of Na^+ from sodium silicate glasses. There are two important process for alkali diffusion in the glass: 1) ionic bonds between the alkali cations and anionic non-bridging oxygens ($Si\text{-}O^-$) must be broken, and 2) the alkali cations must have unobstructed pathways to migrate between sites in the glass [12]. In potassium silicate glasses, ionic bonds of K^+ between $Si\text{-}O^-$ are weaker than those of Na^+ between $Si\text{-}O^-$ in sodium silicate glasses. One of the reasons is ionic field strength of K^+ smaller than that of Na^+. Therefore, it is considered that the process 1) occurs easily. Potassium silicate glasses have larger void volume than sodium silicate glasses because ionic radius of K^+ is larger than that of Na^+ and molar volume of potassium silicate glasses are larger than sodium silicate glasses in same

molar ratio of alkali oxide/silica. This means the process 2) easily takes place. In addition, hydration of the glass during elution treatment can change both bonding interaction and void volume in the glass, exerting a significant influence on alkali diffusion in glass [12]. Consequently, above two important processes for alkali diffusion in glass are satisfied, so it is considered that the elution of alkali ions from potassium silicate glasses was much faster than that from sodium silicate glasses. Bansal also reported the similar difference of alkali elution in alkali silicates and he concluded that the most likely reason for this result is that the hydronium ions has a higher mobility in potassium silicate than sodium silicate glasses because potassium and hydronium ions have about the same effective radius (0.13 nm) [13]. Although our case is in acid solutions, it is considered that elution behavior is similar without silica dissolution. Silica easily dissolve in solution of pH>9, but it dissolves little in solution pH < 9. For the 3.5 Na and 3.5 K glass capillaries, amounts of elution of Si determined by ICP spectrometry were less than 1.8% at the point that alkali ions completely eluted. The effects of various acids on amount of elution of these glass capillaries are not clear in this study, further experiments to elucidate these effects will be planned.

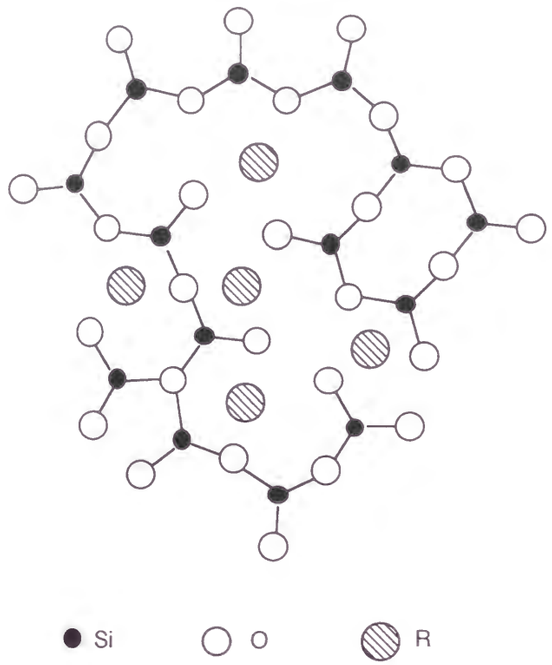

Fig. 1 Schematic representation of the structure of alkali-silicate glass.

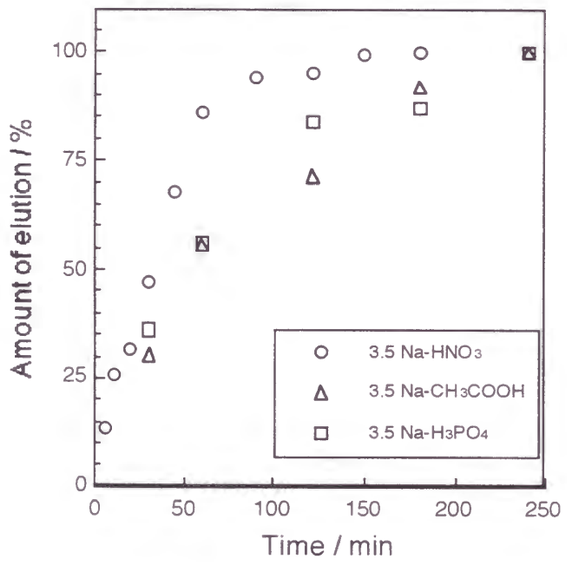

Fig. 2 Elution rate of Na^+ from the 3.5 Na glass capillaries eluted with 3 mol/l HNO_3 (3.5 Na-HNO_3), 3 mol/l CH_3COOH (3.5 Na-CH_3COOH) and 3 mol/l H_3PO_4 (3.5 Na-H_3PO_4).

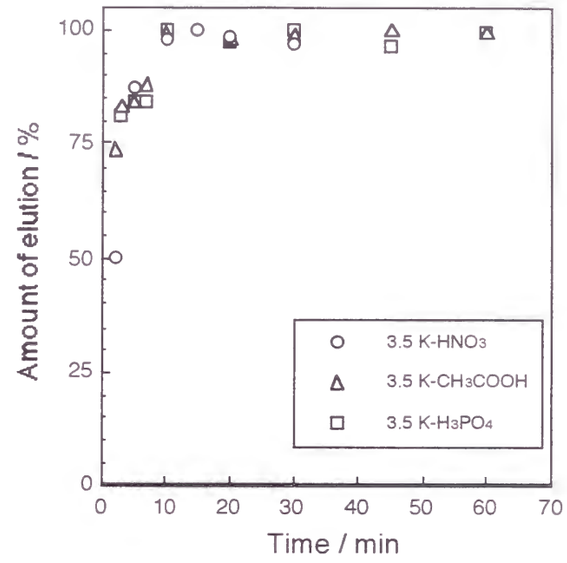

Fig. 3 Elution rate of K^+ from the 3.5 K glass capillaries eluted with 3 mol/l HNO_3 (3.5 K-HNO_3), 3 mol/l CH_3COOH (3.5 K-CH_3COOH) and 3 mol/l H_3PO_4 (3.5 K-H_3PO_4).

3. 4. 2 Pore size distribution

Typical N_2 adsorption-desorption isotherms of the 3.5 Na and the 3.5 K glass capillary membranes eluted with 3 mol/l HNO_3 are shown in Fig. 4, because isotherms of other membranes were similar to those of them, respectively. All of the isotherms of the 3.5 Na were a so-called type IV isotherm but the adsorption amounts were very small and those of 3.5 K were near type I isotherm but hysteresis loops were observed. These hysteresis loops mean the existence of mesopores. These mesopores were probably caused by dissolution and deposition of silica in leached layer during elution treatment. Type I and Type IV isotherms are following the BDDT classification, which is shown in Fig. 5, originally proposed by Brunaer, Deming, Deming and Teller [14,15]. Type I isotherms are often found with a solid which contains micropores and are

characterized by a large amount of adsorbed at low relative pressure and a plateau being nearly or quite horizontal. Type IV isotherms are characteristics of a mesoporous solid and are characterized by a hysteresis loop. Specific surface areas based on BET plot of the 3.5 Na and the 3.5 K glass capillary membranes with various elution treatment are presented in Table 1. The 3.5 Na glass capillary membrane eluted with 3 mol/l CH_3COOH had a larger value than other 3.5 Na samples. But it is not clear the reason why it had a large value. Specific surface areas of the 3.5 K glass capillary membranes eluted with 3 mol/l CH_3COOH and 3 mol/l H_3PO_4 were slightly larger than that of the 3.5 K glass capillary membrane eluted with 3 mol/l HNO_3. It is assumed that those values became slightly large due to dissolution and deposition of silica in leached layer during elution treatments, because those samples needed longer time to completely elute alkali ions. The adsorption amounts of the 3.5 Na glass capillary membranes were smaller than those of the 3.5 K and the specific surface areas of the 3.5 Na were also much smaller those of the 3.5K. It was reported by some researchers [16,17] that the adsorption amounts of N_2 on ultra-microporous materials were also very small. From these results, it is considered that the pores formed by elution of Na^+ were so small that N_2 didn't adsorb on the pores. Thus these values of the 3.5 Na glass capillary membranes were small.

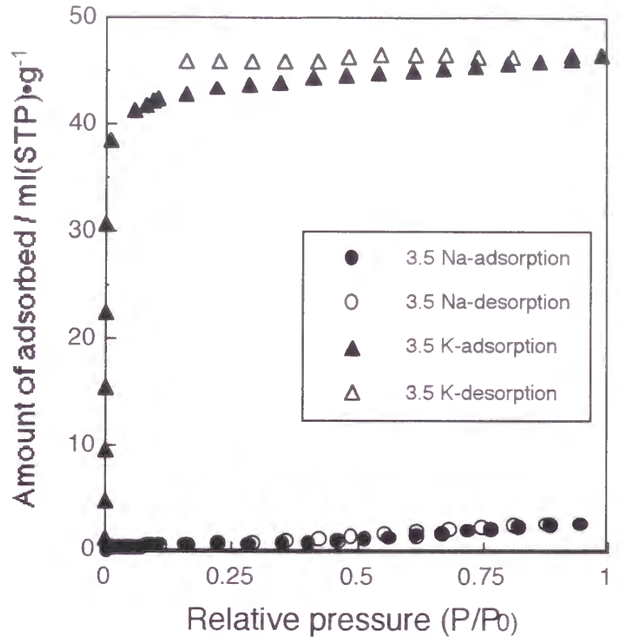

Fig. 4 N_2 adsorption-desorption isotherms at 77 K of the 3.5 Na and 3.5 K glass capillary membranes eluted with 3 mol/l HNO_3.

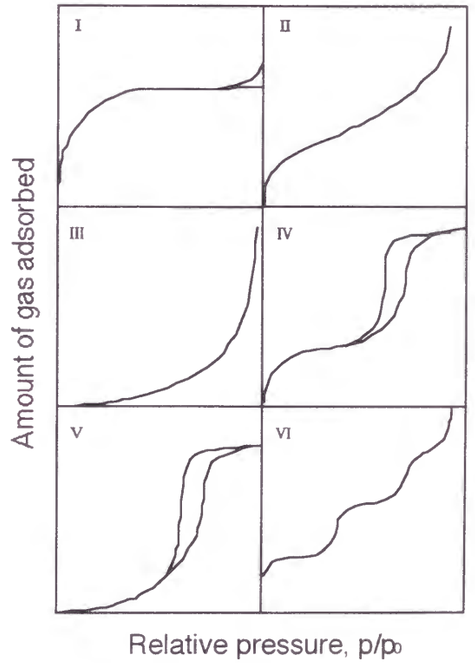

Fig. 5 The five types of adsorption-desorption isothems, I to V, in the BDDT classification, together with Type VI, the stepped isotherm [15].

Table 1 Specific surface areas of the 3.5 Na and 3.5 K glass capillary membranes eluted with 3mol/l HNO_3 (3.5 Na-HNO_3 and 3.5 K-HNO_3), CH_3COOH (3.5 Na-CH_3COOH and 3.5 K-CH_3COOH) and H_3PO_4 (3.5 Na-H_3PO_4 and 3.5 K-H_3PO_4).

Samples	Specific surface area($m^2 \cdot g^{-1}$)
3.5 Na-HNO_3	2.3
3.5 Na-CH_3COOH	15.3
3.5 Na-H_3PO_4	4.0
3.5 K-HNO_3	133.3
3.5 K-CH_3COOH	187.8
3.5 K-H_3PO_4	179.7

Figure 6 shows pore size distribution of the 3.5 K glass capillary membrane eluted with 3 mol/l HNO_3. The mean pore radius was about 0.4 nm. This pore radius was agreement with order of ionic crystal radius of K^+ as shown above. Accordingly, it seems that these pores were mainly made due to elution of alkali metal ions because ionic crystal radii of other easily eluted ions are smaller than that of alkali metal ion. Other samples of the 3.5 K glass capillary membranes showed almost same pore size distributions and they also had same mean pore radius (about 0.4 nm) that is ultra-micro pores (pore diameter less than 1 nm).

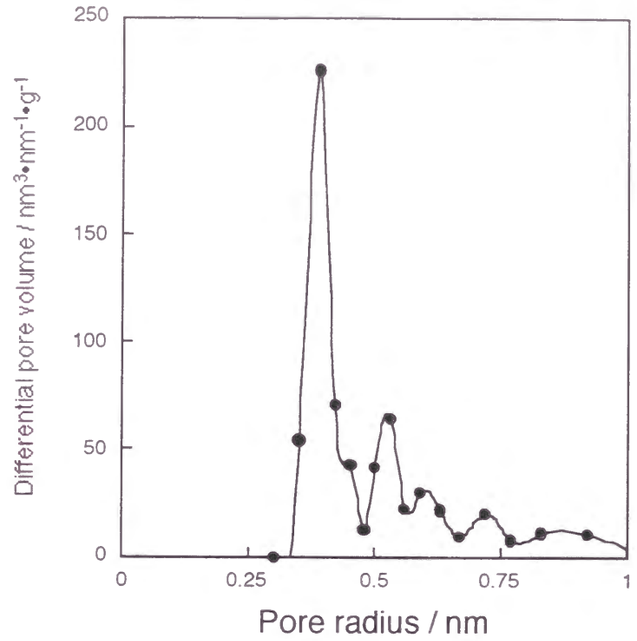

Fig. 6 Pore size distribution of the 3.5 K glass capillary membrane eluted with 3mol/l HNO_3.

3. 4. 3 Gas permeation characteristics

Table 2 and Table 3 show ratios of permeation rates of the 3.5 Na and the 3.5 K glass capillary membranes with various elution treatments, respectively. Theoretical ratios of permeation rates based on Knudsen flow are also indicated in the footnote of these tables. The ratios of permeation rates, CO_2/N_2 and He/N_2, were similar to the theoretical Knudsen value. Permeation rates of the 3.5 Na and 3.5 K glass capillary membranes are presented in Table 4 and 5. Those of the samples indicated similar values (1 - 10^{-1} $cm^3(STP) \cdot cm^{-2} \cdot s^{-1} \cdot cmHg^{-1}$) and significant deferences were not observed. From the results, it is assumed that pores made by elution with various acids didn't have obvious differences on sizes. Thus the kinds of acids affected elution times, but little affected pore sizes after elution. A typical scanning electron microprobe (SEM) photograph of the glass capillary membrane is presented in Fig. 7.

Table 2 The ratio of permeation rate, CO_2/N_2 and He/N_2, through the 3.5 Na glass capillary membranes eluted with 3 mol/l HNO_3 (3.5 Na-HNO_3), 3 mol/l CH_3COOH (3.5 Na-CH_3COOH) and 3 mol/l H_3PO_4 (3.5 Na-H_3PO_4).

	3.5 Na-HNO_3		3.5 Na-CH_3COOH		3.5 Na-H_3PO_4	
Temperature	P_{He}/P_{N_2}[a]	P_{CO_2}/P_{N_2}[b]	P_{He}/P_{N_2}	P_{CO_2}/P_{N_2}	P_{He}/P_{N_2}	P_{CO_2}/P_{N_2}
298 K	2.2	0.8	2.2	0.8	2.2	0.8
373 K	2.1	0.8	2.2	0.8	2.2	0.8
473 K	2.0	0.8	2.1	0.8	2.2	0.8

[a]Theoretical separation factor based on Knudsen flow is 2.6.

[b]Theoretical separation factor based on Knudsen flow is 0.8.

Table 3 The ratio of permeation rate, CO_2/N_2 and He/N_2, through the 3.5 K glass capillary membranes eluted with 3 mol/l HNO_3 (3.5 K-HNO_3), 3 mol/l CH_3COOH (3.5 K-CH_3COOH) and 3 mol/l H_3PO_4 (3.5 K-H_3PO_4).

	3.5 K-HNO_3		3.5 K-CH_3COOH		3.5 K-H_3PO_4	
Temperature	P_{He}/P_{N_2}[a]	P_{CO_2}/P_{N_2}[b]	P_{He}/P_{N_2}	P_{CO_2}/P_{N_2}	P_{He}/P_{N_2}	P_{CO_2}/P_{N_2}
298 K	2.1	0.8	2.1	0.8	2.2	0.8
373 K	2.1	0.8	2.1	0.8	2.2	0.8
473 K	2.1	0.8	2.1	0.8	2.2	0.8

[a]Theoretical separation factor based on Knudsen flow is 2.6.

[b]Theoretical separation factor based on Knudsen flow is 0.8.

Table 4 Permeation rates of the 3.5 Na glass capillary membranes eluted with 3mol/l HNO_3 (3.5 Na-HNO_3), CH_3COOH (3.5 Na-CH_3COOH) and H_3PO_4 (3.5 Na-H_3PO_4).

	3.5 Na-HNO_3			3.5 Na-CH_3COOH			3.5 Na-H_3PO_4		
Temperature	P_{N_2}	P_{He}	P_{CO_2}	P_{N_2}	P_{He}	P_{CO_2}	P_{N_2}	P_{He}	P_{CO_2}
298 K	1.6	3.4	1.3	2.0	4.2	1.6	1.8	3.9	1.4
373 K	1.6	3.2	1.2	1.7	3.7	1.4	1.6	3.5	1.3
473 K	1.3	2.7	1.1	1.6	3.2	1.2	1.4	3.1	1.2

P_{N_2}, P_{He}, P_{CO_2}: Permeation rate X 10 ($cm^3(STP)\cdot cm^{-2}\cdot s^{-1}\cdot cmHg^{-1}$)

Table 5 Permeation rates of the 3.5 K glass capillary membranes eluted with 3mol/l HNO_3 (3.5 K-HNO_3), CH_3COOH (3.5 K-CH_3COOH) and H_3PO_4 (3.5 K-H_3PO_4).

	3.5 K-HNO_3			3.5 K-CH_3COOH			3.5 K-H_3PO_4		
Temperature	P_{N_2}	P_{He}	P_{CO_2}	P_{N_2}	P_{He}	P_{CO_2}	P_{N_2}	P_{He}	P_{CO_2}
298 K	3.2	6.9	2.5	2.6	5.6	2.1	2.7	6.0	2.2
373 K	2.9	6.1	2.3	2.3	4.9	1.8	2.4	5.2	1.9
473 K	2.7	5.4	2.1	2.0	4.2	1.6	2.1	4.7	1.7

P_{N_2}, P_{He}, P_{CO_2}: Permeation rate X 10 ($cm^3(STP)\cdot cm^{-2}\cdot s^{-1}\cdot cmHg^{-1}$)

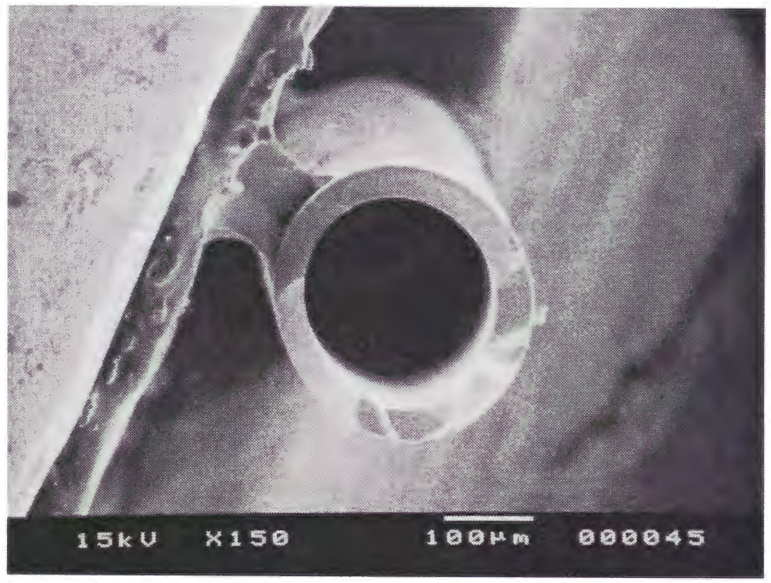

Fig. 7 SEM photograph of the glass capillary membrane

The membrane surface was smooth and no macro-cracks were observed after elution treatment and the following drying. Pore diameters calculated from N_2 adsorption measurement of the membranes were less than 1 nm. From these pore diameters, the membranes can be expected to indicate much higher selectivities (the ratios of permeation rates) and lower permeation rates than that observed above as in the papers reported by Y. H. Ma et al. [1] and J. D. Way et al [2]. It seems that the ratios of permeation rates indicated smaller values and the permeation rates had higher values because those membranes probably had some micro-cracks that couldn't be observed with SEM and N_2 adsorption measurement. When the alkali metal ions were eluted, glasses were stressed. Then those of membranes probably had some micro-cracks.

3. 5 Conclusions

Ultra-microporous glass capillary membranes having pore diameters less than 1 nm were prepared by elution of alkali metal ions from glass capillaries, and gas separation properties of these membranes were measured. It was concluded that the membranes had ultra-micropores less than 1 nm by measuring N_2 adsorption. The ratios of the permeation rates of the 3.5 Na and 3.5 K glass capillary membranes were not high values because of having some micro-cracks made from elution treatment and the following drying. Further experiments are needed to clear the transport mechanism in the ultra-microporous glass capillary membranes.

3. 6 References

1. A.B. Shelekhim, A.G. Dixon and Y.H. Ma, *J. Membrane Sci.*, **75**, 233 (1992).
2. J.D. Way and D.L. Roberts, *Sep. Sci. Tech.*, **27**, 29 (1992).
3. R. Terai and R. Hayami, *J. Non-Cryst. Solids*, **18**, 217 (1975).
4. S. Brunauer, P.H. Emmett and E. Teller, *J. Am. Chem. Soc.*, **60**, 309 (1938).
5. R.S. Mikhail, S. Brunauer and E.E. Bodor, *J. Colloid Interf. Sci.*, **26**, 45 (1968).
6. T. Yazawa and H. Tanaka, *Ceram. Trans.*, **31**, 213 (1993).
7. W.D. Kingery, H.K. Bowen and D.R. Uhlmann, in *Introduction to Ceramics* 98 (John Wiley & Sons, Inc., New York, 1960).
8. R.D. Shannon and C.T. Prewitt, *Acta Cryst.*, **B25**, 925 (1969).
9. M.A. Rana and R.W. Douglas, *Phys. Chem. Glasses*, **2**, 179 (1961).
10. M.A. Rana and R.W. Douglas, *Phys. Chem. Glasses*, **2**, 196 (1961).
11. C.R. Das and R.W. Douglas, *Phys. Chem. Glasses*, **8**, 178 (1967).
12. B.C. Bunker, G.W. Arnold, E.K. Beauchamp and D.E. Day, *J. Non-Cryst. Solids*, **58**, 295 (1983).
13. N.P. Bansal and R.H. Doremus, 646 (Academic Press, Inc., Florida, 1986).
14. S. Brunauer, L.S. Deming, W.E. Deming and E. Teller, *J. Am. Ceram. Soc.*, **62**, 1723 (1940).
15. S.J. Gregg and K.S.W. Sing, *Adsorption, surface area and porosity* (ACADEMIC PRESS INC. (LONDON) LTD, London, 1982).
16. C.J. Brinker, T.L. Ward, R. Sehgal, N.K. Raman, S.L. Hietala, D.M. Smith, D. Hua and T.J. Headley, *J. Membrane Sci.*, **77**, 165 (1993).
17. M.H. Hassan, J.D. Way, P.M. Thoen and A.C. Dillon, *J. Membrane Sci.*, **104**, 27 (1995).

Chapter 4: Preparation of glass hollow fiber membrane and its hydrogen separation property

4. 1 Abstract

Glass hollow fiber membranes with ultra-micropores (pore diameter less than 1 nm) were prepared by acid leaching. The effects of various acids and leaching times on the preparation of the membranes were investigated. It was found from acid leaching that the sodium ions of the Al-0 (composition: $62.5SiO_2$-$28.3B_2O_3$-$9.2Na_2O$ wt%) and Al-3 (composition: $62.5SiO_2$-$27.3B_2O_3$-$7.2Na_2O$-$3.0Al_2O_3$ wt%) glass hollow fibers were completely eluted after 10 and 90 minutes respectively with 3 mol/dm^3 HNO_3, and after 30 and 90 minutes respectively with 3 mol/dm^3 H_3PO_4 or 3 mol/dm^3 CH_3COOH.

Ideal separation factors of H_2/N_2 were measured at 373 K using a gas mixture of 50%H_2-50%N_2. The membranes showed highly selective separation of hydrogen. Values for the Al-0 hollow fiber membrane treated with 3 mol/dm^3 HNO_3 reached more than 80. However, ideal separation factors of H_2/N_2 for the Al-3 hollow fiber membranes were smaller. This is thought to be due to the addition of Al_2O_3. Four coordination aluminum species (AlO^{4-}) are strongly attracted to alkali metal ions because of charge compensation. Sodium ions in the Al-3 glass hollow fibers were therefore prevented from moving within the glass network and the destruction of the glass network during acid leaching caused defects in the Al-3 glass hollow fiber membranes.

The formation mechanism of the ultra-micropores was also investigated. From N_2 adsorption measurement and gas separation measurement, it was concluded that the ultra-micropores of the membranes were formed by elution of the phase-separated sodium borate-rich phase at sub-nanometer level and that these defect-free membranes could only be obtained by using phase separation rather than elution of homogeneously distributed ions from homogeneous glasses (no phase separation) such as the alkali-silicate glasses reported previously.

4. 2 Introduction

Because of their stability in organic solvents and at high temperatures, inorganic membranes have attracted much researches. In particular, glass membrane is seen as promising due to its facility of shaping and its ability to be shaped into hollow fiber. Shaping into hollow fiber has the following advantages: It provides a large membrane area and a compact module; it allows endowment with flexibility; and it allows a high shaping rate (several hundred meters per minute). These properties should facilitate the mass production of glass hollow fiber membranes. In addition, hollow fiber membranes made of glass can be easily formed into modules by melting.

One of the established processes for preparation of inorganic porous materials is acid leaching of phase-separated glasses [1, 2]. Conventional porous glass is produced by this process. However, it is difficult to obtain glass composed of micropores rather than mesopores or macropores using this process. Acid leaching is also applied to homogeneous non-phase-separated glasses. Ion exchange takes place between cations in the glass and hydrogen ions in the acid solution at the initial stage of attack, resulting in a siliceous hydrated layer. Ultra-micropores of the size of the eluted ions are formed in the leached layer. This process has therefore been employed for preparation of ultra-microporous membranes. The author [3] obtained ultra-microporous glass capillary membranes from alkali-silicate glass by this method. These membranes had ultra-micropores, but did not show high selectivity for gas due to the presence of microcracks.

Recently, Ma *et al.* [4] and Way *et al.* [5, 6] reported glass hollow fiber membranes which had high selectivity for gases and were prepared by acid leaching from borosilicate glasses. The gas separation properties and physical properties of these membranes were investigated. However, the composition of the glass hollow fibers and the formation process of ultra-micropores were not studied.

In the present chapter, the author describes the preparation of ultra-microporous glass hollow

fiber membranes by acid leaching from borosilicate glasses, their hydrogen separation properties and the formation process of ultra-micropores.

4. 3 Experimental

4. 3. 1 Preparation of glass hollow fiber membranes

Glass hollow fiber membranes with an outer diameter of about 50 μm and an inner diameter of about 30 μm were made from glass hollow fibers. The glass hollow fibers were prepared as follows. First, glass tubes with an outer diameter of about 5 mm and inner diameter of about 4 mm were made from glass melts. The glass tubes were shaped continuously into glass hollow fibers by redrawing. The compositions of the Al-0 and Al-3 glass hollow fibers were $62.5SiO_2$-$28.3B_2O_3$-$9.2Na_2O$ and $62.5SiO_2$-$27.3B_2O_3$-$7.2Na_2O$-$3.0Al_2O_3$ by wt%, respectively. The glass hollow fibers were cut to about 200 mm in length and immersed in solutions of 3 mol/dm^3 HNO_3, H_3PO_4 CH_3COOH at 371 K for a certain time until the sodium ions were completely eluted. The acid/glass ratio, defined as the ratio of volume of leaching acid to weight of glass hollow fibers, was kept constant at 2000 dm^3/g. After acid leaching, the fibers were washed with distilled water and dried at room temperature.

In order to determine the time required for sodium ions to be completely eluted, a portion of the acid solution in which the glass hollow fibers were immersed was removed at certain time intervals and Na^+ concentrations measured with an atomic absorption/flame emission spectrophotometer (Shimadzu AA-180, Shimadzu). Inductively coupled plasma spectrometry (ICP spectrometry: SPS-1200, Seiko) was used to detect the elution of other ions when the sodium ions had been completely eluted.

4. 3. 2 Measurement of gas permeation

To evaluate the gas separation characteristics and pore size of the membranes, mixed gas separation via the membranes was measured at 373 K using a gas mixture of 50%H_2-50%N_2 as

feed gas. The experimental apparatus is shown in Fig. 1. One side of the glass hollow fiber membranes was sealed and the other side was connected to a Pyrex glass tube with epoxy resin. This membrane module was supported in a gas flow cell. A gas mixture of 50%H_2-50%N_2 was introduced. Pressure of the feed gas was kept at 2 atm and pressure difference of the membrane was kept constant by downstream evacuation. Gas composition of the feed and permeate gas was analyzed by gas chromatography (Shimadzu GC-14A, Shimadzu) with a thermal conductivity detector.

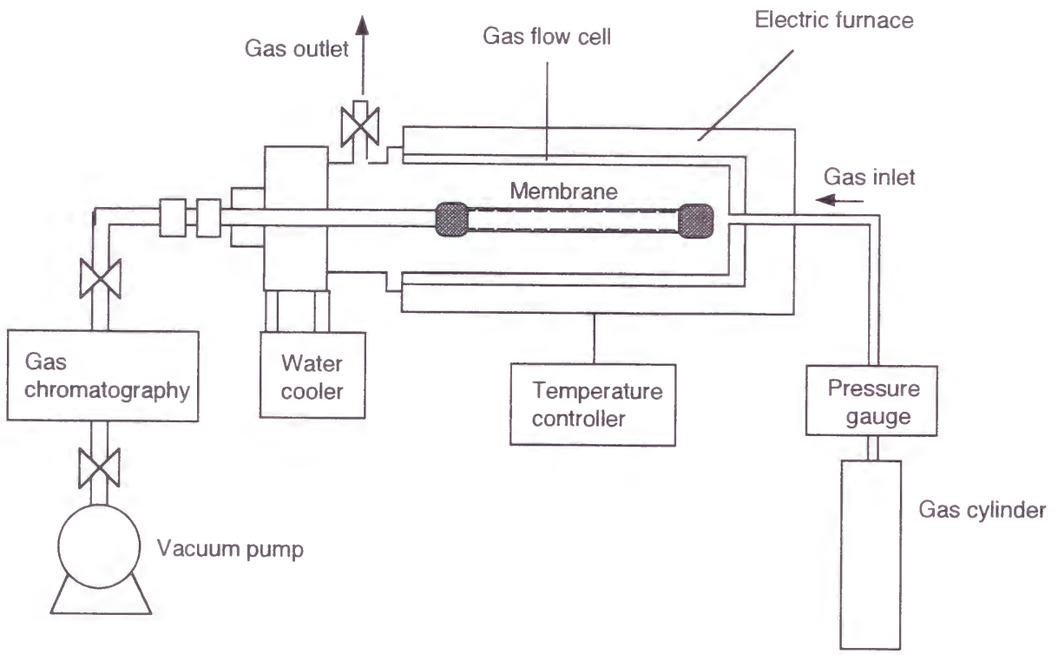

Fig. 1 Schematic diagram of the apparatus used for gas permeation measurement.

The ideal separation factor of H_2/N_2 was calculated from mole fraction of hydrogen in the feed gas and the permeate gas using the following equation [7];

$$\alpha = \frac{y_A}{1-y_A}\,\frac{1-x_A-\Phi(1-y_A)}{x_A-\Phi y_A} \qquad (1)$$

$$\Phi = \gamma + \theta - \gamma\theta \qquad (2)$$

$$\gamma = \frac{P_l}{P_h} \qquad (3)$$

$$\theta = \frac{F_p}{F_f} \qquad (4)$$

where: y_A=mole fraction of hydrogen in feed gas, x_A=mole fraction of hydrogen in permeate gas, Φ=operating factor, γ=operating pressure ratio, θ=cut, P_l=downstream pressure, P_h=upstream pressure, F_p=flux of permeate, F_f=flux of feed.

4. 3. 3 Membrane characterization

To evaluate the pore size and pore size distribution of the membranes, nitrogen adsorption isotherm at 77 K was measured by nitrogen adsorption apparatus (BELSORP 28, BEL JAPAN Inc.).

The morphology of the membrane surface was studied by scanning electron microscopy (JSM-5310LV, JEOL).

4. 4 Results and discussion

4. 4. 1 Elution of ions

Elution rates of sodium ions from the Al-0 glass hollow fibers are shown in Fig. 2. The sodium ions of the glass hollow fibers were completely eluted after 10 minutes with 3 mol/dm^3 HNO_3 and after 30 minutes with 3 mol/dm^3 CH_3COOH or 3 mol/dm^3 H_3PO_4. Figure 3 shows elution rates of sodium ions from the Al-3 glass hollow fibers. The sodium ions were completely eluted after 90 minutes with 3 mol/dm^3 HNO_3, 3 mol/dm^3 CH_3COOH or 3 mol/dm^3 H_3PO_4. The elution rates of sodium ions from the Al-0 glass hollow fibers were faster than those from the Al-3 glass hollow fibers. This is thought to be due to the addition of Al_2O_3. In glass, aluminum atoms fall into four coordination species (AlO_4^-) which accompany alkali metal ions and substitute for a part of the SiO_4 glass network [8]. These aluminum ions are strongly attracted to alkali metal ions because of the charge compensation of AlO_4^-. It was therefore thought that sodium ions in the Al-3 hollow fibers were prevented from moving within the glass network so that their elution rate from these hollow fibers was slower.

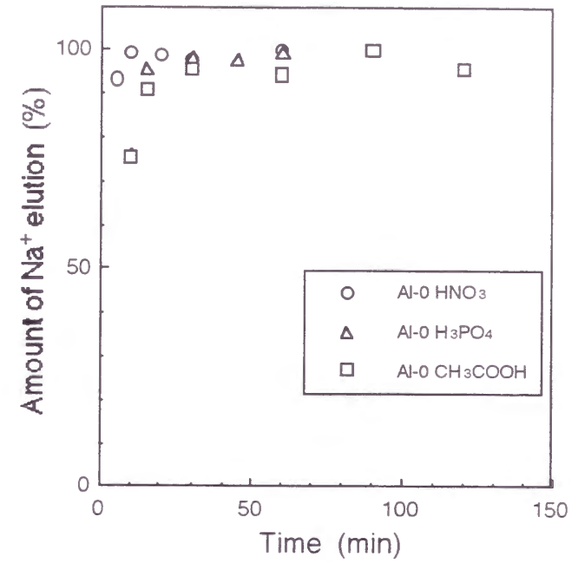

Fig. 2 Elution rate of Na^+ from Al-0 glass hollow fibers treated with 3 mol/dm^3 HNO_3 (Al-0 HNO_3), H_3PO_4 (Al-0 H_3PO_4) and CH_3COOH (Al-0 CH_3COOH).

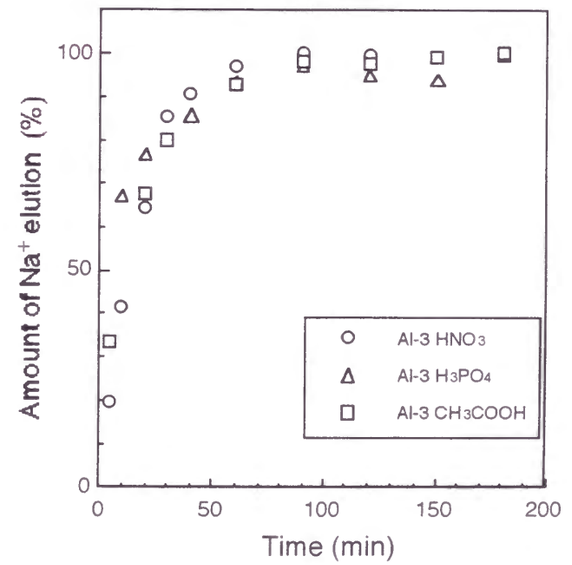

Fig. 3 Elution rate of Na^+ from Al-3 glass hollow fibers treated with 3 mol/dm^3 HNO_3 (Al-3 HNO_3), H_3PO_4 (Al-3 H_3PO_4) and CH_3COOH (Al-3 CH_3COOH).

Table 1 Amounts of elution of other ions for Al-0 glass hollow fibers treated with 3 mol/dm^3 HNO_3 (Al-0 HNO_3), 3 mol/dm^3 H_3PO_4 (Al-0 H_3PO_4) and 3 mol/dm^3 CH_3COOH (Al-0 CH_3COOH).

Sample	Amount of elution (%)	
	B	Si
Al-0 HNO_3	100	2.0
Al-0 H_3PO_4	100	1.3
Al-0 CH_3COOH	100	0.7

Table 2 Amounts of elution of other ions for Al-3 glass hollow fibers treated with 3 mol/dm^3 HNO_3 (Al-3 HNO_3), 3 mol/dm^3 H_3PO_4 (Al-3 H_3PO_4) and 3 mol/dm^3 CH_3COOH (Al-3 CH_3COOH).

Sample	Amount of elution (%)		
	B	Si	Al
Al-3 HNO_3	100	12	50
Al-3 H_3PO_4	100	1.1	1.5
Al-3 CH_3COOH	100	0.4	2.1

After leaching treatment, Al-3 hollow fibers were brittle, and after treatment with 3 mol/dm^3 HNO_3, this prevented their use in membrane modules. Table 1 shows the amounts of other ions eluted from the Al-0 glass hollow fibers after complete elution of sodium ions, as determined by ICP spectrometry when the sodium ions were completely eluted. Table 2 shows the same data for the Al-3 glass hollow fibers. Boron in the Al-0 and Al-3 glass hollow fibers was completely eluted by all acids. The amount of Si eluted was less than 2.0 % except in the Al-3 glass hollow fibers treated with 3 mol/dm^3 HNO_3 (about 14%). Al in the Al-3 glass hollow fibers was eluted to 56% with 3 mol/dm^3 HNO_3, and to about 2 % with 3 mol/dm^3 CH_3COOH or 3 mol/dm^3 H_3PO_4. These results indicate that the brittleness of Al-3 glass hollow fibers treated with 3 mol/dm^3 HNO_3 was caused by destruction of the glass network. As nitric acid is a strong acid (pKa=-1.8 at 298 K) compared to phosphoric acid (pKa=2.15 at 298 K) and acetic acid (pKa=4.56 at 298 K), it attacked strongly and eluted aluminum ions in the glass network together with sodium ions during leaching treatment. This caused the destruction of the glass network and the amount of Si and Al eluted was higher.

4. 4. 2 Gas permeation characteristics

A typical scanning electron microprobe (SEM) photograph of the glass hollow fiber membrane prepared by acid leaching is presented in Fig. 4. The membrane surface was smooth, and no macrocrack was observed after leaching treatment.

Table 3 shows the ideal separation factors of H_2/N_2 at 373 K for Al-0 hollow fiber membranes and Al-3 hollow fiber membranes treated with various acids. The ideal separation factor for the Al-0 hollow fiber membrane treated with 3 mol/dm^3 HNO_3 was more than 80 at 373 K. This value is almost 20 times as large as the theoretical Knudsen value (P_{H_2}/P_{N_2}=3.7). In the case of the

Al-3 hollow fiber membranes, the ideal separation factor of H_2/N_2 at 373 K attained more than 20 for the membrane treated with 3 mol/dm^3 CH_3COOH. However, the membrane treated with 3 mol/dm^3 HNO_3 was too brittle to make into modules and the ideal separation factor for this membrane could not be measured. For other membranes, these high separation factors suggest that the membranes possessed molecular sieving ability due to the presence of ultra-micropores.

Table 3 Ideal selectivity factors of H_2/N_2 at 373 K for Al-0 and Al-3 glass hollow fiber membranes treated with various acids.

Acid	Selectivity of H_2/N_2 at 373 K	
	Al-0	Al-3
HNO_3	82	-
H_3PO_4	20	6.1
CH_3COOH	41	23

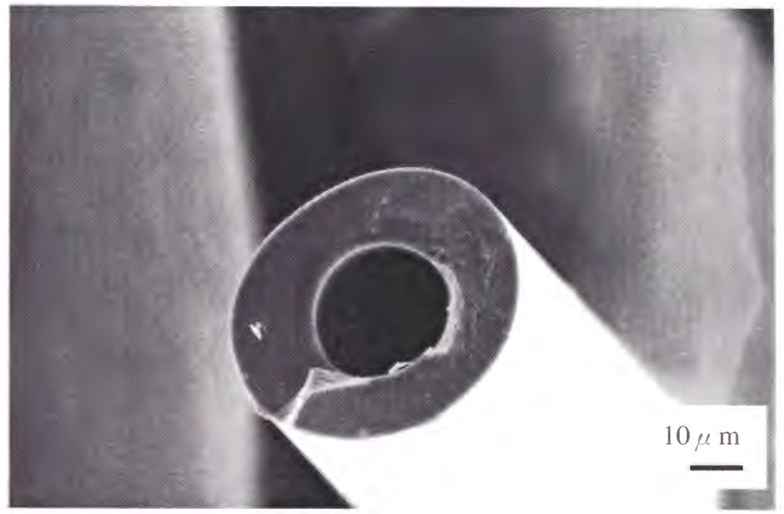

Fig. 4 SEM photograph of the glass hollow fiber membrane

4. 4. 3 Adsorption measurement

N_2 adsorption-desorption isotherms of Al-0 glass hollow fiber membranes treated with various acids are shown in Fig. 5. The isotherms of the membranes were similar to each other. All the N_2 isotherms of the membranes were of the so-called type I isotherm. Type I isotherms follow the BDDT classification, which is shown in Fig. 6 and was originally proposed by Brunauer, Deming, Deming and Teller [9, 10]. It is characteristic of adsorption-desorption on microporous solid and is characterized by a large amount of adsorption at a low relative pressure and a plateau that is nearly horizontal, as shown in Fig. 6. Figure 7 shows N_2 adsorption-desorption isotherms of Al-3 glass hollow fiber membranes treated with various acids. The isotherms of the Al-3 glass hollow fiber membranes treated with 3 mol/dm^3 HNO_3 and CH_3COOH were of the type I isotherm according to the BDDT classification. However, the isotherm of the Al-3 glass hollow fiber membrane treated with 3 mol/dm^3 H_3PO_4 was different and represented a type IV isotherm. This isotherm is characteristic of adsorption-desorption on mesoporous solid and is characterized by a hysteresis loop. The amount of adsorption on this membrane was small. This isotherm is thought to have been caused by closing of micropores and pore-coarsening during acid leaching. It has been reported that prolonged acid treatment causes structural alteration in leached porous glass, which brings about micropore collapse [11], and that the pore size of colloidal silica undergoes coarsening during prolonged acid treatment by Ostwald ripening [12]. Although phosphoric acid (pKa=2.15 at 298 K) is a stronger acid than acetic acid (pKa=4.56 at 298 K), the elution rates of sodium ions from glass hollow fibers treated with H_3PO_4 were the same as for those treated with CH_3COOH. This is due to a reaction of the phosphoric acid with the silica surface formed after ions have leached out. The phosphoric acid molecules are readily sorbed by the surface of the silica, thereby forming donor-acceptor complexes with hydrated silicon atoms [13, 14]. These complexes are thought

to retard the elution of sodium ions. The elution rate from glass treated with H_3PO_4 was therefore slower and acid treatment time longer. The Al-3 glass hollow fiber membrane treated with 3 mol/dm^3 H_3PO_4 thus had a mesoporous structure and low H_2/N_2 selectivity. Specific surface area values based on BET plots [15] of Al-0 and Al-3 glass hollow fiber membranes subjected to various elution treatments are presented in Table 4. Almost all of the membranes showed high values. However, the Al-3 glass hollow fiber membrane treated with H_3PO_4 had a very small specific surface area. This finding also supports the theory that longer acid treatment caused micropore collapse and pore-coarsening.

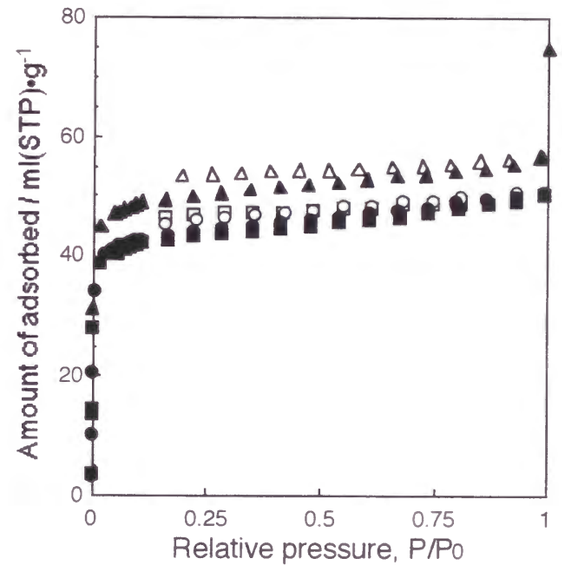

Fig. 5 N_2 adsorption-desorption isotherms of Al-0 glass hollow fiber membranes treated with 3 mol/dm^3 HNO_3 (○), H_3PO_4 (△) and CH_3COOH (□); solid symbols: adsorption, open symbols: desorption.

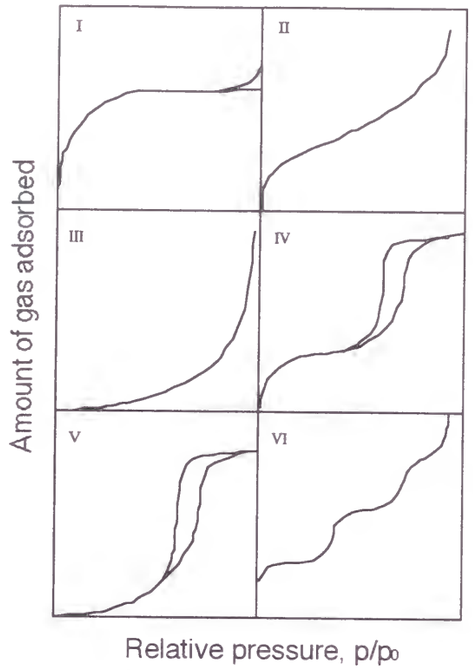

Fig. 6 The five types of adsorption-desorption isotherms, I to V, in the BDDT classification, together with Type VI, the stepped isotherm.

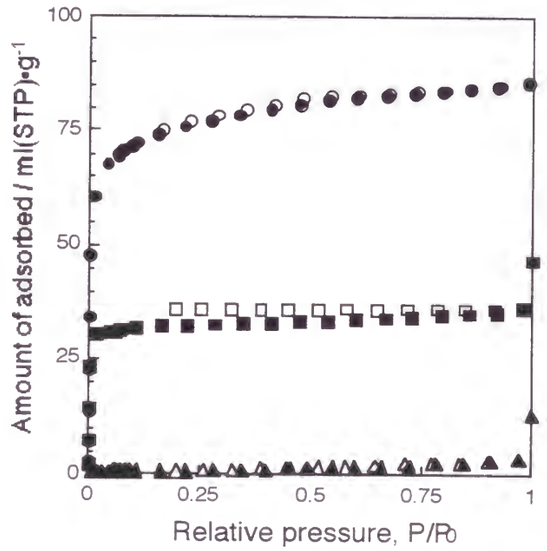

Fig. 7 N_2 adsorption-desorption isotherms of Al-3 glass hollow fiber membranes treated with 3 mol/dm^3 HNO_3 (○), H_3PO_4 (△) and CH_3COOH (□); solid symbols: adsorption, open symbols: desorption.

Figure 8 shows the pore size distributions of the Al-0 glass hollow fiber membrane treated with 3 mol/dm^3 HNO_3 and of the Al-3 glass hollow fiber membrane treated with 3 mol/dm^3 CH_3COOH, as determined by N_2 adsorption isotherms using the MP method [16]. The mean pore radius was about 0.4 nm. Other samples of Al-0 and Al-3 glass hollow fiber membranes with type I isotherms showed almost the same pore size distributions, and also had the same mean pore radii (about 0.4 nm). For the Al-3 glass hollow fiber membrane treated with H_3PO_4, pore size distribution could not be calculated due to the small amount of adsorption.

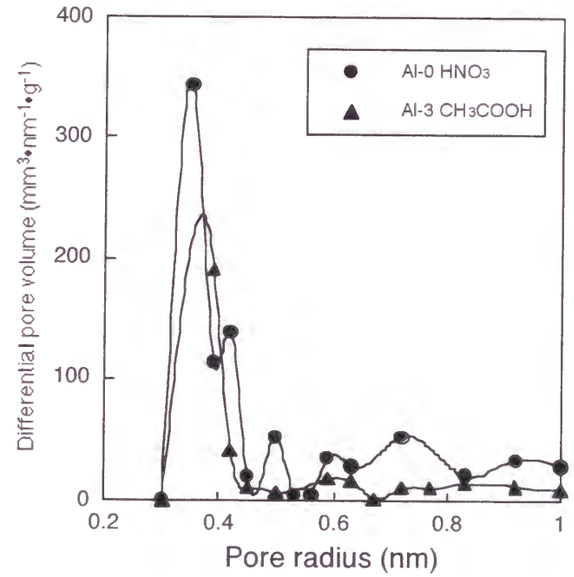

Fig. 8 Pore size distribution of Al-0 glass hollow fiber membranes treated with 3 mol/dm^3 HNO_3 (Al-0 HNO_3) and Al-3 glass hollow fibers treated with 3 mol/dm^3 CH_3COOH (Al-3 CH_3COOH).

4. 4. 4 Mechanism of micropore formation

In alkali-silicate glass, alkali metal ions are present between SiO_2 networks as shown in Fig. 9[17]. The ionic crystal radius of Na^+ is 0.102 nm [18]. Under acidic conditions, H^+ ions easily diffuse into the glass matrix and replace the alkali metal ions. The alkali metal ions also move within the glass, and are therefore eluted in solution and create pores with diameters similar to their own. Membranes prepared by acid leaching using alkali-silicate glass have been reported [3]. These membranes had ultra-micropores from N_2 adsorption. However, as reported here, they did not show high selectivity for gas separation due to the development of microcracks.

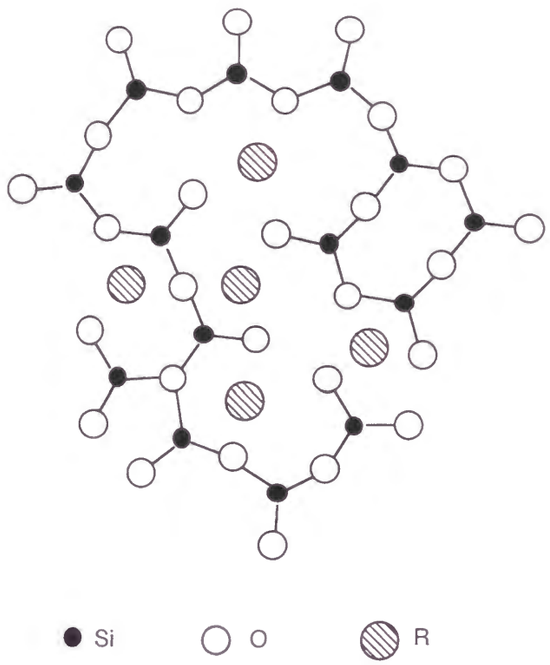

Fig. 9 Schematic representation of the structure of alkali-silicate glass.

In the present study, Al-0 and Al-3 glass hollow fiber membranes were also prepared by acid leaching. The membranes had ultra-micropores as shown in Fig. 8 and showed high H_2 selectivity. The difference between the above-mentioned membranes and the Al-0 and Al-3 glass hollow fiber membranes of the present study was in the compositions of the original glass. The compositions of the Al-0 and Al-3 glass hollow fibers were $62.5SiO_2$-$28.3B_2O_3$-$9.2Na_2O$ and $62.5SiO_2$-$27.3B_2O_3$-$7.2Na_2O$-$3.0Al_2O_3$ by wt%, respectively. These are compositions in which phase separation is well-known to occur [19]. These glasses were separated into two phases (silica-rich phase and sodium borate-rich phase) by spinodal decomposition during heat treatment. White *et al.* [20] reported that phase separation in these glasses also occurred in the as-drawn state and that the size of phase separation was of atomic scale (less than 1 nm). Recently, Yazawa *et al.* [21] reported the effect of cooling rate on pore distribution in quenched sodium borosilicate glasses. In their study, it was found that phase separation occurred in sodium borosilicate glasses obtained by the roller-quenching method (quenched at 10^6 K/s) and pore size after acid leaching was less than 1 nm. They concluded that these micropores were based on spinodal phase separation.

Boron in the Al-0 and Al-3 glass hollow fibers was completely eluted by all acids after complete elution of the sodium ions, as shown in Table 1. The pore diameters of the membranes were less than 1 nm and the membranes had high H_2 selectivity. These results and other reports [21] suggest that the pore formation mechanism is as schematically shown in Fig. 10. Already during shaping and redrawing of the glasses, phase separation occurred through spinodal decomposition. The glasses were separated into two phases (silica-rich phase and sodium-borate rich phase) and these two phases were highly interconnected in a three-dimensional continuum (Fig. 10 (a)). The sodium borate-rich phase was then readily eluted by acid leaching due to its high solubility in acids and, due to the continuity, it created continuous pores without microcracks (Fig. 10 (b)). Without

phase separation, sodium and boron ions existed homogeneously in the glass network, and it is difficult to elute them without stress due to destruction of the glass network. A previous report on alkali-silicate glasses [3] supports this theory. The glass compositions used in the report in question were $77.2SiO_2$-$22.8Na_2O$ and $69.1SiO_2$-$30.9K_2O$ by wt%, which are beyond the phase separation range. Phase separation therefore did not occur in these glasses and the membranes obtained after acid leaching did not show high selectivity for gas separation due to the development of microcracks. It was thus concluded that the ultra-micropores of these membranes were created by elution of the phase-separated sodium borate-rich phase at sub-nanometer level.

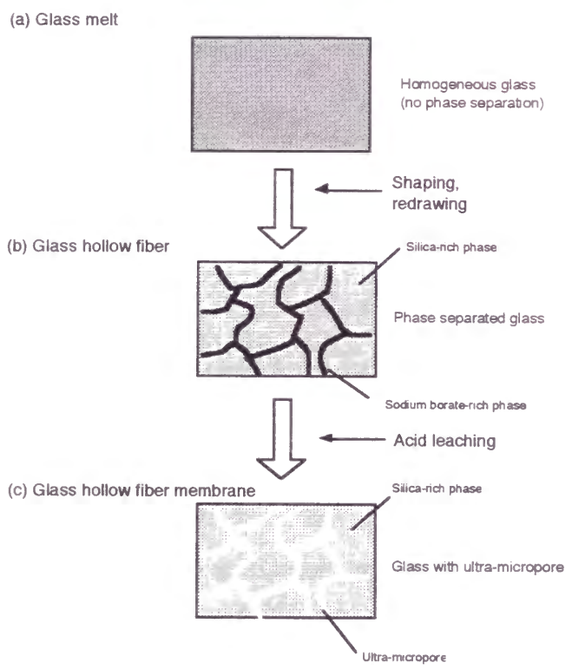

Fig. 10 Schematic diagram of the formation mechanism of the pore on the glass hollow fiber membranes.

4. 5 Conclusions

Ultra-microporous glass hollow fiber membranes were prepared by acid leaching with various acids. It was found from acid leaching that the sodium ions of the Al-0 (composition: $62.5SiO_2$-$28.3B_2O_3$-$9.2Na_2O$ wt%) and Al-3 (composition: $62.5SiO_2$-$27.3B_2O_3$-$7.2Na_2O$-$3.0Al_2O_3$ wt%) glass hollow fibers were completely eluted after 10 and 90 minutes respectively with 3 mol/dm^3 HNO_3, after 30 and 90 minutes respectively with 3 mol/dm^3 H_3PO_4 or 3 mol/dm^3 CH_3COOH. These membranes exhibited highly selective separation for H_2/N_2: For instance, the ideal separation factor of H_2/N_2 for the Al-0 hollow fiber membrane treated with 3 mol/dm^3 HNO_3 reached more than 80 at 373 K. These membranes exhibited a molecular sieving effect due to the presence of ultra-micropores. However, ideal separation factors of H_2/N_2 for the Al-3 hollow fiber membranes were smaller than those for the Al-0 hollow fiber membranes. This is thought to be due to the addition of Al_2O_3. Four coordination aluminum species (AlO4-) are strongly attracted to alkali metal ions because of charge compensation. Sodium ions in the Al-3 glass hollow fibers were therefore prevented from moving within the glass network and destruction of the glass network during acid leaching caused defects in the Al-3 glass hollow fiber membranes. From N_2 adsorption measurement and gas separation measurement, it was concluded that the ultra-micropores of the membranes were created by elution of the phase-separated sodium borate-rich phase at sub-nanometer level and that these defect-free membranes could be obtained only by using phase separation rather than elution of homogeneously distributed ions from homogeneous glasses (no phase separation) such as the alkali-silicate glasses reported previously.

4. 6 References

1. H.P. Hood and M.E. Nordberg, USA Patent, 2,106,744 (1938).
2. H.P. Hood and M.E. Nordberg, USA Patent, 2,221,709 (1940).
3. K. Kuraoka, Z. Qun, K. Kushibe and T. Yazawa, *Sep. Sci. Tech.*, **33**, 297 (1998).
4. A.B. Shelekhin, A.G. Dixon and Y.H. Ma, *J. Membrane Sci.*, **75**, 233 (1992).
5. J.D. Way and D.L. Roberts, *Sep. Sci. Tech.*, **27**, 29 (1992).
6. M.H. Hassan, J.D. Way, P.M. Thoen and A.C. Dillon, *J. Membrane Sci.*, **104**, 27 (1995).
7. Y. Shindo, in *Designs for membrane separation processes* (ed. The Membrane Society of Japan) 25 (Kitami syobo, Tokyo, 1985).
8. Y. Moriya, *J. Ceram. Soc. Japan*, **78**, 24 (1970).
9. S. Brunauer, L.S. Deming, W.E. Deming and E. Teller, *J. Am. Ceram. Soc.*, **62**, 1723 (1940).
10. S.J. Gregg and K.S.W. Sing, *Adsorption, surface area and porosity* (ACADEMIC PRESS INC. (LONDON) LTD, London, 1982).
11. H. Tanaka, K. Kuraoka, H. Yamanaka and T. Yazawa, *J. Non-Cryst. Solids*, **215**, 262 (1997).
12. H. Tanaka, *J. Ceram. Soc. Japan*, **85**, 587 (1977).
13. N.H. Ray, *J. Non-Cryst. Solids*, **5**, 71 (1970).
14. B.M. Mitsyuk, *Russ. J. Inorg. Chem.*, **17**, 471 (1972).
15. S. Brunauer, P.H. Emmett and E. Teller, *J. Am. Chem. Soc.*, **60**, 309 (1938).
16. R.S. Mikhail, S. Brunauer and E.E. Bodor, *J. Colloid Interf. Sci.*, **26**, 45 (1968).
17. W.D. Kingery, H.K. Bowen and D.R. Uhlmann, in *Introduction to Ceramics* 98 (John Wiley & Sons, Inc., New York, 1960).
18. R.D. Shannon and C.T. Prewitt, *Acta Cryst.*, **B25**, 925 (1969).
19. O.V. Mazurin and E.A. Porai-Koshits, *Phase separation in glass* (Elsevier Science Publishers B. V., Amsterdam, 1984).
20. W.B. White, *J. Non-Cryst. Solids*, **49**, 321 (1982).
21. T. Yazawa, K. Kuraoka and W.-F. Du, *J. Phys. Chem. B*, **103**, 9841 (1999).

Part II Vapor phase method

Part II-1 CVD (Chemical Vapor Deposition) method

Chapter 5: Preparation of silica membrane and its methanol vapor separation property

5. 1 Abstract

Silica membranes were prepared by depositing silica on porous glass tubes with the aid of evacuation using tetraethoxysilane as a reactant in the temperature range of 673-773 K. The basic permeation properties of methanol vapor in gas phase were investigated. This membrane appears to hinder permeation of methanol vapor. This behavior is quite different from the original porous glass and other reported membranes. The separation factors of He/CH_3OH were 7.1 at 373 K and 16.9 at 473 K. These value are much higher than the Knudsen value (He/CH_3OH=2.8). The permeances of He and N_2 through this membrane were also measured at varying temperatures in order to investigate the permeation mechanism. Gas permeation through the membrane was predominantly governed by an activated diffusion mechanism.

5. 2 Introduction

The recent development of inorganic molecular sieving membranes, which can be used at high temperature and in the presence of reactive chemicals, has opened up many possible applications for high temperature gas separation and membrane reactor with catalyst. Chemical vapor deposition (CVD) techniques have been used for preparing inorganic molecular sieving membranes with an ultramicroporous layer of silica, zirconia or titania. Gavalas et al. first reported the deposition of amorphous silica inside the pore wall of a Vycor glass tube using SiH_4/O_2 and $SiCl_4/H_2O$ as the reactants [1, 2]. These membranes gave highly selective separation of hydrogen due to an activated diffusion mechanism. Other researchers also reported the deposition of metal oxides on porous substrates by CVD method [3-7]. An important property of these membranes is that they have pores with diameters less than 1 nm and indicate molecular sieving performance. Advantage is taken of this property in the present study on permeation of methanol vapor and other gases. Because the membrane is made of silica, which is often used for catalyst supports, the separation with this membrane can be applied to membrane reactors, in which reaction and separation occur simultaneously.

In order to recover energy from low level waste heat at about 423~473 K, membrane reactor that employs the endothermic methanol decomposition reaction can be used [8, 9]. The permeation of methanol vapor in the gas phase is very important for this application. There have been numerous studies on methanol-water system by pervaporation [10], however few researchers reported methanol vapor separation in the gas phase [11]. The purpose of this chapter is therefore to examine the basic permeation property of methanol vapor in gas phase.

In this chapter, molecular sieving silica membrane using the CVD method with the aid of evacuation was prepared. This process is quite effective at reducing the pore size only near the

surface (deposition side) because the deposition of silica preferentially occurred near the pores with aid of evacuation. The permeation properties of methanol vapor, He and N_2 through the membrane were also reported.

5. 3 Experimental

5. 3. 1 Materials

Porous glass tubes (about 97%SiO_2) with outer diameter 5 mm, inner diameter 4 mm and mean pore diameter 4 nm were used as the supports. Tetraethoxysilane (TEOS, $Si(OC_2H_5)_4$, 99.9%) was purchased from Kanto Chemical Co., Inc. High purity N_2 (>99.99%) and high purity O_2 (>99.5%) was used as a carrier gas and as a reacting gas with TEOS, respectively.

5. 3. 2 Membrane preparation by the CVD

Figure 1 shows the schematic diagram of the apparatus used for the CVD. The membrane module is about 10 cm length porous glass sealed by melting at one side with nonporous quarts tube with outer diameter 8 mm and at the other side closed. This module was located at the center of an electric tubular furnace. The inside of the module was evacuated with a vacuum pump to deposit silica near the pores preferentially. In this respect, this CVD process is different from conventional CVD process as reported Gavalas et al. [12]. TEOS vapor was fed to the reactor with nitrogen carrier and oxygen was also introduced to the reactor. The flow rate of N_2 was kept at 200 cc/min. Other conditions were changed to optimize the CVD conditions as follows: O_2 flow rate of 1000, 2000 cc/min, TEOS concentrations of 0.8, 1.6, 2.3%, and reaction temperature of 673, 723, 773 K.

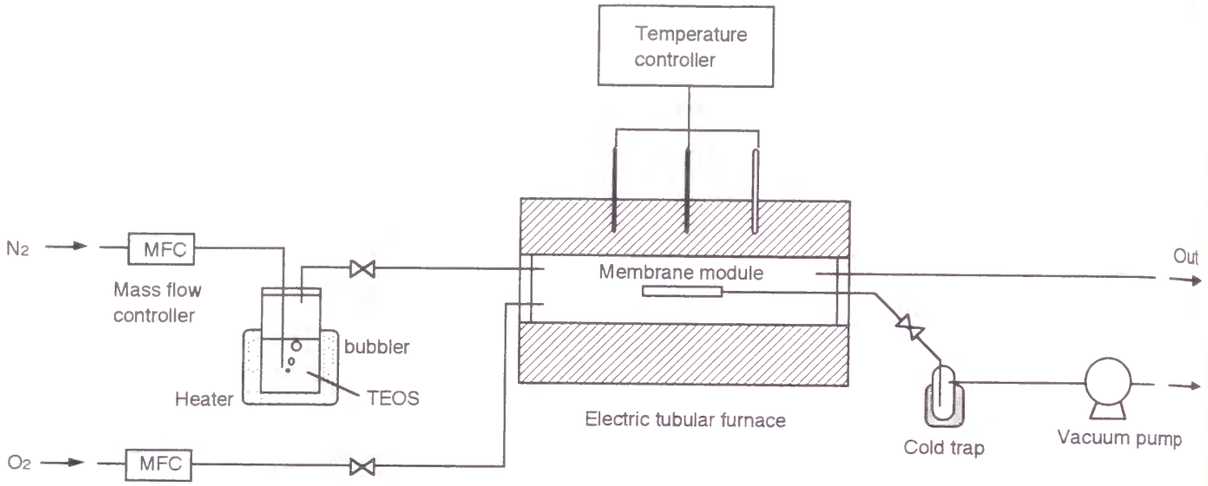

Fig. 1 Schematic diagram of the apparatus used for the CVD.

5. 3. 3 Measurement of permeation

Permeations of methanol vapor through the membranes were measured at 373 K and 473 K using a mixture of CH_3OH and He or N_2 for the feed gases. The experimental apparatus is shown in Fig. 2. The membranes were supported in a gas flow cell. Methanol vapor and He or N_2 were mixed and introduced into the gas flow cell. Methanol content of the feed gas was about 10%. The pressure of the feed gas was kept at 2 atm (2.026×10^5 Pa) and the permeate gas was carried using an argon stream for sweep gas. Gas compositions of the feed and permeate gas were analyzed by a gas chromatography (Shimadzu GC-8A, Shimadzu) with a thermal conductivity detector.

The separation factor of He/CH_3OH or N_2/CH_3OH was calculated from mole fraction of He or N_2 in feed gas and in the permeate gas by using the following equation,

$$\alpha = \frac{y_A}{1 - y_A} \frac{1 - x_A}{x_A} \qquad (1)$$

where: x_A=mole fraction of He or N_2 in the feed gas

y_A=mole fraction of He or N_2 in the permeate gas.

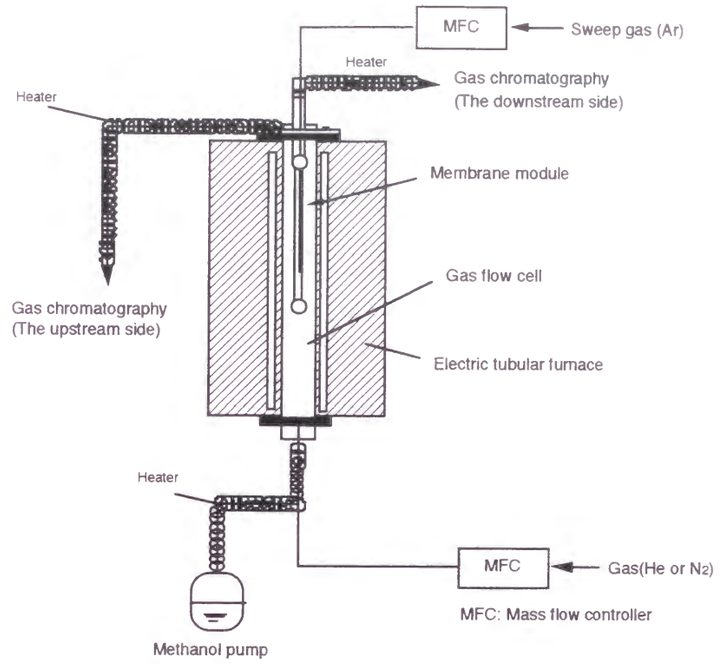

Fig. 2 Schematic diagram of the apparatus used for the measurement of methanol vapor permeation.

Pure gas permeations through the membranes were also measured at 298 K, 373 K and 473 K using He, N_2 by the same procedure described previously [12] after drying at 373 K in a vacuum oven. The membrane modules were supported in a gas flow cell. Pressure differences of the gases through the membranes were kept at 1 atm (1.013×10^5 Pa) and the permeances were measured by a mass flow meter.

5. 3. 4 Membrane characterization

The specific surface areas and the pore size distributions of the original porous glass membrane and the membrane prepared by the CVD were measured by a nitrogen adsorption (BELSORP 28, BEL JAPAN Inc.). The specific surface areas were determined by BET plots [13] and the pore size distributions were analyzed by BJH method [14].

The morphologies of the membrane surfaces were studied by a scanning electron microscopy, SEM (JSM-5310LV, JEOL).

5. 4 Results

5. 4. 1 Optimizing the CVD condition

To optimize the CVD condition, O_2 flow rate, TEOS concentration, reaction time and reaction temperature of the CVD were changed. Two kinds of O_2 flow rate were examined as shown in Table 1. The ratio of the permeances, He/N_2 (P_{He}/P_{N_2}) of the membrane prepared by the CVD at O_2 flow rate of 2000 cc/min was higher than that at O_2 flow rate of 1000 cc/min. The effect of TEOS concentration on the ratio of the permeances, He/N_2 (P_{He}/P_{N_2}) of the membranes prepared by the CVD is presented in Table 2. The maximum ratio of permeance, He/N_2 was obtained at TEOS concentration of 1.6 %. The change in the ratios of the permeances, He/N_2 of the membranes prepared by the CVD at 373 K on reaction time is shown in Fig. 3. No appreciable change in the ratios of the permeances, He/N_2 was observed after reaction time of 3 hours. From these results, O_2 flow rate of 2000 cc/min, TEOS concentration of 1.6% and reaction time of 3 hours were kept constant. Figure 4 shows the change in the ratios of the permeances, He/N_2 of the membranes prepared by the CVD at 298 K and 373 K on reaction temperature. The ratio of permeance, He/N_2 was indicated the highest value (P_{He}/P_{N_2}=31 at 373 K) on reaction temperature at 723 K. This value was more than 10 times as large as the theoretical Knudsen value (P_{He}/P_{N_2}=2.6). Consequently, O_2 flow rate of 2000 cc/min, TEOS concentration of 1.6% and reaction time of 3 hours and reaction temperature of 723 K are the best CVD condition among the selected conditions in our experiments.

Table 1 Effect of O_2 flow rate on the ratio of the permeances, He/N_2 (P_{He}/P_{N_2}) of the membranes prepared by the CVD.

O_2 flow rate (cc/min)	TEOS concentration (%)	P_{He}/P_{N_2} at 373 K
1000	2.3	2.3
2000	2.3	6.6

All membranes were coated for 5 hours at 673 K.

Table 2 Effect of TEOS concentration on the ratio of the permeances, He/N_2 (P_{He}/P_{N_2}) of the membranes prepared by the CVD.

TEOS concentration (%)	O_2 flow rate (cc/min)	P_{He}/P_{N_2} at 373 K
0.8	2000	2.5
1.6	2000	8.3
2.3	2000	6.6

All membranes were coated for 5 hours at 673 K.

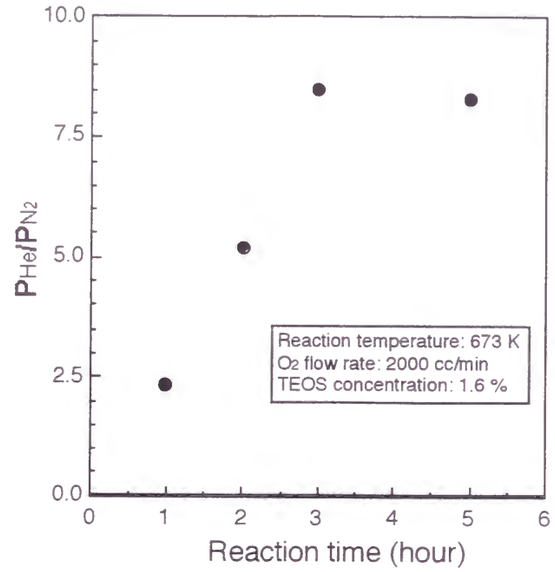

Fig. 3 Change in the ratios of permeance, He/N_2 (P_{He}/P_{N_2}) of the membranes prepared by the CVD at 373 K on reaction time.

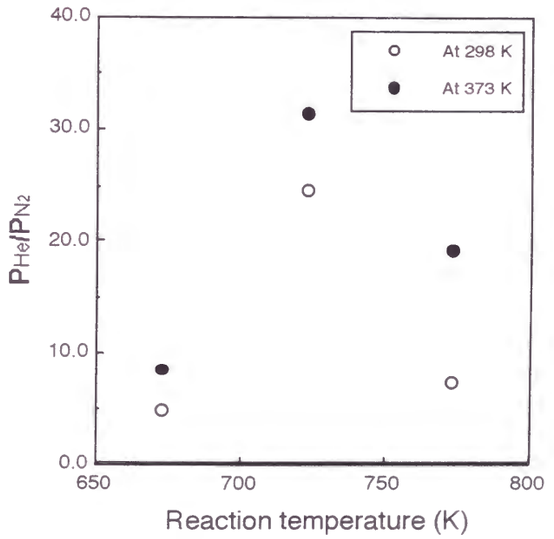

Fig. 4 Change in the ratios of permeance, He/N_2 (P_{He}/P_{N_2}) of the membranes prepared by the CVD at 298 K and 373 K on reaction temperature.

5. 4. 2 Methanol vapor separation

Figure 5 shows the results of the separation factors for He/CH_3OH and N_2/CH_3OH mixtures (X/CH_3OH, X=He, N_2) at 373 K and 473 K with the silica membrane prepared by the CVD. The separation factors of He/CH_3OH were 7.1 at 373 K and 16.9 at 473 K. These values were higher than those of the original porous glass membrane (He/CH_3OH= 0.4 at 373 K and 1.3 at 473 K). At 473 K, the separation factor was more than 5 times as large as the theoretical Knudsen value (He/CH_3OH=2.8). Those of N_2/CH_3OH for the membrane prepared by the CVD were 0.8 at 373 K and 473 K. These values were slightly higher than the porous glass membrane (N_2/CH_3OH= 0.2 at 373 K and 0.5 at 473 K) and slightly lower than the theoretical Knudsen value (N_2/CH_3OH=1.1).

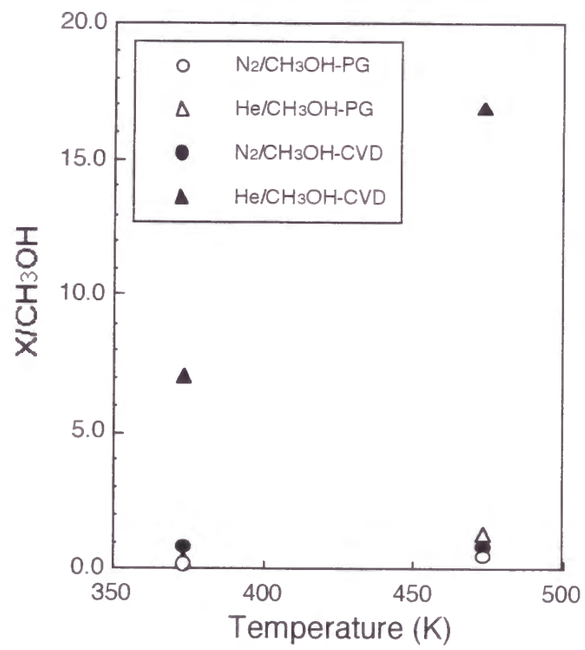

Fig. 5 Separation factors of X/CH_3OH (X=He, N_2) for the membrane prepared by the CVD and the original porous glass membrane.

5. 4. 3 Gas permeation properties of the membranes

The permeances of He and N_2 through the membrane prepared by the CVD were also measured at varying temperatures in order to investigate the permeation mechanism. The relationships between the permeances of He (P_{He}), N_2 (P_{N_2}) and temperatures for the membrane prepared by the CVD, the membrane prepared by the CVD without the aid of evacuation and the original porous glass membrane are shown in Fig. 6. The permeances of N_2 through the membrane prepared by the CVD were extremely low. However the permeances of He through this membrane were decreased to only one-fifth to half compared with those of the original porous glass membrane. The permeances of He and N_2 through the membrane prepared by the CVD without the aid of evacuation were reduced to about one-half of those of the original porous glass membrane. As shown in Fig. 6, the permeances of N_2 through the membrane prepared by the CVD without the aid of evacuation, the permeances of He and N_2 through the original porous glass membrane decreased with increasing temperature. The permeances of He through the membrane prepared by the CVD without the aid of evacuation slightly increased with increasing temperature. However the ratio of the permeances, He/N_2 were low (P_{He}/P_{N_2}=2.4 at 298 K, 2.7 at 373 K and 3.4 at 473 K) and close to the theoretical Knudsen value (P_{He}/P_{N_2}=2.6). Therefore, the gas permeations through these membranes were mainly governed by the Knudsen diffusion. On the other hand, the permeances of He and N_2 through the membrane prepared by the CVD increased with increasing temperature, suggesting that gas permeation was predominantly governed by an activated diffusion mechanism. The calculated activation energies for He and N_2 permeations based on Fig. 6 were 6.2 and 2.8 kJ/mol, respectively. The activation energy for He obtained in the present work is comparable with that previously reported by Hassan et al. [15] and Shelekhin et al. [16] for silica hollow fibers with ultra-micro pores. From this result, it was assumed that the membrane prepared by the CVD had ultra-micro pores as with the silica hollow fibers.

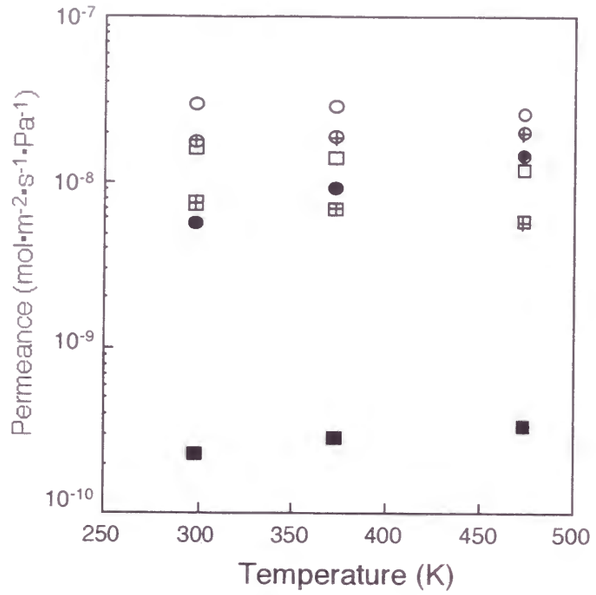

Fig. 6 Relations between the permeances of He (P_{He}), N_2 (P_{N_2}) and temperatures for the membrane prepared by the CVD (P_{He}: ●, P_{N_2}: ■), the membrane prepared by the CVD without the aid of evacuation (P_{He}: ○, P_{N_2}: □) and the original porous glass membrane (P_{He}: ○, P_{N_2}: □).

5. 4. 4 Pore structure controlled by the CVD

The pore size distributions and the specific surface areas of the original porous glass and the membrane prepared by the CVD were measured by nitrogen adsorption measurement. The pore size distributions calculated by BJH method [14] are shown in Fig. 7. The pore size distribution of the membrane does not change from that of the original porous glass and the mean pore diameters are almost the same.

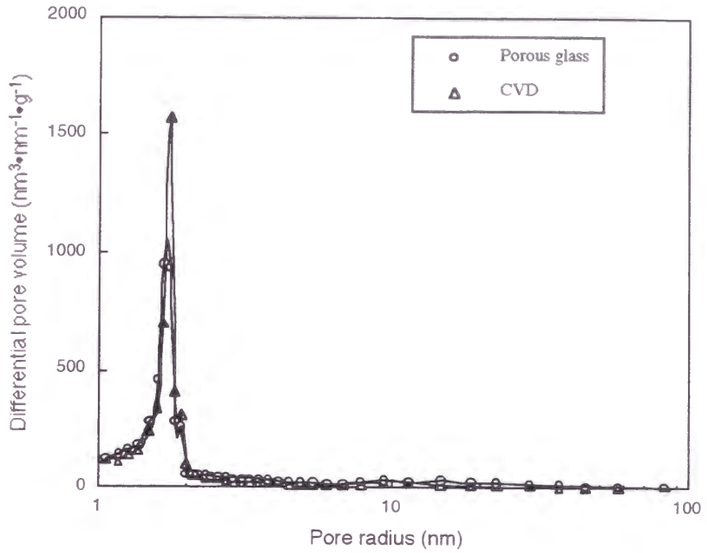

Fig. 7 Pore size distributions of the membrane prepared by the CVD (CVD) and the original porous glass membrane (Porous glass).

Mean pore radii, pore volumes and specific surface areas measured by nitrogen adsorption measurement are presented in Table 3. Both pore volumes and specific surface areas of the membrane were almost the same as those of the original porous glass.

Table 3 Mean pore radii, pore volumes and specific surface areas of the original porous glass membrane (Porous glass) and the membrane prepared by the CVD (CVD).

Sample	Mean pore radius (nm)	Pore volume ($cm^3 \cdot g^{-1}$)	Specific surface area ($m^2 \cdot g^{-1}$)
Porous glass	1.7	0.126	167.4
CVD	1.7	0.118	163.0

The CVD condition; O_2 flow rate: 2000cc/min, TEOS concentration: 1.6 %
Reaction temperature: 723 K, Reaction time: 3 hours

5. 4. 5 Morphology of the membrane

SEM micrographs of the membrane prepared by the CVD are shown in Fig. 8. The CVD was carried out under the optimum condition. Fig. 8 (a) shows the morphology of the outer surface of the membrane (Deposition side). The surface was smooth and no crack was observed. A fractured surface of the membrane is shown in Fig. 8 (b). From these micrographs, the thickness of silica deposition zone was estimated to be about 500 nm.

(a)

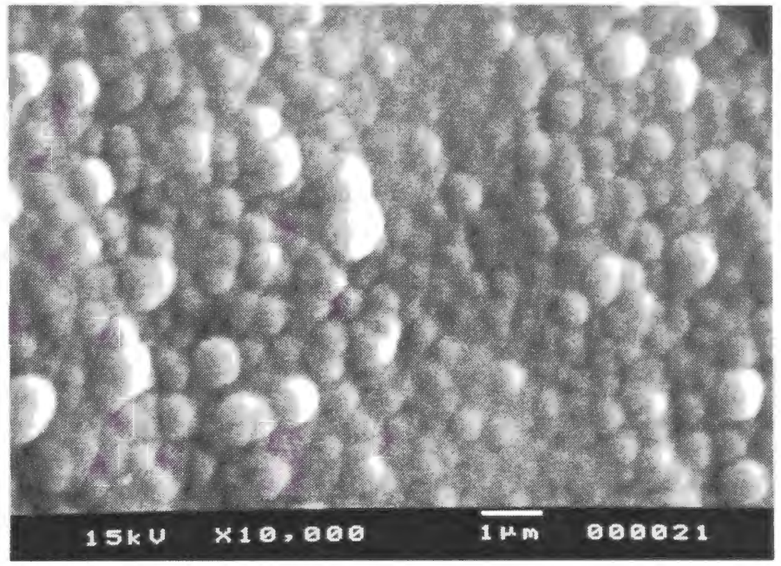

(b)

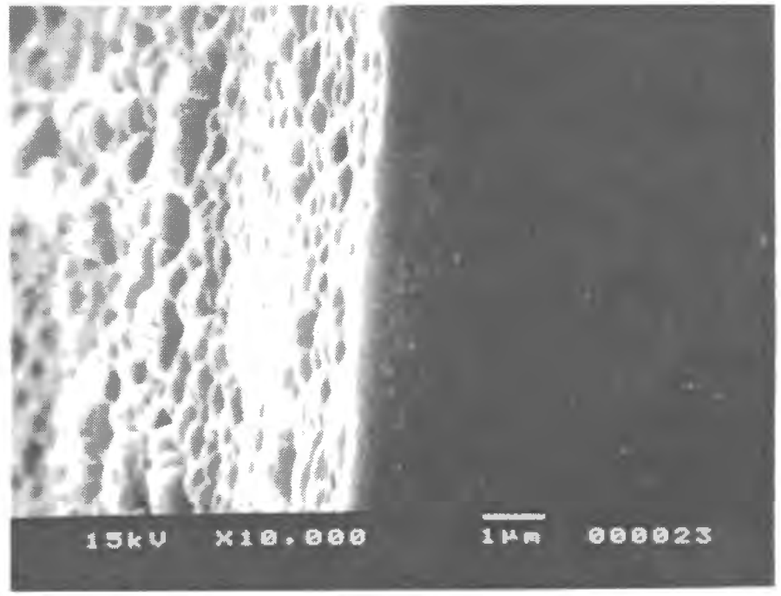

Fig. 8 SEM micrographs showing the membrane prepared by the CVD: (a) the outer surface and (b) the fractured surface.

5. 5 Discussion

5. 5. 1 Structure of the deposition zone on the membrane

The membrane prepared by the CVD had the same mean pore radius and pore size distribution as the original porous glass as indicated in Fig. 7. And the pore volume and specific surface area of the membrane were also almost same as those of the original porous glass as shown in Table 3. However it had different gas permeation properties that prevented permeation of methanol vapor and molecular sieving ability (Fig. 5 and Fig. 6). On the other hand, the membrane prepared by the CVD without the aid of evacuation didn't indicate molecular sieving ability. From these results, it is suggested that the structure of the deposition zone on the membrane prepared by the CVD was schematically shown in Fig. 9. First, silica was preferentially deposited on the pore entrances due to the aid of evacuation and also deposited on the outer surface (Fig. 9 (a)). Therefore, the pore entrances were reduced. After that, the reactants were difficult to enter the pores and silica depositions occurred on the outer surface (Fig. 9 (b)). This silica deposition layer was assumed to be not a quite dense silica because the permeance of He through the membrane was not extremely low compared with the original porous glass membrane. The deposition zone on the outer surface of the membrane was estimated about 500 nm thickness by the SEM observation. If the deposition layer was a quite dense silica, the permeance of He through the membrane would become one-tenth or one percent of the observed value due to the low permeance of silica [17]. Thus the reduced pores with depositions of silica mainly governed the gas permeation through the membrane prepared by the CVD. Consequently, the suggesting structure is reasonable, and the CVD with the aid of evacuation is quite effective to reduce only the pore size near surface due to depositing silica on the pore entrances preferentially. The pore radius determined by nitrogen adsorption measurement is based on measurement of pore volume. Thus it is not sensitive if the deposition zone on the pore entrance and the outer surface of the membrane are quite narrow as suggested, due to its very small volume. Therefore the pore size distributions, mean pore radii, pore volumes and specific surface areas of the original porous glass membrane and the membrane

prepared by the CVD were almost same despite the result that the membrane prepared by the CVD indicated preventing permeation of methanol vapor and molecular sieving ability.

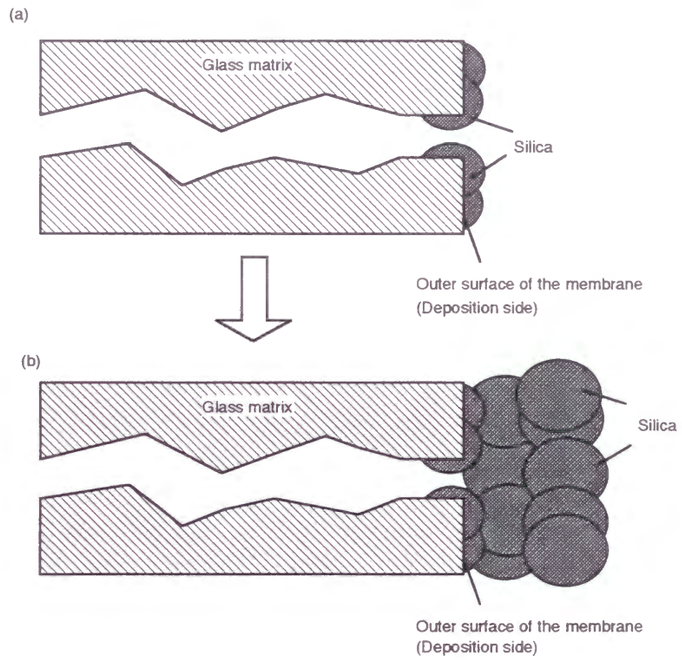

Fig. 9 Schematic diagram of the silica deposition layer.

5. 5. 2 Methanol vapor separation

The results presented in the previous section indicated that the silica membrane prepared by the CVD was the highly selective membrane for He/CH_3OH. However the separation factors of He/CH_3OH for the original porous glass membrane used for the substrate were indicated to be 0.4 at 373 K and 1.3 at 473 K, respectively. There have been numerous studies on methanol-water system by pervaporation [10], however few researchers have reported methanol vapor separation in gas phase [11]. Although it was not a same system, Noble et al. reported the separation factors of H_2/CH_3OH at 473 K for a NaOH-poisoned γ-alumina membrane with 4 nm diameter pores [11]. These values were between 0.25 and 0.67. From these results, it was found to be difficult to prevent

permeation of methanol vapor through small pores of about 4 nm in size. If pore size is not small enough to prevent permeation of methanol molecules, methanol is easy to permeate due to the surface flow or the capillary condensation mechanism. In such a pore, methanol is easy to condense because the saturated vapor pressure is decreased as the pore radius becomes small, according to the Kelvin equation. Therefore, these membranes preferentially permeated methanol (the separation factor of H_2/CH_3OH or He/CH_3OH became small.). On the other hand, the pore size of the membrane reported in this chapter was too small to introduce methanol molecules, so helium permeated dominantly and the separation factor of He/CH_3OH became large. A significant increase of the ratio of the permeances, He/N_2 after the CVD also supports this. However, the pore size distributions of the original porous glass and the membrane prepared by the CVD were almost same as shown in Fig. 7. There were some very narrow parts on the pore entrances by the deposition of silica as schematically indicated in Fig. 9 (a), but the amount was very small. These very narrow parts played a very important role in separation.

5. 6 Conclusions

It is shown that the membrane minimizing permeation of methanol vapor and displaying molecular sieving performance could be synthesized by depositing silica on the porous glass tubes using TEOS as a reactant in the temperature range of 673-773 K. The basic permeation property of methanol vapor in gas phase was investigated. This membrane appears to hinder permeation of methanol vapor. This behavior is quite different from the original porous glass and other reported membranes. The separation factors of He/CH_3OH were 7.1 at 373 K and 16.9 at 473 K. These values are higher than the Knudsen value. The permeances of He and N_2 through this membrane were also measured at varying temperatures in order to investigate the permeation mechanism. Gas permeation through the membrane was predominantly governed by an activated diffusion mechanism.

5. 7 References

1. G.R. Gavalas, C.E. Megiris and S.W. Nam, *Chem. Eng. Sci.*, **44**, 1829 (1989).
2. M. Tsapatsis, S. Kim, S.W. Nam and G. Gavalas, *Ind. Eng. Chem. Res.*, **30**, 2152 (1991).
3. L.G.J.d. Haart, Y.S. Lin, K.J.d. Vries and A.J. Burggraaf, *J. Europ. Ceram. Soc.*, **8**, 59 (1991).
4. Y.S. Lin and A.J. Burggraaf, *AIChE J.*, **38**, 445 (1992).
5. J.C.S. Wu, H. Sabol, G.W. Smith, D.L. Flowers and P.K.T. Liu, *J. Membrane Sci.*, **96**, 275 (1994).
6. S. Morooka, S. Yan, K. Kusakabe and Y. Akiyama, *J. Membrane Sci.*, **101**, 89 (1995).
7. H.Y. Ha, S.W. Nam, T.H. Lim, I.-H. Oh and S.-A. Hong, *J. Membrane Sci.*, **111**, 81 (1996).
8. A. Yabe, *Denki-kyokai-zasshi*, **3**, 27 (1993).
9. H. Ishida, *Nenryo oyobi Nensyou*, **62**, 249 (1995).
10. Q. Liu, R.D. Noble, J.L. Falconer and H.H. Funke, *J. Membrane Sci.*, **117**, 163 (1996).
11. R.D. Noble, J.L. Falconer, M.-D. Jia and T.W. Perkins, *J. Membrane Sci.*, **79**, 123 (1993).
12. T. Yazawa and H. Tanaka, *Ceram. Trans.*, **31**, 213 (1993).
13. S. Brunauer, P.H. Emmett and E. Teller, *J. Am. Chem. Soc.*, **60**, 309 (1938).
14. E.P. Barrett, L.G. Joyner and P.P. Halenda, *J. Am. Chem. Soc.*, **73**, 373 (1951).
15. M.H. Hassan, J.D. Way, P.M. Thoen and A.C. Dillon, *J. Membrane Sci.*, **104**, 27 (1995).
16. A.B. Shelekhim, A.G. Dixon and Y.H. Ma, *J. Membrane Sci.*, **75**, 233 (1992).
17. F.J. Norton, *J. Am. Ceram. Soc.*, **36**, 90 (1953).

Part II-2 Sputtering method

Chapter 6: Preparation of silica membrane and its gas permeation property

6. 1 Abstract

The silica tubular glass membranes with thin, dense silica layers on porous glass supports were prepared by sputtering using the novel sputtering apparatus for tubular supports. This apparatus has holder for tubular supports and a rotation mechanism. The sputtering conditions of the membranes were investigated. It was found that the support temperature of 573 K was the best among the selected temperatures in our experiments. From SEM observation, the surfaces of the membranes became smooth with increasing sputtering time and had no cracks. Permeances of He, N_2 and carbon dioxide were measured at 373 K. The order of permeances for the membranes was 10^{-9} mol•m^{-2}•s^{-1}•Pa^{-1} (10^{-5} cm^3(STP)•cm^{-2}•s^{-1}•cmHg^{-1}). The ratios of permeances, He/N_2, were similar to the theoretical Knudsen value. These values were much lower than the values expected from the dense silica glass. It was considered that this was due to the presence of micro cracks during the sputter deposition.

6. 2 Introduction

The high selectivity of dense silica glass (e.g. fused quartz) at 873-973 K for He and H_2 over N_2, O_2 and Ar is well known [1]. The reason for high selectivity is as followed: He and H_2 can permeate through small free volume of glass network of silica, on the other hand, N_2, O_2 and Ar cannot permeate through such a small free volume. However, permeances of He and H_2 are too small to use in actual usages even at high temperature. To get high permeance, it is important to make the thickness of a silica layer thin.

The sputtering method is very effective to make thin films which cannot be prepared by other methods, such as sol-gel method, electroless plating and so on. Recently, this method is used to make thin effective separation layer on various substrates for inorganic membranes. For instance, Lin et al. reported palladium-silver alloy membranes, which Pd-Ag films were coated on γ-alumina disc [2], and Mercea et al. reported a silica coated PET membrane [3]. In actual membrane separation system, almost actual membrane modules were tubular membranes to get large surface area and mechanical strength. However, these reported membranes were flat membranes and few researcher reported tubular membranes prepared by the sputtering method. Because it is difficult to use a conventional sputtering apparatus for making tubular type membranes. Basil et al. reported the membrane deposited with Pd-Ag alloy on the outer surface of a commercial tubular ceramic membrane with the magnetron sputtering technique [4]. But they didn't investigate the sputtering conditions and didn't succeed in covering the pores with Pd-Ag alloy. The size of the pores remained almost same after alloy deposition. Their experimental equipment and conditions are not described in detail.

There were, however, no reports investigating the preparation of thin silica layer on a tubular membrane with sputtering technique. The objective of this chapter is to report the preparation of

the silica tubular glass membranes with thin, dense silica layers on porous glass substrate by sputtering using the novel sputtering apparatus for tubular supports to improve the gas permeances.

6. 3 Experimental

Silica tubular membranes were prepared by the sputter deposition technique on porous glass supports. Porous glass tubes with mean pore diameter of 4 nm, outer diameter of 5 mm, inner diameter of 4 mm and length of approximately 10 cm were used as the supports.

Silica layers were then coated onto the porous glass supports by a radio-frequency (RF) sputter deposition machine (Model SH-350-D06S, ULVAC JAPAN Ltd.). This machine is a special machine for the sputter deposition of tubular supports and has a holder for tubular supports and a rotation mechanism as shown in Fig. 1. Prior to deposition the supports were heated at 873 K to clean and then placed in the sputtering equipments. SiO_2 glass plate was used as the target for sputtering. The target to support distance was kept constant at 40 mm. Before deposition, the sputtering chamber was evacuated 4.0 X 10^{-5} Pa (3 X 10^{-7} Torr) and then back filled with high purity Ar. All silica layers were deposited at 9.3 X 10^{-1} Pa (7 X 10^{-3} Torr) partial pressure of pure Ar. The RF power was maintained at 500 W and rotation speed was kept constant at 35 rpm. Under this condition, the measured sputtering rate was about 5 nm/min. Before the actual deposition pre-sputtering was done for 5 min to clean the SiO_2 target surface. During pre-sputtering time, the support was masked from the target by means of a shutter. Hence the actual deposition on the support starts only after the target is cleaned completely.

Single gas permeations of the membranes were measured using He, N_2 and carbon dioxide by a procedure described previously [5] for evaluation of the defects of the membranes. One end of the tubular membrane was sealed and the other end was connected to a Pyrex glass tube with epoxy resin. This membrane module was supported in a gas flow cell. The pressure difference of the gases through the membranes was kept at 1.013 X 10^5 Pa (1 atm), and the permeances at 373 K were measured with a mass flow meter.

The surface morphologies of the membranes were studied by a scanning electron microscopy, SEM (JSM-5310LV, JEOL).

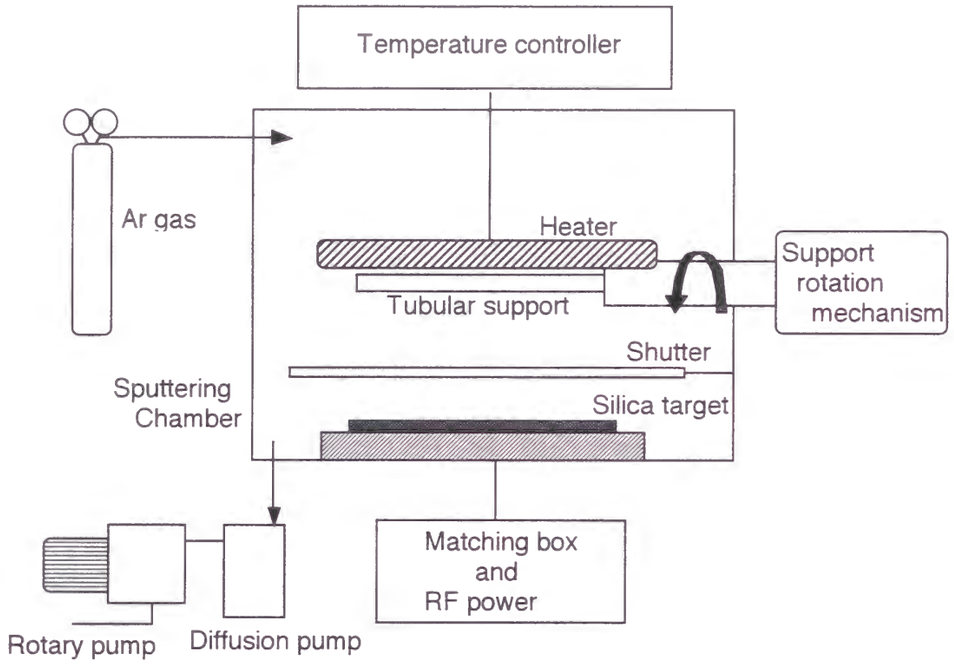

Fig. 1 Schematic diagram of the apparatus used for sputtering deposition.

6. 4 Results and discussions

To optimize the sputtering conditions, first, the support temperature was changed. Table 1 shows the permeances of He, N_2 and CO_2, and the ratios of the permeances, He/N_2 and CO_2/N_2 at 373 K for the membranes with various support temperatures and original porous glass membrane (as support). Sputtering time of 2 hours and other conditions were kept constant. The permeances for the membrane on the support temperature at 573 K (S2) were indicated as the lowest value. These values were less than half of the values for the original porous glass. However, the permeances for the membranes on the other support temperatures were almost the same as those of the original porous glass.

Table 1 The permeances of He, N_2, CO_2, and the ratios of the permeances, He/N_2 and CO_2/N_2 at 373 K for the membranes with various support temperatures (S1, S2, S3) and original porous glass membrane (PG).

Samples	Sputtering temp. (K)	Permeance			The ratio of permeance	
		He	N_2	CO_2	He/N_2	CO_2/N_2
PG	–	26	13	16	2.0	1.2
S1	473	22	11	18	2.0	1.6
S2	573	11	3.7	4.3	2.8	1.2
S3	673	27	12	18	2.2	1.5

Permeance: $X10^{9}$ $mol \cdot m^{-2} \cdot s^{-1} \cdot Pa^{-1}$

SEM photographs of the surface morphologies for those membranes and original porous glass are shown in Fig. 2. Original porous glass had rough surface (Fig. 2 (a)). This rough surface morphology is attributed to the acid leaching treatment for making porous glass. The surface of the membrane on the support temperature at 573 K (Fig. 2 (c)) was smoother than those of the other membranes. This result supports that the permeance for this membrane was indicated as the lowest value. The lowest permeance was due to silica deposited layers covered on the pore. On the other hand, the membranes on the other support temperatures indicated almost the same permeance as the original porous glass and didn't have smooth surfaces (Fig. 2 (b) and (d)). According to the previous paper [6], the microstructure of sputter-deposited coatings was classified as a function of T/T_m (T: substrate temperature, T_m: melting point of coating material). The low temperature ($T/T_m<0.3$) zone 1 structure was columnar, consisting of tapered units defined by voided growth boundaries. The zone 2 structure ($0.3<T/T_m<0.5$) consisted of columnar grains, which defined by metallurgical grain boundaries and increased in width with T/T_m in accordance with activation energies typical of surface diffusion. The high temperature zone 3 ($T/T_m>0.5$) structure consisted of equiaxed grains, which increased in accordance with activation energies typical of bulk diffusion. A fourth zone consisting of a dense array of poorly defined fibrous grains was identified in the region between zones 1 and 2 and termed zone T since it was believed to be a transition state between the two zones. From this model, it is considered that the silica deposition layer didn't become smooth at low support temperature due to the sputtered silica particles couldn't move on the support surface by the surface diffusion (zone 1), and the silica deposition layer became coarse at high support temperature because the particle growth occurred during the deposition (zone 2). Therefore, the membranes under these two conditions didn't have smooth surfaces and the permeances for the membranes were not decreased. From these results, the support temperature of 573 K was the best among the selected temperatures in our experiments.

Secondly, the sputtering time was changed. Permeances of He, N_2 and CO_2 at 373 K for the membranes with various sputtering time and original porous glass membrane (as support) are summarized in Table 2. The permeances for the membranes were 10^{-9} mol•m^{-2}•s^{-1}•Pa^{-1} (10^{-5} cm^3(STP)•cm^{-2}•s^{-1}•cmHg^{-1}) order and decreased comparing with the original porous glass support. Theoretical ratios of permeances, He/N_2 and CO_2/N_2, based on Knudsen flow are 2.6 and 0.8, respectively. The ratios of permeances, He/N_2, were similar to the theoretical Knudsen value. However the ratios of permeances, CO_2/N_2, were higher than that value.

Table 2 The permeances of He, N_2, CO_2, and the ratios of the permeances, He/N_2 and CO_2/N_2 at 373 K for the membranes with various sputtering time (S4, S2, S5) and original porous glass membrane (PG).

Samples	Sputtering time (h)	Permeance			The ratio of permeance	
		He	N_2	CO_2	He/N_2	CO_2/N_2
PG	0	26	13	16	2.0	1.2
S4	1	23	10	16	2.3	1.6
S2	2	11	3.7	4.3	2.8	1.2
S5	4	14	6.0	10	2.3	1.7

Permeance: X10^9 mol•m^{-2}•s^{-1}•Pa^{-1}

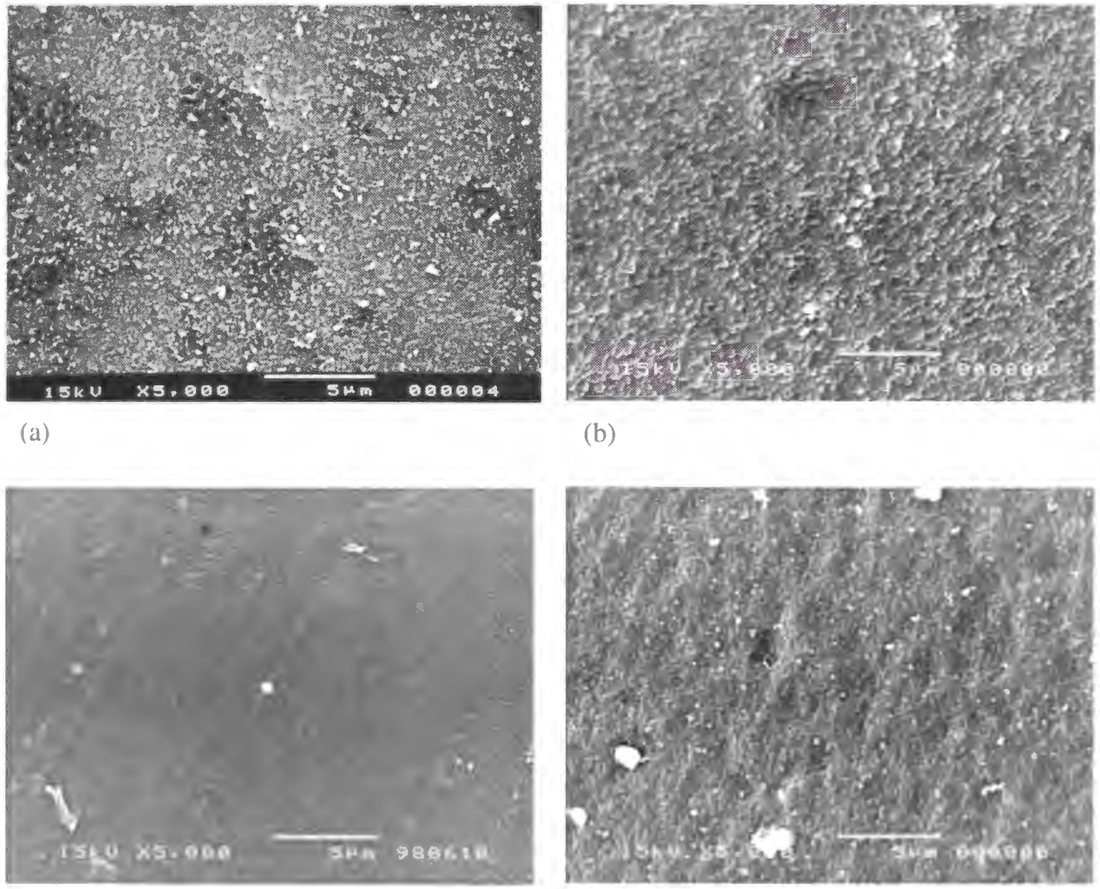

(a) (b)

(c) (d)

Fig. 2 SEM micrographs showing the surface morphology of (a) the original porous glass, (b) the membrane at a support temperature of 473 K, (c) the membrane at a support temperature of 573 K, and (d) the membrane at a support temperature of 673 K.

Figure 3 shows SEM photographs of the surface morphologies for the membranes with various sputtering time and original porous glass. Original porous glass had rough surface (Fig. 3 (a)) as described above. After 1 hour sputtering, the surface of the membrane dramatically became smooth but some coarse particles were observed here and there (Fig. 3 (b)). However, as sputtering time was increased, the surfaces of the membrane became much smooth and no crack was observed in SEM. After 4 hours sputtering, the surface was very smooth and no crack was observed in SEM (Fig. 3 (d)).

From the results of gas permeation, the sputter deposition layers couldn't be prepared as a defect free layer even after 2 and 4 hours sputtering because the ratios of permeances, He/N_2, for the membranes were very small. Those values were expected to be very large value (more than 1000) if the deposition layers were defect free. However, the surfaces of the membranes were smooth and cracks were not observed in SEM. It seems that the ratios of permeances indicated smaller values because the membranes had some micro cracks that couldn't be observed in SEM. The ratios of permeances, CO_2/N_2, for these membranes were larger than the theoretical Knudsen value. For this result, it could be assumed that surface flow of CO_2 might take place in parallel with Knudsen flow. This fact also supported the defects were not macro size because surface flow did not occur in macro pores.

The permeances of the membrane after 2 hours sputtering were smaller than the other membranes. Thickness of deposited layer was estimated to be about 600 nm from sputtering rate under this condition. After 4 hours sputtering, it became about 1200 nm but the permeances became slightly large again. From SEM observation, the surface of the membrane after 4 hours sputtering was smoother than that after 2 hours sputtering and there was no macro crack. On the microscopic scale (about 1 - 10 μm), the result of SEM observation is reasonable because silica continuously deposited on the surface of the membrane during the sputter deposition. However it is

difficult to explain the result of gas permeation. Although the reason of this phenomenon is not clearly proved, it is considered that the increase of the permeances was due to generation of micro cracks, which couldn't be observed with SEM, in the deposition layer after 4 hours sputtering. A deposition layer on a tubular support seems to have a large stress compared with that on a flat support because of its curvature. This stress makes sputtering on a tubular support more difficult. Consequently, as the deposition layer became thicker, the stress became larger and the generation of micro cracks occurred more easily. This caused the permeances became slightly large after 4 hours sputtering and the ratios of the permeances, He/N_2, for the membranes were small.

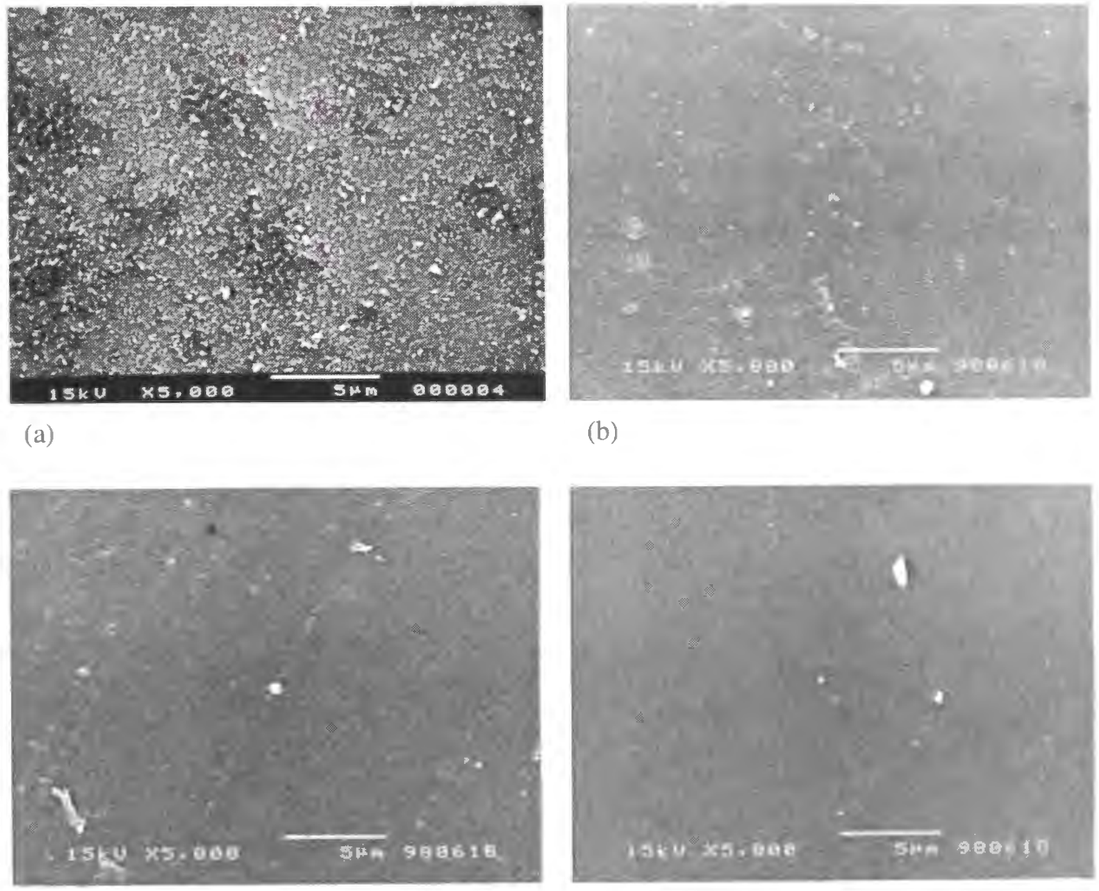

Fig. 3 SEM micrographs showing the surface morphology of (a) the original porous glass, (b) the membrane after sputtering for 1 h, (c) the membrane after sputtering for 2 h, and (d) the membrane after sputtering for 4 h.

6. 5 Conclusions

The silica tubular glass membranes with thin, dense silica layer on porous glass supports were prepared by sputtering using the novel sputtering apparatus for tubular supports, and the sputtering conditions of the membranes were investigated.

The support temperature of 573 K was the best among the selected temperatures in our experiments. From SEM observations, the surface of the membranes became much smooth as sputtering time was increased and there was no macro crack. However, the ratios of permeances, He/N_2, were similar to the theoretical Knudsen value (He/N_2=2.6). These values were much lower than the value expected from the dense silica glass (more than 1000). It was considered that this was due to the generation of micro cracks during the sputter deposition.

6. 6 References

1. F.J. Norton, *J. Am. Ceram. Soc.*, **36**, 90-96 (1953).
2. V. Jayaraman and Y.S. Lin, *J. Membrane Sci.*, **104**, 251-262 (1995).
3. P. Mercea and M. Bârçan, *J. Membrane Sci.*, **59**, 353-358 (1991).
4. A. Basile, E. Drioli, F. Santella, V. Violante, G. Capannelli and G. Vitulli, *Gas. Sep. Purif.*, **10**, 53-61 (1996).
5. T. Yazawa and H. Tanaka, *Ceram. Trans.*, **31**, 213-222 (1993).
6. J.H. Thornton, *J. Vac. Sci. Technol. A*, **4**, 3059-3065 (1986).

Part III Surface modification by organosilane compounds

Chapter 7: Preparation of surface modified porous glass membrane and its hydrocarbon gases separation property

7. 1 Abstract

The synthesis and properties of the surface modified porous glass membranes using organosilane compounds with different hydrocarbon length, $C_nH_{2n+1}(CH_3)_2SiCl$ (n=1, 3, 8, 18) are described. Single gas permeations through the membranes were measured at 298 K, and 333 K and 373 K using He, N_2, CO_2, CH_4, C_2H_6, C_3H_8, n-C_4H_{10} and i-C_4H_{10}. The membranes indicated highly selective separation of hydrocarbon gases with high permeances. Hydrocarbon gas selectivities were increased with increased carbon chain length of hydrocarbon gases and with increased carbon chain length of organosilane compounds which were used for the surface modification. For C18 membrane (surface modified with dimethyloctadecylchlorosilane), the ratios of the permeances, n-C_4H_{10}/N_2 were 66.6 at 298 K, 22.5 at 333 K and 14.0 at 373 K, respectively. The value at 298 K is about 100 times as large as the theoretical Knudsen value (n-C_4H_{10}/N_2=0.69). The binary gas permeation at 373 K was also investigated using a gas mixture of 90% CH_4 and 10% n-C_4H_{10}. The ideal separation factor of n-C_4H_{10}/CH_4 through C18 membrane was 8.8. This value was higher than that from single gas measurement due to hindering of adsorbed molecules. To evaluate adsorption affinities of hydrocarbon gases, CH_4, C_2H_6, C_3H_8, n-C_4H_{10} and i-C_4H_{10}, on the surface modified membranes at high temperature, dynamic flow adsorption measurement was performed at 373 K. All the isotherms obtained in the present work were almost followed Henry's adsorption equation due to the low relative pressures. Adsorption amounts of hydrocarbon gases were increased with increasing length of carbon chain of organosilane compounds.

7. 2 Introduction

In general, almost all membranes used in industrial gas separation are organic polymer membranes except for Pd membranes. The main advantage of organic polymers is its easy handling and its functionality (high selectivity). However, organic polymer membranes have several limitations; low permeance, high temperature instability, swelling and decomposition in organic solvents. These limitations can be overcome by inorganic membranes. Several approaches are known for preparation of inorganic membranes [123]: phase separation and acid leaching, particle dispersion and slipcasting, anodic oxidation, sol-gel methods. Porous glasses having narrow pore distribution are made using phase separation and acid leaching [456]. However, smallest pore diameter of porous glass prepared by this method is 4 nm. This size is slightly large for gas separation. Permeance of gases is much higher than that of organic polymer membranes, but selectivity is low.

It is well-known that organosilane compounds such as chlorosilane compounds are easy to react with any kind of hydroxyl groups, generating hydrochloric acid. To utilize this reaction, organic functional groups can be introduced on the surface of porous glasses with covalent bonds [7]. The chemical reaction between silanols on the porous glass surface and organosilane compounds can be described as shown in Fig. 1. Surface modification of porous glass membranes by covalently bonded molecular monolayer is a special way to alter membrane performance. These surface modified membranes are expected to show high thermal stability, high permeance with organic functionality (high selectivity). This is due to the existence of rigid inorganic pores and covalently bonded organic monolayer.

In this chapter, the author reports preparation of the surface modified porous glass membranes using organosilane compounds with different hydrocarbon length, $C_nH_{2n+1}(CH_3)_2SiCl$ (n=1, 3, 8, 18). Thermal stability of these membranes and its adsorption property for hydrocarbon

gases at 373 K were investigated. Single gas permeation of hydrocarbon gases and permeation of binary gas (n-C_4H_{10}-CH_4) were also investigated.

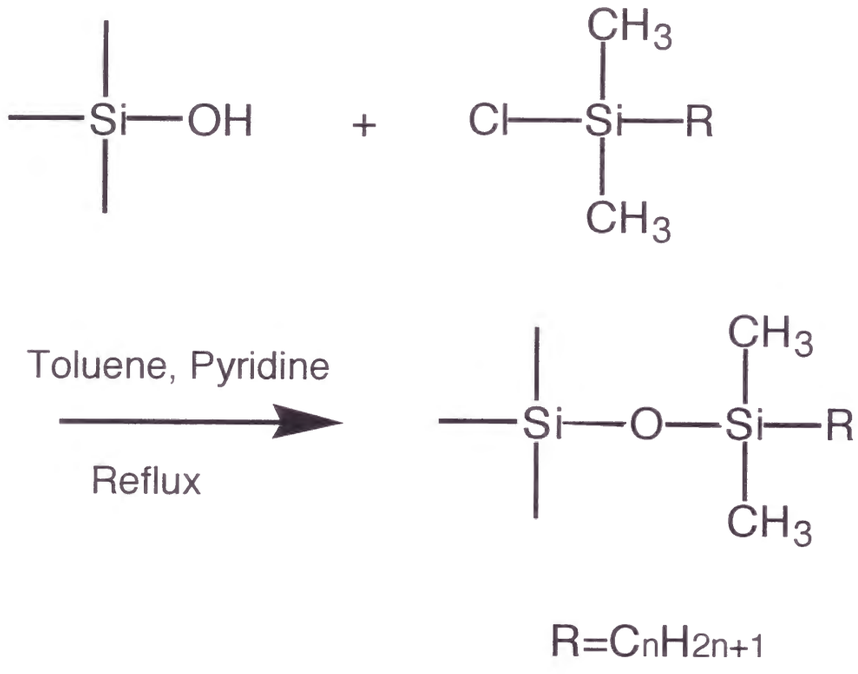

Fig. 1 Schematic of the reaction between silanol groups and organosilane compounds.

7. 3 Experimental

7. 3. 1 Membrane modification by organosilane compounds

Porous glass tubes with mean pore diameter of 4 nm, outer diameter of 5 mm, inner diameter of 4 mm, and length of approximately 10 cm were used as the supports. Before surface modification being done, the porous glass tube was dehydrated at 443 K for 3 hours in vacuum to evaporate molecular water which was harmful to the surface modification as well as to leave only surface hydroxyl groups. This porous glass tube was introduced in a flask equipped with a reflux condenser. The organosilane compounds used in this chapter were trimethylchlorosilane, dimethylpropylchlorosilane, dimethyloctylchlorosilane and dimethyloctadecylchlorosilane. Commercially available reagent grade chemicals were used. A mixture of 1.3 g of organosilane compound and 30 ml dry toluene was introduced in the flask and the porous glass tube then being completely immersed in the mixture. After 10 minutes, 1 ml pyrizine was added into the flask to neutralize the reaction product, hydrochloric acid. And it was refluxed at 383 K for 20 hours. After reflux, the porous glass tube was removed, and the mixture was refluxed again in dry toluene at 383 K for 3 hours to remove unreacted organosilane compounds and reaction products. Then the surface modified membranes were reheat-treated at 373 K for several hours in vacuum to evaporate toluene trapped in the membranes. The surface modified membranes synthesized by the above method are described as C0 membrane (the original porous glass), C1 membrane (using trimethylchlorosilane), C3 membrane (using dimethylpropylchlorosilane), C8 membrane (using dimethyloctylchlorosilane) and C18 membrane (using dimethyloctadecylchlorosilane).

7. 3. 2 Measurement of gas permeation

Single gas permeations through the membranes were measured at 298 K, and 333 K and 373 K using He, N_2, CO_2, CH_4, C_2H_6, C_3H_8, n-C_4H_{10} and i-C_4H_{10} by the same procedure described previously [8] after drying at 373 K in a vacuum oven. One end of the tubular membrane was sealed and the other end was connected to a Pyrex glass tube with epoxy resin. The membrane modules were supported in a gas flow cell. Pressure differences of the gases through the membranes were kept constants and the permeances were measured by a mass flow meter.

Due to evaluate hydrocarbon gas separation characteristics, binary gas separation of the membranes was measured at 373 K using a gas mixture of 90% CH_4 and 10% n-C_4H_{10} as the feed gas. The experimental apparatus is shown in Fig. 2. The membrane module prepared by the same procedure described above was supported in a gas flow cell. The gas mixture of 90% CH_4 and 10% n-C_4H_{10} was introduced into the gas flow cell. Pressure of the feed gas was kept at 2 atm (2.026×10^5 Pa) and the permeate gas was introduced to a gas chromatography. Gas compositions of the feed and permeate gas were analyzed by gas chromatography (Shimadzu GC-14A, Shimadzu) with a thermal conductivity detector.

The ideal separation factor of n-C_4H_{10}/CH_4 was calculated from mole fraction of n-C_4H_{10} in the feed gas, in the permeate gas and by using the following equation [9].

$$\alpha = \frac{y_A}{1 - y_A} \frac{1 - x_A - \Phi(1 - y_A)}{x_A - \Phi y_A} \quad (1)$$

$$\Phi = \gamma + \theta - \gamma\theta \quad (2)$$

$$\gamma = \frac{P_l}{P_h} \quad (3)$$

$$\theta = \frac{F_p}{F_f} \quad (4)$$

where: y_A=mole fraction of n-C_4H_{10} in feed gas, x_A=mole fraction of n-C_4H_{10} in permeate gas, Φ=operating factor, γ=operating pressure ratio, θ=cut, P_l=pressure of downstream, P_h=pressure of upstream, F_p=flux of permeate, F_f=flux of feed.

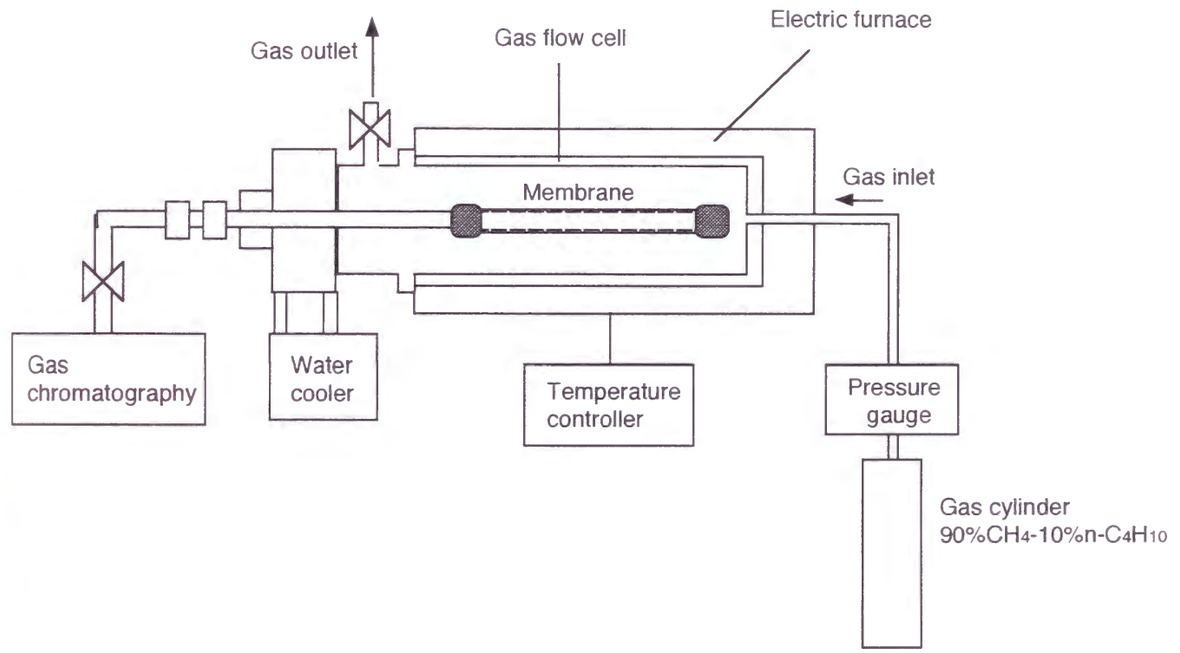

Fig. 2 Schematic diagram of the apparatus used for binary gas permeation measurement.

7. 3. 3 Pore size measurement

The specific surface areas and the pore volumes of the original porous glass membrane and the surface modified membranes were measured by nitrogen adsorption (BELSORP 28, BEL JAPAN Inc.) to evaluate the pore structures of the membranes. The specific surface areas were determined by BET plots [10] and the pore size distributions were analyzed by BJH method [11].

7. 3. 4 Thermal stability measurement

Thermal stability of the samples was measured by thermal gravimetric analysis (TGA) using TGA equipment (TGA-7, Perkin Elmer). Powder sample was prepared by the same procedure described above. The TGA experiments were performed with a heating rate of 5 K/min to 773 K in an air.

7. 3. 5 Adsorption measurement of hydrocarbons

Gravimetric set-up was used to obtain dynamic flow adsorption data at 373 K for hydrocarbons. The experimental set-up for adsorption measurement is shown in Fig. 3. An electro-microbalance (TGA-7, Perkin Elmer) was used to measure the changes in the sample weight. Original porous glass and surface modified samples were prepared by the same procedure described above. The samples were crushed and sieved to particle size of 149-420 μm (35-100 mesh). This powder sample was set to a quartz glass cell in the electro-microbalance. Base gas (N_2) and hydrocarbon gases (CH_4, C_2H_6, C_3H_8, n-C_4H_{10} and i-C_4H_{10}) were mixed with certain ratios, and total flux was kept 100 ml/min. Before measurements, the samples were set in the equipment at 373 K and N_2 flowed until the samples were dried completely.

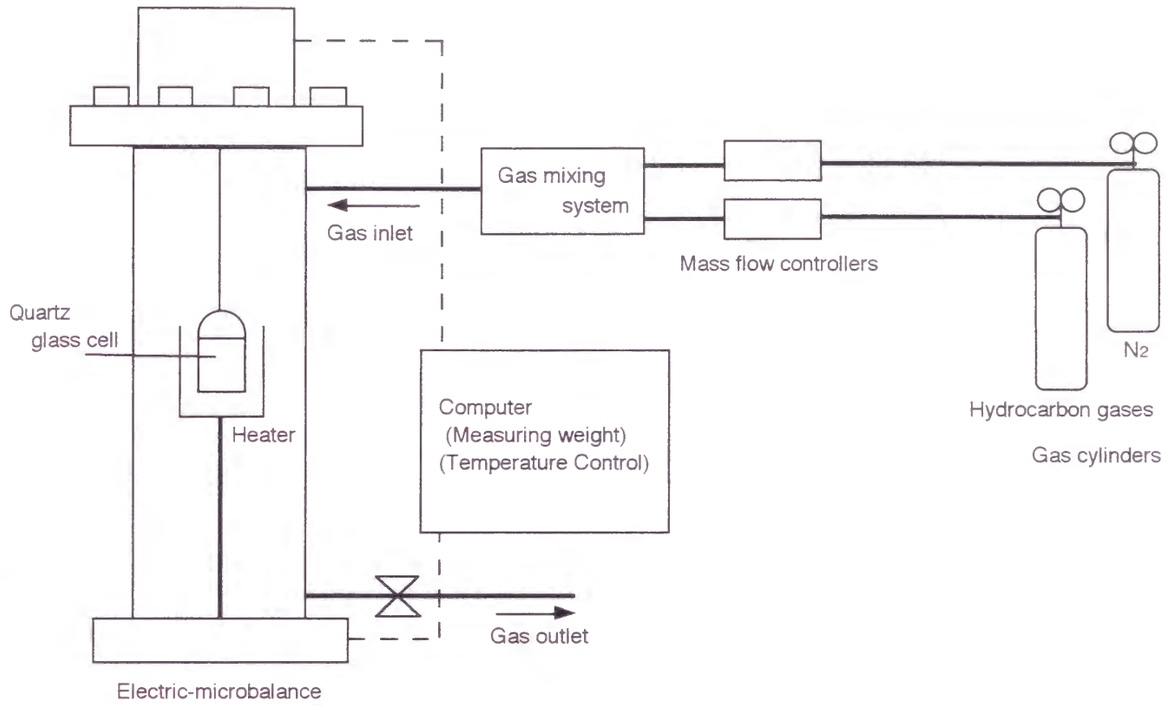

Fig. 3 Schematic representation of the apparatus for adsorption measurement.

7. 4 Results

7. 4. 1 Surface areas and pore volumes of the membranes

N_2 adsorption-desorption isotherms at 77 K of the surface modified membranes are shown in Fig. 4. These isotherms were the so-called type IV isotherm. Type IV isotherm follows the BDDT classification, which was originally proposed by Brunaer, Deming, Deming and Teller [12, 13]. This isotherm is characteristic of adsorption-desorption on mesoporous solid and is characterized by a hysteresis loop. Amounts of adsorption were decreased with increasing length of carbon chain of organosilane compounds. Specific surface area values based on BET plots [10] and pore volumes of the membranes are presented in Table 1. These two values were also decreased with increasing length of carbon chain of organosilane compounds.

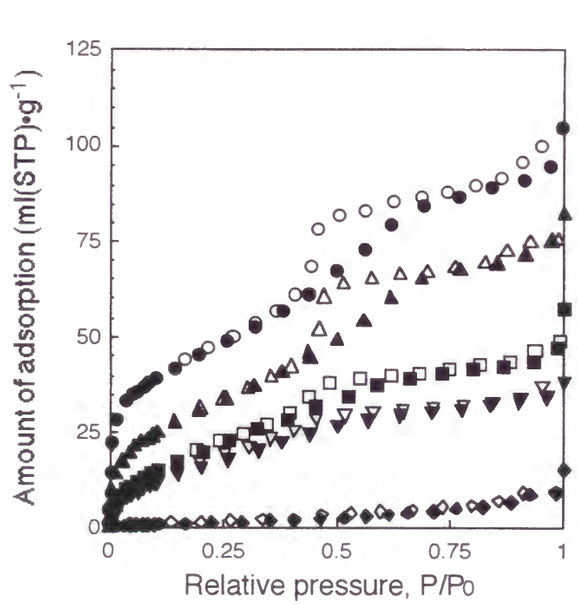

Fig. 4 N_2 adsorption-desorption isotherms of C0 (○), C1 (△), C3 (□), C8 (▽) and C18 membrane (◇); solid symbols: adsorption, open symbols: desorption.

Table 1 Specific surface areas and pore volumes of C0, C1, C3, C8 and C18 membrane.

Sample	Specific surface area ($m^2 \cdot g^{-1}$)	Pore volume ($cm^3 \cdot g^{-1}$)
C0	162.0	0.143
C1	117.4	0.113
C3	81.3	0.073
C8	65.9	0.053
C18	5.9	0.017

7. 4. 2 Thermal stability of the membranes

Figure 5 shows relative weight loss of the surface modified membranes at temperatures between 323-773 K. At 773 K, relative weight loss of C0, C1, C3, C8 and C18 membrane were 4.2, 7.5, 9.1, 12.1 and 8.8 % respectively. The weight loss of the membranes except for C18 membrane was increased with increasing length of carbon chain of organosilane compounds. About C18 membrane, it is considered that not all carbon atoms of octadecyl groups were removed from C18 membrane because the pores of C18 membranes were almost filled with C-H chains. At 373 K, relative weight losses of all membranes were less than 1.2 %. And the permeances of gases were not changed after measuring at 373 K. From these results, it is considered that these surface modified membranes were stable at least at 373 K. Because the main component of the surface modified membranes was inorganic material (a porous glass) and the covalent bonds between silanol and organosilane compounds were strong. Thus, the membranes were stable at high temperature.

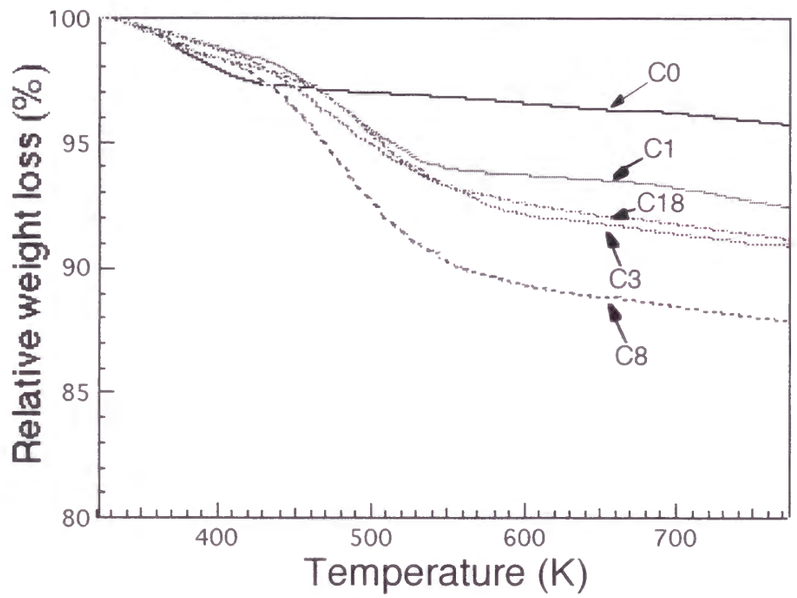

Fig. 5 Relative weight loss of C0, C1, C3, C8 and C18 membrane at temperatures between 323 K-773 K.

7. 4. 3 Single gas permeation measurement

Table 2 shows ratio of the permeance, CH_4, C_2H_6, C_3H_8, n-C_4H_{10}, i-C_4H_{10}/N_2 and n-C_4H_{10}/CH_4, through the surface modified membranes at 298 K, 333 K and 373 K. Theoretical ratios of the permeances based on the Knudsen flow are also indicated in the footnote of Table 2. The surface modified membranes indicated highly hydrocarbon gas selectivity even at high temperature. For C18 membrane, the ratios of the permeances, n-C_4H_{10}/N_2 were 66.6 at 298 K, 22.5 at 333 K and 14.0 at 373 K. The value at 298 K is about 100 times as large as the theoretical Knudsen value (n-C_4H_{10}/N_2=0.69). The ratios of the permeances, n-C_4H_{10}/CH_4, through the surface modified membranes were also higher than theoretical Knudsen value (n-C_4H_{10}/CH_4=0.53). For C18 membrane, even at 373 K, this value was kept high (n-C_4H_{10}/CH_4=6.7). This value is more than 10 times as large as the theoretical Knudsen value.

Table 2 Ratio of permeances, CH_4, C_2H_6, C_3H_8, n-C_4H_{10}, i-C_4H_{10}/N_2 and n-C_4H_{10}/CH_4, through C1, C3, C8 and C18 membrane at 298 K, 333 K and 373 K.

Sample	Temp. (K)	Ratio of permeances					
		CH_4/N_2	C_2H_6/N_2	C_3H_8/N_2	n-C_4H_{10}/N_2	i-C_4H_{10}/N_2	n-C_4H_{10}/CH_4
C1	298	1.5	2.2	3.0	8.5	4.5	5.5
	333	1.5	1.9	2.3	3.6	2.8	2.3
	373	1.6	1.9	2.4	4.1	3.0	2.6
C3	298	1.6	2.0	3.2	9.0	5.0	5.7
	333	1.6	2.1	2.5	4.2	3.3	2.6
	373	1.6	2.0	2.4	4.4	3.9	2.8
C8	298	1.8	3.3	5.2	6.8	4.8	3.7
	333	2.0	3.7	5.1	6.8	5.8	3.3
	373	1.8	3.0	3.9	6.9	5.5	3.9
C18	298	5.2	15.9	48.3	66.6	45.0	12.9
	333	2.8	6.2	11.5	22.5	16.8	8.2
	373	2.1	4.9	8.6	14.0	12.6	6.7

Theoretical Knudsen values: CH_4/N_2=1.3, C_2H_6/N_2=0.97, C_3H_8/N_2=0.80, n-C_4H_{10}/N_2=0.69, i-C_4H_{10}/N_2=0.69, n-C_4H_{10}/CH_4=0.53

Figures 6-9 show the relationships between the permeances of He, N_2, CO_2, CH_4, C_2H_6, C_3H_8, n-C_4H_{10}, i-C_4H_{10} and temperatures through the surface modified membranes. The permeances through the membranes were 10^{-11} to 10^{-7} mol•m^{-2}•s^{-1}•Pa^{-1}. The permeances of He, N_2, CO_2 through the membranes except for C18 membrane were decreased with increased temperature suggesting that these gas permeation through the membranes were predominantly governed by the Knudsen diffusion. However, those permeances through C18 membranes were increased with increased temperature. Thus, it was considered that the gas permeation through this membrane was predominantly governed by the activated diffusion mechanism. The length of octadecyl group is about 2.5 nm. This length was almost same as pore radius of original porous glass (mean pore diameter of 4 nm) and the pores of C18 membrane were supposed to be filled with C-H chains of dimethyloctadecylchlorosilane. This was supported by the result that the pore volume measured by N_2 adsorption were very small (see Table 1). He, N_2, CO_2 can permeate through the space of C-H chains. Therefore, C18 membrane had dense structure, having micropores, which the activated diffusion mechanism occurred. The permeances of hydrocarbon gases through the surface modified membranes were higher than those of N_2. The differences between the permeances of hydrocarbon gases and those of N_2 were increased with increased length of carbon chains of organosilane compounds.

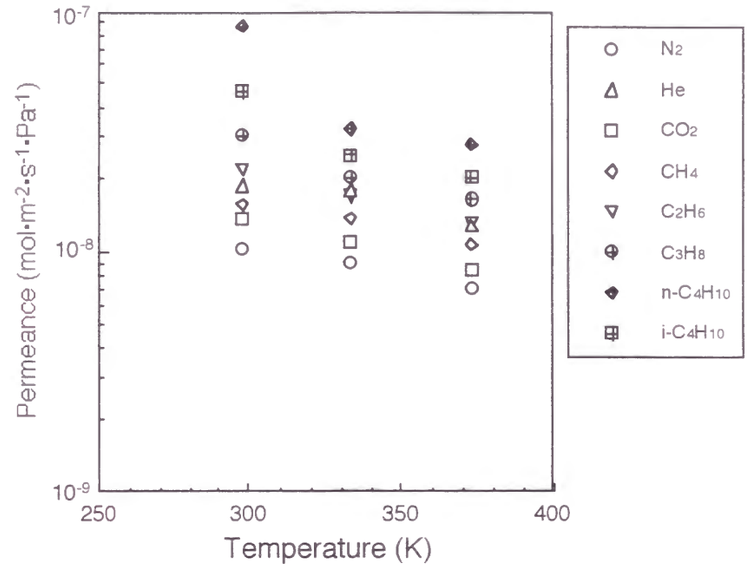

Fig. 6 Relations between the permeances of gases and temperatures through C1 membrane.

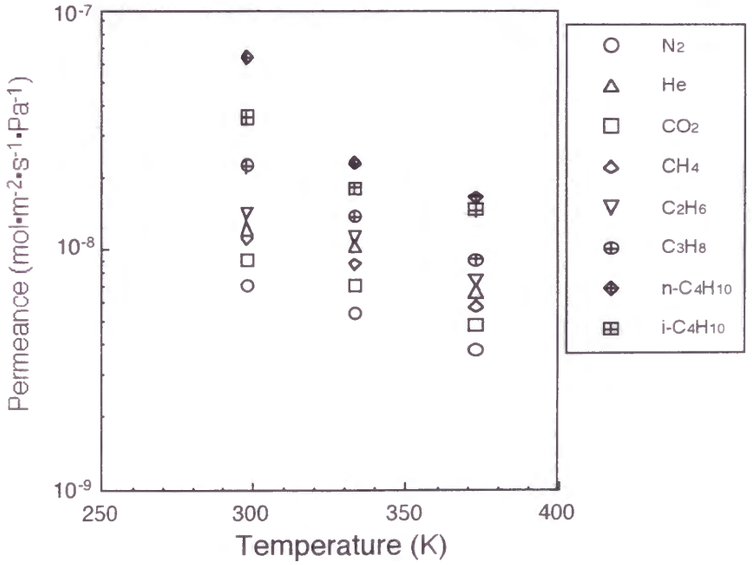

Fig. 7 Relations between the permeances of gases and temperatures through C3 membrane.

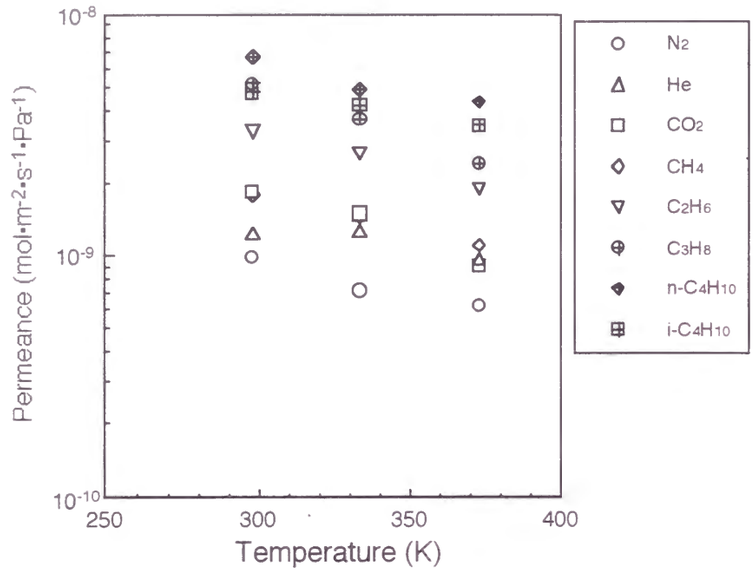

Fig. 8 Relations between the permeances of gases and temperatures through C8 membrane.

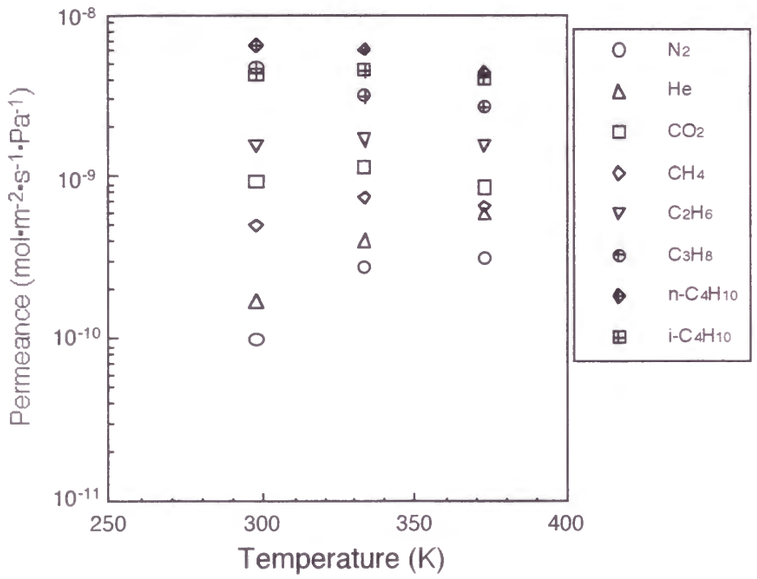

Fig. 9 Relations between the permeances of gases and temperatures through C18 membrane.

7. 4. 4 Binary gas permeation measurement

Table 3 shows the ideal separation factors of n-C_4H_{10}/CH_4 from single gas measurement and binary gas measurement at 373 K. The ideal separation factors from binary gas measurement through C8 and C18 membranes were higher than those of the single gas measurement. However, the ideal separation factors from binary gas measurement through C1 and C3 membranes were almost same as those of the single gas measurement. One of the reasons considerably attributes to the spaces in the pores of the surface modified membranes. The pores of C1 and C3 membranes were not filled with C-H chains due to their short carbon chain length, and CH_4 molecules can by-pass the strongly adsorbed n-C_4H_{10} molecules through the spaces in the pores. On the other hand, C8 and C18 membranes were almost filled with C-H chains, and the strongly adsorbed n-C_4H_{10} molecules were hindered permeation of CH_4. Therefore, ideal separation factor of n-C_4H_{10}/CH_4 from binary gas measurement was higher than that from single gas measurement.

Table 3 Ideal separation factors of n-C_4H_{10}/CH_4 from single gas measurement and binary gas measurement at 373 K for C1, C3, C8 and C18 membrane.

Sample	Ideal separation factor of n-C_4H_{10}/CH_4	
	From single gas measurement	From binary gas measurement
C1	2.6	2.1
C3	2.8	2.5
C8	3.9	5.3
C18	6.7	8.8

At 373 K

Theoretical Knudsen value: n-C_4H_{10}/CH_4=0.53

7. 4. 5 Adsorption of hydrocarbon gases

To investigate adsorption affinities of hydrocarbon gases on the surface modified membranes at high temperature, dynamic flow adsorption measurement was performed at 373 K. Adsorption isotherms at 373 K of CH_4, C_2H_6, C_3H_8, n-C_4H_{10} and i-C_4H_{10} on the surface modified membranes are presented in Fig. 10-13. All the isotherms obtained in the present work were almost followed Henry's adsorption equation due to the low relative pressures [14]. Adsorption amounts of hydrocarbons were increased with increasing length of carbon chain in surface modified agents. Table 4 shows solubility constant, based on Henry's equation, of C_3H_8, n-C_4H_{10} and i-C_4H_{10} for the surface modified membranes. Adsorption amounts of CH_4 and C_2H_6 for the membranes were too small to calculate solubility constants. Solubility constant for C18 membrane was the largest of all. The values for C_3H_8, n-C_4H_{10} and i-C_4H_{10} were 13.0, 41.0 and 32.8 respectively. These values were the same order as those of polyethylene films at 298 K reported previously [15]. Therefore, the surface modified membranes had high affinity for hydrocarbon gases even at high temperature. Thus the surface modified membranes indicated highly selective separation of hydrocarbon gases even at 373 K.

Table 4 Solubility constants of C_3H_8, n-C_4H_{10}, i-C_4H_{10} for C1, C3, C8 and C18 membrane.

Sample	Solubility constant X 10^6 (ml(STP)•g^{-1}•Pa^{-1})		
	C_3H_8	n-C_4H_{10}	i-C_4H_{10}
C1	9.26	27.3	22.3
C3	9.19	30.3	24.4
C8	12.0	39.1	31.6
C18	13.0	41.0	32.8

at 373 K

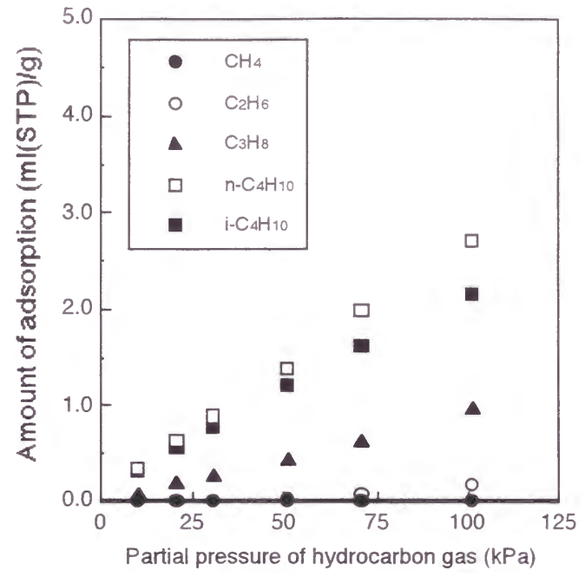

Fig. 10 Adsorption isotherms of hydrocarbon gases on C1 membrane at 373 K.

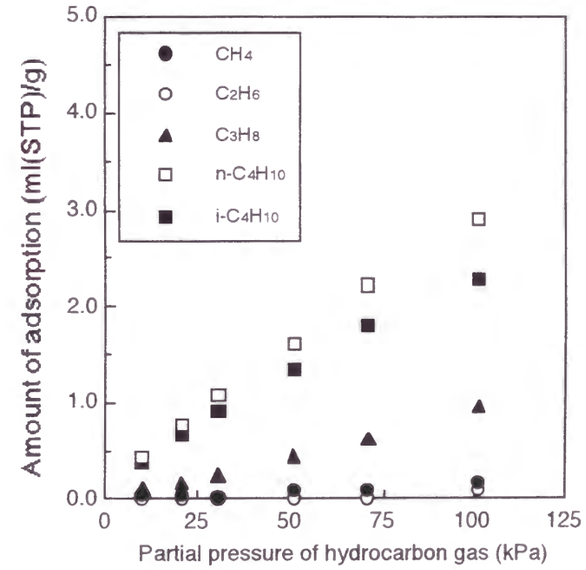

Fig. 11 Adsorption isotherms of hydrocarbon gases on C3 membrane at 373 K.

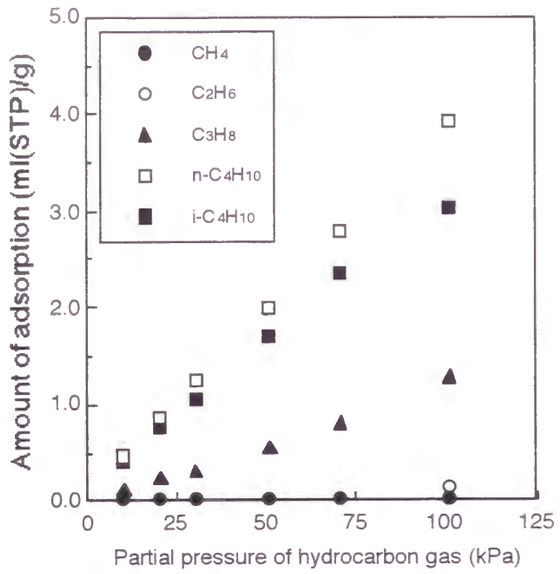

Fig. 12 Adsorption isotherms of hydrocarbon gases on C8 membrane at 373 K.

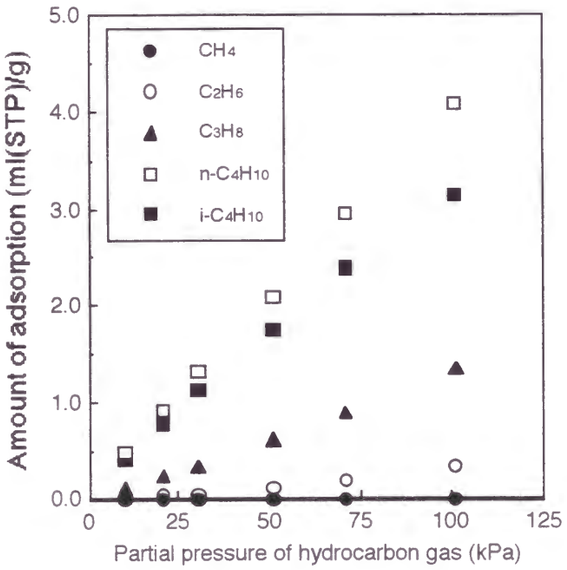

Fig. 13 Adsorption isotherms of hydrocarbon gases on C18 membrane at 373 K.

7. 5 Discussion

7. 5. 1 Pore structure of the surface modified membranes

The amounts of N_2 adsorption, the specific surface areas and the pore volumes of the surface modified membranes were decreased with increased length of carbon chain of organosilane compounds used for surface modification as shown in Fig. 4 and Table 1. The organosilane compounds were reacted with silanol groups in the pores. From these results, it is suggested that the pore structure of the surface modified membranes is schematically shown in Fig. 14. Therefore, the pores were filled with C-H chains with increased length of carbon chains and the amounts of adsorption, specific surface areas and pore volumes were decreased. Estimated values of surface modification amounts from the changes of the pore volumes, using density of organosilane compounds, were about 2.0-4.0 μmol/m^2. These values were similar to the reported values of surface modified porous glasses previously [7] and the almost same as the amounts of silanol for the porous glasses [16]. From these results, it is considered that organosilane compounds were successfully introduced on the pore surface and they covered pore surface as indicated in Fig. 14.

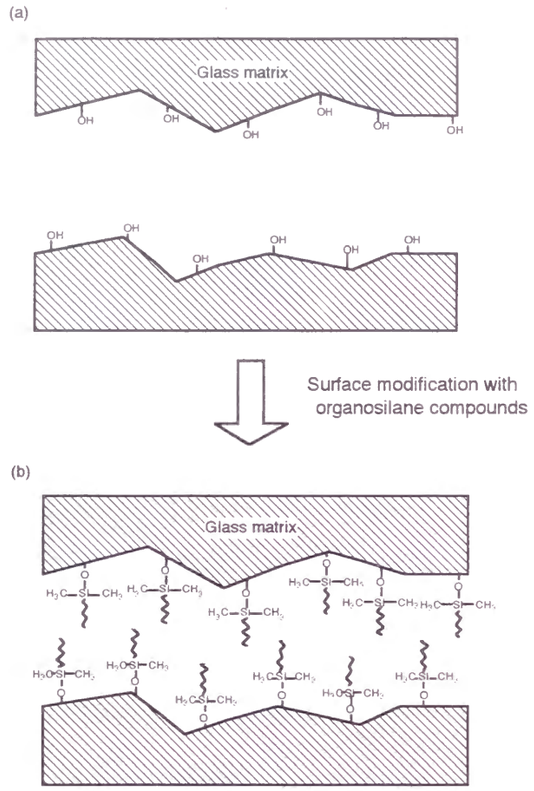

Fig. 14 Schematic representation of the pore structure of the surface modified membranes: (a) before surface modification, (b) after surface modification.

7. 5. 2 Hydrocarbon gases separation

The results presented in the previous section indicated that the surface modified membranes were highly selective membranes for hydrocarbon gases even at high temperature. Hydrocarbon gas selectivities were increased with increased carbon chain length of hydrocarbon gases and with increased carbon chain length of organosilane compounds which were used for the surface modification as indicated in Table 2. However, these selectivity were decreased with increasing temperature. The ratios of the permeances, n-C_4H_{10}/N_2 through C18 membrane were 66.6 at 298 K and 14.0 at 373 K. These values were considerably higher than those of polyethylene films, which

composed of C-H chains, reported previously (n-C_4H_{10}/N_2=10.4 at 298 K) [15]. The ratios of the permeance, n-C_4H_{10}/CH_4, through the surface modified membranes were also high. These high selectivities for hydrocarbon gases were thought to be due to affinity of C-H chains introduced by surface modification for hydrocarbon gases. Longer C-H chains (C18) had higher affinity for hydrocarbon gases. Thus, C18 membrane indicated the highest selectivity among all membranes.

The permeability coefficients of He, N_2, CO_2, CH_4, C_2H_6, C_3H_8, n-C_4H_{10}, i-C_4H_{10} through the surface modified membranes were $5X10^{-14}$ to $5X10^{-11}$ mol•m•m^{-2}•s^{-1}•Pa^{-1}. Theses values were about more than 1000 times as high as those of polyethylene films reported previously [15]. The surface modified membranes had rigid pores attributed to inorganic nature. This maintains permeation pass of the gases in the membranes. Therefore, the surface modified membranes indicated high gas permeances compared to the polyethylene films. The permeances of C_3H_8, n-C_4H_{10} and i-C_4H_{10} through the surface modified membranes were higher than those of He and N_2 as presented in Fig. 6-9. The differences between the permeances of hydrocarbon gases and those of He and N_2 were increased with increased length of carbon chains of organosilane compounds. The adsorption amounts of C_3H_8, n-C_4H_{10} and i-C_4H_{10} on the surface modified membranes were large even at high temperature as shown in Fig. 10-13. These results imply that the surface modified membranes had strong affinity for these gases. Therefore, it is considered that the surface modified membranes had strong affinity for hydrocarbon gases and hydrocarbon gases were preferentially permeated through the membranes by the surface diffusion or solubility diffusion mechanism.

7. 6 Conclusions

The surface modified porous glass membranes were prepared by surface modification using organosilane compounds with different hydrocarbon length, $C_nH_{2n+1}(CH_3)_2SiCl$ (n=1, 3, 8, 18). It was found that organosilane compounds were successfully introduced onto the pore surface completely and they covered pore surface from N_2 adsorption measurement, and these membranes were stable at 373 K from TGA analysis. The single gas permeation of He, N_2, CO_2, CH_4, C_2H_6, C_3H_8, n-C_4H_{10} and i-C_4H_{10} were measured at 298 K, 333 K and 373 K. The membranes indicated highly selective separation of hydrocarbon gases with high permeances. Hydrocarbon gas selectivities were increased with increased carbon chain length of hydrocarbon gases and with increased carbon chain length of organosilane compounds which were used for the surface modification. For C18 membrane (surface modified with dimethyloctadecylchlorosilane), the ratios of the permeances, n-C_4H_{10}/N_2 were 66.6 at 298 K, 22.5 at 333 K and 14.0 at 373 K. The value at 298 K is about 100 times as large as the theoretical Knudsen value (n-C_4H_{10}/N_2=0.69). The binary gas permeation at 373 K was also investigated using a gas mixture of 90% CH_4 and 10% n-C_4H_{10}. The ideal separation factor of n-C_4H_{10}/CH_4 through C18 membrane was 8.8. This value was higher than that from single gas measurement due to hindering of adsorbed molecules. To evaluate adsorption affinities of hydrocarbon gases, CH_4, C_2H_6, C_3H_8, n-C_4H_{10} and i-C_4H_{10}, on the surface modified membranes at high temperature, dynamic flow adsorption measurement was performed at 373 K. All the isotherms obtained in the present work were almost followed Henry's adsorption equation due to the low relative pressures. Adsorption amounts of hydrocarbons were increased with increasing length of carbon chains of organosilane compounds.

7. 7 References

1. R.R. Bhave, *Inorganic membranes synthesis, characteristics and applications* (CHAPMAN & HALL, London, 1991).
2. H.P. Hsieh, *Inorganic membranes for separation and reaction* (ELSEVIER, Amsterdam, 1996).
3. A.J. Burggraaf and L. Cot, *Fundamentals of inorganic membrane science and technology* (ELSEVIER SCIENCE B.V., Amsterdam, 1996).
4. H.P. Hood and M.E. Nordberg, USA Patent, 2,106,744 (1938).
5. H.P. Hood and M.E. Nordberg, USA Patent, 2,221,709 (1940).
6. O.V. Mazurin and E.A. Porai-Koshits, *Phase separation in glass* (Elsevier Science Publishers B. V., Amsterdam, 1984).
7. T. Yazawa, H. Tanaka and K. Eguchi, *J. Ceram. Soc. Japan*, **96**, 630 (1988).
8. T. Yazawa and H. Tanaka, *Ceram. Trans.*, **31**, 213 (1993).
9. The Membrane Society of Japan, *Designs for membrane separation processes* (Kitami syobo, Tokyo, 1985).
10. S. Brunauer, P.H. Emmett and E. Teller, *J. Am. Chem. Soc.*, **60**, 309 (1938).
11. E.P. Barrett, L.G. Joyner and P.P. Halenda, *J. Am. Chem. Soc.*, **73**, 373 (1951).
12. S. Brunauer, L.S. Deming, W.E. Deming and E. Teller, *J. Am. Ceram. Soc.*, **62**, 1723 (1940).
13. S.J. Gregg and K.S.W. Sing, *Adsorption, surface area and porosity* (ACADEMIC PRESS INC. (LONDON) LTD, London, 1982).
14. D.M. Young and A.D. Crowell, *Pysical adsorption of gases* (Butterworth & Co. Ltd., London, 1962).
15. W.W. Brandt, *J. Polymer Sci.*, **41**, 403 (1959).
16. T. Yazawa, H. Nakamichi, H. Tanaka and K. Eguchi, *J. Ceram. Soc. Japan*, **95**, 1186 (1987).

List of Publications

Chapter 1. K. Kuraoka, H. Tanaka and T. Yazawa, *J. Mater. Sci. Lett.*, **15**, 1-3 (1996).

K. Kuraoka, N. Kubo and T. Yazawa, *J. Sol-Gel Sci. Tech.*, in press.

Chapter 2. K. Kuraoka, Y. Chujo and T. Yazawa, *J. Am. Ceram. Soc.*, submitted.

Chapter 3. K. Kuraoka, Z. Qun, K. Kushibe and T. Yazawa, *Sep. Sci. Tech.*, **33**, 297-309 (1998).

Chapter 4. K. Kuraoka, R. Amakawa, K. Matsumoto and T. Yazawa, *J. Membrane Sci.*, in press.

Chapter 5. K. Kuraoka, Z. Shugen, K. Okita, T. Kakitani and T. Yazawa, *J. Membrane Sci.*, **160**, 31-39 (1999).

Chapter 6. K. Kuraoka and T. Yazawa, *J. Am. Ceram. Soc.*, **82**, 1325-1328 (1999).

Chapter 7. K. Kuraoka, Y. Chujo and T. Yazawa, *J. Membrane Sci.*, submitted.

List of Other Publications

T. Yazawa, K. Kadono, H. Tanaka, T. Sakaguchi, S. Tsubota, K. Kuraoka, M. Miya and D.-X. Wang, *J. Non-Cryst. Solids*, **170**, 105-108 (1994).

H. Tanaka, T. Yazawa and K. Kuraoka, *Bull. Osaka National Research Inst., AIST*, **45**, 137-154 (1994).

K. Kuraoka and T. Yazawa, *NEW GLASS*, **11(4)**, 45-48 (1996).

H. Tanaka, K. Kuraoka, H. Yamanaka and T. Yazawa, *J. Non-Cryst. Solids*, **215**, 262-270 (1997).

C.V. Avadhani, Y. Chujo, K. Kuraoka and T. Yazawa, *Polymer Bull.*, **38**, 501-508 (1997).

Y. Matsumura, K. Kuraoka, T. Yazawa and M. Haruta, *Catalysis Today*, **45**, 191-196 (1998).

N. Murase, K. Kuraoka and T. Yazawa, *Mol. Cryst. Liq. Cryst.*, **314**, 273-278 (1998).

R. Tamaki, Y. Chujo, K. Kuraoka and T. Yazawa, *J. Mater. Chem.*, **9**, 1741-1746 (1999).

W.-F. Du, K. Kuraoka and T. Yazawa, *J. Mater. Chem.*, **9**, 2723-2725 (1999).

T. Yazawa, K. Kuraoka and W.-F. Du, *J. Phys. Chem. B*, **103**, 9841-9845 (1999).

W.-F. Du, K. Kuraoka, T. Akai and T. Yazawa, *J. Ceram. Soc. Japan*, **107**, 1151-1155 (1999).

W.-F. Du, K. Kuraoka, T. Akai and T. Yazawa, *J. Solid State Chem.*, **149**, 459-464 (2000).

T. Yazawa, K. Kuraoka, T. Akai, N. Umesaki and W.-F. Du, *J. Phys. Chem. B*, **104**, 2109-2116 (2000).